

Review Article

Physical Models of Plasma Microfield

A. V. Demura

Hydrogen Energy & Plasma Technology Institute, Russian Research Center "Kurchatov Institute," Kurchatov Square 1, Moscow 123182, Russia

Correspondence should be addressed to A. V. Demura, alexander.demura@hepti.kiae.ru

Received 22 April 2009; Accepted 15 July 2009

Academic Editor: Elisabeth Dalimier

Copyright © 2010 A. V. Demura. This is an open access article distributed under the Creative Commons Attribution License, which permits unrestricted use, distribution, and reproduction in any medium, provided the original work is properly cited.

The present review is devoted to the current status of microfield notion that was so successful and profitable for experimental and theoretical studies of plasma in gas discharges and thermonuclear modeling installations for many decades. The physical aspects and ideas of the main generally used microfield models are described and analyzed in detail. The review highlights the remaining vague and unclear questions in the subject.

1. Microfield Notion

1.1. The Term of Microfield. The term “microfield” was introduced to designate the electric and magnetic fields, whose action is essential on microscales intra different media [1–12]. This was done to distinguish microfield from the fields of other origin essential, for example, for macroscopic description of a medium. As a rule the average microfield over macroscopic volume is equal to zero.

Plasma on microscales is characterized by noticeable deviation from quasineutrality conditions and appearance of strong electric fields due to separation of charges [3–12]. Namely, those electric fields, essential on microscales, usually are implied under term “microfield.” The magnitude of this field and its direction are subjected to fortuitous variations from point to point in space and in time.

Thus, from the very beginning, the microfield calculations represent itself challenging, complex, statistical, and kinetic problems. Being defined by the medium properties and composing it separate particles, the microfields action in its turn affects the medium characteristics and physical processes between these composing particles. Hence, the physical phenomena that somehow or other became involved and connected with microfields are very diverse. The voluminous literature [1–198], which is not confined so far by the named list and devoted to the study of various physical processes related to microfield characteristics and its affect on

medium properties and composing it particles, just confirms the variety of aspects and complexity of a problem.

The characteristics of microfields could be, in principle, determined with the help of hydrogen-like atoms placed inside plasma, which experience the Stark or Zeeman effects in electric or magnetic fields correspondingly [1, 2]. Those effects lead to the line splitting into separate sublines—Stark or Zeeman components. Thereby, the simplest quantum systems could serve as some kind of microprobes for the measurements of plasma parameters on microscales and perform the role of the so-called test particles. The measured signal from these microprobes on microscales is their emission in spectral lines or other spectral characteristics, perturbed by plasma environment.

However, the emission of spectral lines practically impossible to register locally from the volume with characteristic microsizes. That is why the radiation is registered simultaneously from different microvolumes. As far as the probability of field realization with the given magnitude and direction is different in space, this is equivalent to average of observed spectral lines profiles over the field configurations with various microfield magnitudes and directions, which leads to some extent to the smoothed-broadened contour.

Basing on pointed out dependencies spectral lines of atoms, molecules and ions with simple energetic structure are used for diagnostics of plasma parameters [1, 2]. Usually the methods of measurements correspond to the

so-called passive diagnostics, when the observed quantities are the distributions of intensity and polarization in discrete spectrum, emitted by plasmas. However, as meanwhile the measurements mainly has integral character, the success of their interpretation depends on construction of adequate model notions on the interaction of radiator with plasma medium, better corresponding to observed characteristics.

The formation of spectral line contour is influenced by dynamics of interaction of radiator of the electric field with that or another frequency spectrum, and by statistics of such interactions, describing the average over probabilities of appearance of the fields in plasmas. The real problem is complicated due to the strong difference in masses of negative and positive charges in plasmas, which leads to the strongly differing characteristic time scales of corresponding electric fields alterations [3–12]. For example, in equilibrium plasmas with density in a range of 10^{17} cm^{-3} and temperature about 1 eV, the ions of the electric fields vary more slowly than the electrons ones. So, the conventional picture of spectra formation is composed by splitting the energy levels in slowly varying ion microfield into Stark sublevels, broadening of these sublevels due to transitions between them, induced by more swift electron flights, and further averaging of spectrum over ion microfield distribution in plasmas [1, 2].

Near the series limit, the lines strongly overlap, and their intensity starts to decrease due ionization in plasma microfields [1]. However, the contribution of continuum noticeably increases in this region, and that is why visually the lines, located in sequence of decreasing intensity to the series limit, look as if ascending up the hillside, describing the increasing intensity of continuum.

For emitters with more complex internal structure, the contribution of line satellites, induced by transitions from doubly excited states of ions with preceding ionization stage, becomes important. On the other hand, under plasma creation by femtosecond laser pulses ionization evolves from K—and L—atomic shells of the targets, and the ions of hole configurations are created. In this case, the observed spectrum acquires quasicontinuous character. The plasma microfield even in these more complex conditions noticeably modifies the discrete spectrum of radiation.

The plasma microfield is stipulated as by Coulomb electric fields of charged particles, as by self-oscillations of plasma, playing the decisive role in nonequilibrium conditions. These fields are subdivided by terms of “individual” and “collective” components of microfield, respectively [1, 3].

In the wide range of plasma parameters, the quasistatic approximation is efficient for the description of interactions with ion microfield. It is grounded on the notion of instantaneous static microfield distribution function [1, 2]. However, in these conditions, the broadening by some part of ions has impact character, and this is of principal significance for a family of simulation methods [13].

It would seem, from general considerations, that the solution of spectral line broadening problem in a medium could be found using only statistical, and even, moreover, thermodynamic methods. However, in truth, a phenomenon

of spectral lines broadening has inseparably linked to each other dynamical and statistical aspects. For example, the processes of spectral line shape formation and population of quantum states are interrelated, and have to be considered self-consistently [108, 109]. The important factor in finding the solution is physically a correct choice of zero-order wave functions of a problem and its direction of quantization, adequately corresponding to physical observables [53].

Thus inadequacy of only statistical or only dynamical descriptions of a problem makes necessary the search of solutions based more or less on synthesis of these notions [104–109]. To a considerable extent, the necessity of such synthesis is stipulated also by actually restricted power of recent supercomputers for numerical modeling of complex multidimensional problems [14–17].

It should be noted that the whole row of phenomena exists in which microfield plays the important role but more amply its characteristics show up just in spectra of atoms and ions, immersed into plasmas. That is why in this introductory part the main attention was paid for the broadening of spectral lines.

This work presents the review of current ideas about plasma microfields, physical models, and methods for describing the quasistatic instantaneous distribution functions and temporary microfield evolution. The most ample previous reviews of this problem could be found in [1, 2, 11, 14–17] and the recently published papers [195–198].

1.2. Dipole Approximation as Basement of Microfield Formalism. So, a consideration of medium influence on test particles serves as a source of information on origin and character of interactions in various media and in its turn about the media state.

In plasmas this impact is due first of all to charged particles—plasma electrons and ions. If to expand the interaction potential of test particles with the medium into series over multipoles, assuming large remoteness of the medium (field) particles from the test ones in comparison with distances between the test particles, then the first term of expansion becomes zero due to condition of quasineutrality. (Here the case of charged plasmas, where this condition does not fulfill is not considered.)

The first not equal to zero term of this expansion just is due to the electric fields of plasma particles and proportional to the scalar product of the vector of dipole moment of a system of test particles and the summary electric field strength vector of plasma particles. This summary electric field of medium on microscales, becoming zero under average over macrovolume due to quasineutrality condition, was called microfield, as its action shows up at microscales, where the quasineutrality condition does not hold and the charge separation is essential.

Thereby, a possibility to describe the test particles interaction with environment (plasma) in terms of microfield is linked with conditions of predominance of long range components of potential over short range ones, when the distances between particles in a test system are less than the distances between particles of a medium. On the other hand, the possibility of such description depends on the

existence of dipole moment in a test system. That is why approximate representation of potential in terms of microfield corresponds to the dipole approximation.

In the case of the electric fields of collective plasma oscillations, the implementation of dipole approximation is evidently admissible, as the sizes of test systems are typically much less than the wavelength of those oscillations.

1.3. Applicability Criteria for Quasistatic Approach. Notion of quasistatic microfield is based as a rule on a simple reasoning that summary electric plasma microfield does not alter on some effective for radiation time scales [1, 2]. Within such settings, this condition turns out depending not only on microfield statistical properties but also on quantum properties of a radiator. For example, the smallness of frequency of temporary microfield changes \vec{F} in comparison with the hydrogen atom dipole moment d_n (n —the principal quantum number) [1, 2] frequency precession in this field is considered as such aforementioned condition:

$$\frac{d_{nn} F}{\hbar} \gg \left| \frac{\dot{\vec{F}}}{\vec{F}} \right|. \quad (1)$$

For the other condition of this kind, the smallness of life time of atom quantum state τ_{eff} in comparison with characteristic life time of microfield might serve or, when the characteristic frequency of atomic decay exceeds the characteristic frequency of microfield changes

$$\left| \frac{\dot{\vec{F}}}{\vec{F}} \right| \ll \tau_{\text{eff}}^{-1}, \quad (2)$$

indicating that an atom could not have enough time to response to temporary microfield variation. Often both these conditions are considered in aggregate with each other.

Besides the mentioned criteria, which are called “integral,” there are other types of conditions, requesting, for example, smallness of spectra variations, calculated using quasistatic microfield distribution functions $W_{st}(F)$ with small corrections $I_{st}(\Delta\omega) + \delta I(\Delta\omega)$, accounting to microfield evolution with time $W_{st}(F) + \delta W(F(t))$

$$\begin{aligned} I_{st}(\Delta\omega) &\gg \delta I(\Delta\omega), \\ W_{st}(F) &\gg \delta W(F(t)), \end{aligned} \quad (3)$$

where $\Delta\omega = \omega - \omega_0$, ω is the circular frequency of radiation, ω_0 is the unperturbed circular frequency of transition.

Per se this requires the complete solution within perturbation theory in assumption of small effective times [1, 2]. Such type of criteria dependent on circular frequency detuning from the line centers $\Delta\omega$ are used to call “spectral.”

More definitive quantitative characteristics are provided by integral and spectral criteria, derived from consideration of power law potentials of binary interaction of particles with respect to problems of spectral line broadening theory (see [2]).

1.4. Quantum and Classical Theory. The necessity of quantum microfield description mainly appears in connection with degeneracy of electron plasma component [7]. That is why from practical point of view the account of “quantumness” or the extent of degeneracy of electron gas in this concrete case touches upon mainly the character of plasma ions shielding by electrons [3–12]. Prescriptively, this could be reduced to the function of plasma ions shielding by electrons, which sufficiently well describes all limiting cases (see [7–12]).

However, for example, for plasma of metals very often, the range of parameters, where the effective charge of field ions noticeably differs from the charge of bare nuclear, is of main interest. Then, the appearance of quantum exchange and correlation effects due to ion core becomes essential. Evidently, the consequent account of quantum structure of radiator also has definite contribution. The description of these effects was suggested to perform in terms of formalism of local density functional, the application of which will be discussed in Section 2.7.

Additionally, for very low temperatures, the account of quantum description might become necessary even for the translational motion.

1.5. Significance of Models. We have to comprehend that plasma is a medium with very complicated physical characteristics [3–11].

Namely, due to this complexity, it was not possible to elaborate universal rigorous and self-consistent theory of plasma microfield in spite of numerous papers published on the subject up to now [1–198]. However, each time, some tractable but limited picture is achieved only in the frames of more or less trustable assumptions, obvious physical ideas, some solvable mathematical formalism, and various approximations. All the aforementioned components together constitute that or another physical model for microfield description.

For example, plasma could be considered as continuous medium [175] or as medium, which constitutes from many separate discrete particles [18]. Indeed, the commonly used ion-sphere model for microfield description is the typical sample of continuous models (see, e.g., [11, 45, 110]). So, it is natural to divide models on continuous and discrete ones. There are also some mixed models, where continuous and discrete approaches are applied to the different subsystems (see, e.g., [9, 11, 110]). One can consider point particles [18] and particles with finite sizes as well [176].

The deviation of plasma main parameters temperature and density also provides a variety of physical conditions—weakly and strongly coupled plasmas [9, 11], nonrelativistic and relativistic plasmas [177], degenerate electron plasma component [43], and so forth.

There is also a lot of complications connected with the choice of interaction potential, that is different for weakly and strongly coupled plasmas, for moving particles and particles at rest [42, 125]. Its working form depends on effective characteristic time scales that are prescribed to the microfield action [84, 85, 135–137], which in their turn

due to Fourier transform could be determined further by detunings from the line center [83, 95].

The microfield in plasma could be due to many-body interactions with discrete charged particles, or due to plasma self-oscillations or plasma waves [18, 30, 31, 49–52]. Moreover, it is important on what space and time scales it is necessary to define microfield. The space scales could be limited by formalism as well, and introduction of additional constraints such as energy conservation law [178, 179]. Indeed, for weakly coupled plasma on the microdistances less than Debye radius, the fluctuations of energy of particles is of the order of temperature. So, there is no reason to implement energy conservation law, but on macroscales, the fluctuations are much smaller and this restriction starts to hold. Interestingly, both mentioned restrictions or usage of the formalism, which from very beginning is derived for macro scales like the formalism of dielectric functions, should lead to the different from discrete models microfield distributions. In this context, we remind the old dispute around Hunger and Larenz works [178], who obtained instead of Holtsmark distribution Gauss type distributions introducing additionally energy conservation law constraints. The illuminating analysis of these results and polemics around them is presented in the work of Kogan and Selidovkin [179], who found explicit mistakes in analytical derivations of Hunger and Larenz works.

The distribution functions of microfield conventionally are obtained in the case of the so-called thermodynamical limit for $\mathcal{N} \rightarrow \infty$ and $\mathcal{V} \rightarrow \infty$, so that $\mathcal{N}/\mathcal{V} = \text{const} = N$ (\mathcal{N} is total number of particles in the system, \mathcal{V} is the system volume, N is the density of particles) [14–16]. However, it is possible to introduce microfield distribution functions for the finite number of particles as well [135–137]. There are obvious contradictions between various views on microfield definitions. For example, the different notions of instantaneous static ion microfield and ion microfield, obtained as a result of thermodynamic average, appeared from the consideration of the same physical object. However, the difference between output distributions, based on the distinct initial assumptions could result only in difference of the shielding constants that had to be used in the expression of “elementary” ion microfield.

The classification of microfield models in terms of their accounting for correlations between subsystems of plasma electrons and plasma ions was presented, for example, in the work of Ortner et al. [188]. These plasma models accounting for correlations are called “Two Component Plasma” (TCP) models in distinction from “One Component Plasma” (OCP) models [9].

The microfield models are additionally subdivided on those that attempt to describe static fields and ones depending on time. Using some assumptions on microfield statistics and some other approximations, the Method of Model Microfield (MMM) [86–94], Collective Coordinates for Ion Dynamics [180], Frequency Fluctuation Model (FFM) [99, 100], and Frequency Separation Technique (FST) [181] were proposed. Also, the direct computer simulations methods were elaborated firstly for static microfield distributions like the Monte-Carlo method [27–29, 35–39, 110, 113] and

after for modeling the evolution of electric microfields versus time: Computer Simulations (CS) with particles moving along prescribed type of trajectories [101–105, 142–145] and Method of Molecular Dynamics (MD) [107, 109, 135–139, 182, 183].

Thus we see that notions of microfield and models that are designed for its description are complicated and diverse, reflecting the diverse and complex plasma properties.

2. Quasistatic Distribution Functions

It is used to distinguish (although it could be done only approximately) plasma microfield additive components, having essentially different frequency and spatial characteristics. Firstly, it is possible to single out the electric fields of high and low frequency plasma collective oscillations and individual component of electric microfield, being a summary field of separate plasma particles.

Furthermore, an individual component in its turn could be divided into high frequency, induced by plasma electrons, and low frequency, induced by plasma ions, parts. Evidently, such separation should happen automatically under implementation of sufficiently adequate mathematic approaches to the complete system and specifics of that or another problem. Although such attempts were done, they did not lead to formulated goal. In fact, as was underlined in the previous subsection, the microfield theory is constructed based on model and intuitive ideas as necessary solutions for a whole row of problems could not be obtained using conventional thermodynamic methods.

The interaction of the point field ions with an emitter in dipole approximation could be represented in terms of the electric ion microfield \vec{F} in assumption, that perturbing particles are situated sufficiently far from emitter, so that the radius-vector of radiating electron is much less than radius-vectors of perturbing particles with respect to the emitter nuclear. Using the condition of vector additivity of electric fields of all ions \vec{F}_j , we have

$$\vec{F} = \sum_{j=0}^{\infty} \vec{F}_j. \quad (4)$$

Then the statistical microfield distribution function \vec{F} could be obtained from the next thermodynamic average

$$W(\vec{F}) = \left\langle \delta \left(\vec{F} - \sum_{j=0}^{\infty} \vec{F}_j \right) \right\rangle, \quad (5)$$

where symbol $\langle \dots \rangle$ designates the average over plasma ensemble of ions. Moreover, as a rule, this average encircles passage to the limit, under which the number of particles (ions) in ensemble \mathcal{N}_i and the system volume \mathcal{V} are indefinitely increasing, while their ratio is kept constant and equal to the particle density $\lim_{\mathcal{N}_i \rightarrow \infty, \mathcal{V} \rightarrow \infty} \mathcal{N}_i/\mathcal{V} = \mathcal{N}_i$.

The field strength of electric microfield \vec{F} and its components \vec{F}_j in assumption of a point test particle is evaluated in the place of its localization, which usually is

chosen as an origin of reference frame of coordinates (in the case of test particles at rest).

The average value calculation, mentioned earlier, is a complex problem due to its many-body character, vector properties of quantities under evaluation, multicomponent system of plasma particles, correlations and interactions between them, and specific peculiarities of a test system.

It is important to comprehend what a function in the sense of performed average character would more correctly correspond to the posed problem. From the arsenal of mathematical methods of statistical physics the average over canonical or microcanonical ensembles, chaotic phases, fast subsystems, and so forth [3–12] could be recovered.

However, for obtaining such averages as a rule, the infinite time interval is needed, while the used in many physical solutions Fourier transform itself limits the effective duration of time average. For example, under Fourier transform for line profile calculation at the circular frequency detuning from the line center $\Delta\omega = \omega - \omega_0$, the effective time of profile formation is of the order $\Delta\omega^{-1}$, where ω , ω_0 are perturbed and unperturbed circular frequencies of radiation. The value $\Delta\omega^{-1}$ determines thereby the allowed characteristic scales of average over the time of stochastic variables entering expression for line contour versus the frequency detuning. As a rule, it is implicitly assumed that instantaneous distribution function of ion microfield, when the average could be performed before ions would change essentially their space configuration, is used. Here is evidently some mismatch of descriptive methods and requested from physical consideration result. However, spectra depend not only on line profiles but also on spectral lines intensities, proportional to population of excited levels. The populations in many cases are determined by the balance of thermodynamically equilibrium processes. Hence, the real situation is rather diverse. The elaborated up-to-date approaches give only approximate solutions for the aforementioned row of problems. In this paper, only those that are used more often will be enlightened.

2.1. Holtsmark Function. Historically, the Holtsmark function [18] became the first and physically significant solution of a problem of static microfield distribution, derived for isotropic ideal gas of charged particles with the same sign of charges [1, 2, 14–21]. This function describes the probability of outcome for ions configuration for the given value of microfield module F without account of plasma ion-ion and ion-electron interactions versus the reduced dimensionless microfield value $\beta = F/F_0$, where $F_0 = 2\pi(4/15)^{2/3}eZ_iN_i^{2/3}$ is the normal Holtsmark field value:

$$\mathcal{H}(\beta) = \frac{2\beta}{\pi} \int_0^\infty dx x \sin(\beta x) \exp[-x^{3/2}]. \quad (6)$$

The important characteristic of this distribution is its asymptotic behavior at small $\beta \ll 1$ and large $\beta \gg 1$. At large β , it is proportional to $\beta^{-5/2}$ and stems to the distribution of the nearest neighbor, which corresponds to small distances between the perturbing and emitting (test) particles. At small β , this distribution is proportional to β^2 , which corresponds

to the many-body law of summary field formation at large distances between field particles, when the field values due to separate particles are small. Those asymptotic dependencies in fact are universal features and of more realistic microfield distributions [1, 2, 14–17]. The basic technical element for obtaining this and other results is the Fourier-transform of δ -function, which allows to reduce the problem in the isotropic case to calculation of characteristic function $A(k)$:

$$W(\beta) = \frac{2\beta}{\pi} \int_0^\infty dk k \sin(k\beta) A(k), \quad (7)$$

$$\int_0^\infty d\beta W(\beta) = 1.$$

This expression is universal and based only on isotropy of distribution function, does not depend on density, which enters only in the definition of the normal field. At the same time, the functional dependence of $\ln A(k)$ is determined by the Coulomb law of electric field. The graph of universal Holtsmark distribution function will be given in what follows in comparison with more sophisticated distributions of Ecker-Müller [22, 23], and Hooper [27–29].

2.2. Ecker-Müller Distribution. The first step to account of plasma specifics became the Ecker and Ecker-Müller microfield distribution functions [22, 23]. In its derivation, it is assumed that the potential of plasma field ion is shielded by plasma electrons and obeys Debye law. The interaction between field ions is neglected. So, the difference from the Holtsmark distribution is only using the expression for electric field for plasma ions, shielded by plasma electrons according to Debye:

$$\vec{E}(\vec{r}) = -Z_p e \left(1 + \frac{r}{r_{De}}\right) \exp\left(-\frac{r}{r_{De}}\right) \frac{\vec{r}}{r^3}, \quad (8)$$

where $Z_p e$ is the charge of field ion, e is the electron charge, r_d is the electron Debye radius [3–11]. In various publications, the total Debye radius is substituted in this expression, simultaneously including the shielding by electrons and ions [14–17]. However, from physical point of view, it is not always justified.

The Ecker-Müller distribution became a function of two variables—the reduced electric field value β and dimensionless parameter δ , proportional to the number of field ions in the Debye sphere:

$$\delta = \frac{4\pi}{3} N_i r_{De}^3. \quad (9)$$

However, later, the labeling of distribution functions with the parameter

$$a = \delta^{1/3} = \frac{R_0}{r_{De}} \quad (10)$$

became conventional, where R_0 is the mean distance between field ions.

For weakly coupled plasmas, only for which there is a sense to apply this distribution, the parameter value a is limited from above by unity. At $a = 0$, the Ecker-Müller distribution coincides with the Holtsmark distribution, and its maximum is shifted to the lesser reduced values of microfield while parameter a is increasing. As due to quasineutrality condition, the ion density could be expressed via electron density, and from the aforementioned, it follows that the Ecker-Müller distribution is also a function of electron temperature, of course, via dependence on parameter δ or a .

The comparison of Ecker-Müller distribution and Holtsmark function versus parameter δ and values of electric reduced field values $\mathcal{E}/\mathcal{E}_0$ is presented in Figure 1.

2.3. Baranger-Mozer Cluster Expansion. The Baranger-Mozer papers [24, 25] appeared approximately 2 years after the works of Ecker and Müller and were significant advance as according to the physical formulation as to the development of adequate mathematical formalism.

The notions of high-frequency electronic and low-frequency ionic components of plasma microfield, ion-ion correlations were introduced in [24, 25]. It was pointed out on inadmissibility of usage the total Debye radius in expression for ion microfield and was demonstrated the different character of distributions in the neutral and charged points.

The adequate formalism in [24, 25] is based on the cluster expansion methods, developed firstly for virial coefficients [7–12] and giving the possibility to represent $\ln[A(k)]$ in power series over density ordered versus the extent of correlations weakening. Let us consider in more detail the instructive derivation of these results. The summary field of ions \vec{F} satisfies the vector additivity condition, that is,

$$\vec{F} = \vec{F}_1 + \vec{F}_2 + \vec{F}_3 + \cdots + \vec{F}_{\mathcal{N}}. \quad (11)$$

The distribution function of summary microfield $W(\vec{F})$ could be transformed to the form

$$\begin{aligned} W(\vec{k}) &= \frac{1}{(2\pi)^3} \int d^3k \exp(-ik\vec{F}) A(\vec{k}), \\ A(\vec{k}) &= \int \cdots \int d^3x_1 \cdots d^3x_{\mathcal{N}} \\ &\cdot \exp[i \vec{k}(\vec{F}_1 + \vec{F}_2 + \cdots + \vec{F}_{\mathcal{N}})] \\ &\cdot P(\vec{x}_1, \vec{x}_2, \dots, \vec{x}_{\mathcal{N}}), \end{aligned} \quad (12)$$

where $P(\vec{x}_1, \vec{x}_2, \dots, \vec{x}_{\mathcal{N}})$ designates the probability of given configuration from \mathcal{N} particles.

Further on, the standard procedure, which is performing the identical operations with each of multiplicands $\exp(i\vec{k}\vec{F}_j)$ in the integrand, is applied:

$$\begin{aligned} \exp(i\vec{k}\vec{F}_j) &= 1 + \varphi_j, \\ \prod_{j=1}^{\mathcal{N}} (1 + \varphi_j) &= 1 + \sum_i \varphi_i + \sum_{i,i'} \varphi_i \varphi_{i'} + . \end{aligned} \quad (13)$$

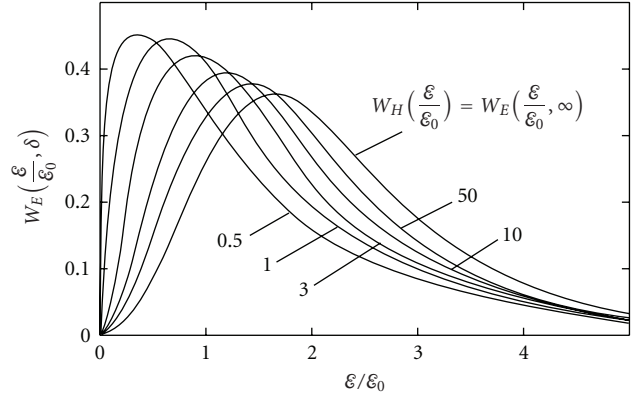


FIGURE 1: Comparison of Ecker-Müller microfield distribution $W(\mathcal{E}/\mathcal{E}_0)$ and Holtsmark function $W_H(\mathcal{E}/\mathcal{E}_0)$ versus parameter δ and values of reduced field $\mathcal{E}/\mathcal{E}_0$ according to [22, 23].

Then integrating over free variables, the characteristic function could be represented as a sum

$$A(\vec{k}) = \sum_{\mathcal{M}} A_{\mathcal{M}}(\vec{k}), \quad (14)$$

$$\begin{aligned} A_{\mathcal{M}} &= \int \cdots \int d^3x_i \cdots d^3x_s \cdot \varphi_i \cdots \varphi_s \\ &\cdot P_{\mathcal{M}}(\vec{x}_i, \dots, \vec{x}_s), \end{aligned} \quad (15)$$

where the summation is extended on all combinations of \mathcal{M} particles from \mathcal{N} .

Then the idea about strong decreasing of correlations versus increasing their order is explicitly implemented:

$$\begin{aligned} \mathcal{V}^{\mathcal{M}} P_{\mathcal{M}}(\vec{x}_i, \dots, \vec{x}_s) &= \prod_i g_1(\vec{x}_i) + \sum_2 g_2(\vec{x}_j, \vec{x}_k) \prod_i g_1(\vec{x}_i) \\ &+ \sum_{22} g_2(\vec{x}_j, \vec{x}_k) \cdot g_2(\vec{x}_l, \vec{x}_m) \prod_i g_1(\vec{x}_i) \\ &+ \sum_{222} \cdots + \cdots + \sum_3 g_3(\vec{x}_j, \vec{x}_k, \vec{x}_l) \\ &\cdot \prod_i g_1(\vec{x}_i) + \sum_{33} g_3(\vec{x}_j, \vec{x}_k, \vec{x}_l) \\ &\cdot g_3(\vec{x}_m, \vec{x}_n, \vec{x}_p) \prod_i g_1(\vec{x}_i) + \sum_{333} \cdots + \cdots \\ &+ \sum_{32} g_3(\vec{x}_j, \vec{x}_k, \vec{x}_l) \cdot g_2(\vec{x}_m, \vec{x}_n) \prod_i g_1(\vec{x}_i) \\ &+ \sum_4 \cdots + \cdots, \end{aligned} \quad (16)$$

where \mathcal{V} is the system volume, and the single particle probability function is

$$P_1(\vec{x}) = \frac{1}{\mathcal{V}} g_1(\vec{x}). \quad (17)$$

The sum \sum_2 designates the summation over all pairs of particles from \mathcal{M} particles, the sum \sum_{22} over two different pairs of particles from \mathcal{M} particles. In the sum \sum_{32} , the summation goes over all possible combinations of different triplets and pairs of particles from \mathcal{M} particles. In each term of this series, those particles, included in the product from \mathcal{M} particles, do not constitute triplets, pairs, and so forth. The g functions due to the extraction of factor $\mathcal{V}^{-\mathcal{M}}$ are defined so that do not depend on volume \mathcal{V} for large values of \mathcal{V} . Generally speaking, the cluster diagram could be confronted to each term of this expansion [7].

In the limit of large $\mathcal{N} \rightarrow \infty$ and large $\mathcal{V} \rightarrow \infty$, but for constant concentration $N = \mathcal{N}/\mathcal{V} = \text{const}$, $A(\vec{k})$ could be represented as

$$A(\vec{k}) = G_1(\vec{k})G_2(\vec{k})G_3(\vec{k})\dots, \quad (18)$$

$$\begin{aligned} G_p(\vec{k}) = & 1 + \mathcal{V}^{-P} \sum_P \int \varphi_i \cdots \varphi_s g_P(\vec{x}_i, \dots, \vec{x}_s) \\ & \cdot d^3x_i \cdots d^3x_s \\ & + \mathcal{V}^{-2P} \sum_{PP} \int \varphi_i \cdots \varphi_v g_P(\vec{x}_i, \dots, \vec{x}_s) \quad (19) \\ & \cdot g_P(\vec{x}_t, \dots, \vec{x}_v) d^3x_i \cdots d^3x_v \\ & + \sum_{PPP} \cdots + \cdots \end{aligned}$$

Here, the single sum covers all possible combinations with P particles from \mathcal{N} ones, the double sum over all possible combinations of different two clusters with P particles from \mathcal{N} ones, while all particles in a cluster are being different, and so forth.

The difference of expression (18) from (14) is that there are no the same particles in each term from (14), represented as the expansion according to (15)–(17), whereas according to definition (18), one particle, entering in G_p , could coincide with one of particles, that compose G_Q . That is why (18) contains a part of additional terms which do not appear in (14). However, as stated in [24, 25], the number of coinciding terms in both expansions, under the tendency of the total number of particles to infinity, is \mathcal{N} times larger the number of additional terms, whose contribution to the total sum thus occurs negligible [24, 25].

If to take into account that under $\mathcal{N} \rightarrow \infty$ all terms in each sum become equal, then calculating the number of those terms, one could obtain the following closed expression for $G_p(\vec{k})$

$$\begin{aligned} G_p(\vec{k}) = & \exp\left(\frac{N^p}{p!} h_p(\vec{k})\right), \\ h_p(\vec{k}) = & \int \int \cdots \int \varphi_1 \varphi_2 \cdots \varphi_p \quad (20) \\ & \cdot g_p(\vec{x}_1, \vec{x}_2, \dots, \vec{x}_p) d^3x_1 d^3x_2 \cdots d^3x_p, \end{aligned}$$

and hence the expression for $A(\vec{k})$ takes the form

$$A(\vec{k}) = \exp\left[\sum_{p=1}^{\infty} \frac{N^p}{p!} h_p(\vec{k})\right]. \quad (21)$$

In contrast to the virial expansion, the convergence of integrals $h_p(\vec{k})$ and its sum are more rapid due to the appearance of powers of additional factors $\varphi_j(\vec{k})$ in the integrands for terms of cluster expansion series, which drastically narrows the range of effective values of variables, providing the main contribution to integrals.

As the Bogoliubov-Born-Green-Kirkwood-Yvon chain [7–12], the cluster expansion is based on two very significant semi-intuitive notions: (i) about monotonous decreasing of correlation functions versus increase of the correlation order; (ii) about a sufficiently rapid decrease of correlation functions versus increase of the distance between particles.

For the low-frequency distribution of ion microfield, the electric field produced by single-field ion at the origin of reference frame was taken in the form of Coulomb electric field statically shielded by plasma electrons according to Debye as was already mentioned in the previous paragraph. The Debye approximation was implemented in expressions for pair correlation functions, and calculations were limited by the pair correlations in neutral point and the triple correlations in charged point. In the case of the electric field distribution in charged point, the triple correlation function was disentangled with the help of the Kirkwood superposition approximation [7–12]. Thereby, only the two first terms of cluster expansion of $\ln[A(k)]$ were taken into account, where the second term describes ion-ion correlations. For the pair correlations function of field ions, the linearized Debye approximation was used for description of ion-ion correlations, which is the first not equal to zero term of expansion [3–12].

The high-frequency function, describing the Coulomb field of plasma electrons, practically was not used later, but the low frequency component of plasma microfield had got applications in spectroscopy.

Formally, this distribution due to ion-ion correlation additionally to the dependencies on β and T_e also is a function of ion temperature T_i through dependence on additional dimensionless parameter $R_c/R_0 = e^2 Z_p^2 / T_i R_0$, which practically coincides with the definition of ionic coupling parameter Γ_i , where R_c is the ionic Coulomb radius. It should be pointed out that in the second of cited works [24, 25], the linearized Debye pair correlation function, used for description of ion-ion correlations, contains as a shielding length the total Debye radius, where the ion-ion shielding also is accounted for [24, 25].

Regretfully, in the tabulation of ion microfield distribution functions in [24, 25] the numerical mistakes were detected, which led to undeserved disavowal of developed approach. Later, Pfennig and Trefftz found and removed these inaccuracies [26] together with distrust to approach in general.

The important advantage of Baranger-Mozer formalism is the possibility of its generalization for arbitrary plasma

ionization composition, that is presented, particularly, in 2.9.1. The explicit results of 2.9.1. allow to obtain more ample apprehension on practical receipts of Baranger-Mozer approach implementations.

The graphical behavior of Baranger-Mozer distribution functions after removal of numerical inaccuracies coincides with the Hooper distributions, obtained within the different model and represented in the following subsection.

The main progress of these two works is distinguishing the high-frequency electric microfield component, whose time variation is governed by the motion of electrons, and the low-frequency electric microfield component, whose characteristic time scale is determined by ion motion. At the same time, it is assumed that the average of high-frequency component on the ion microfield time scale contributes to the summary low-frequency microfield component via the Debye electronic shielding of ion electric field due to the electron clouds surrounding ion charges [24, 25]. Having in mind the problem of the Stark broadening of spectral lines, the authors aimed to obtain the distribution of, namely, “instant” microfield and not the average “thermodynamic” microfield. It should be underlined, thus these declarations although quite sound and reasonable from physical sense contradict with the available formalism, which is, of course, thermodynamic in its origin [24, 25].

As the properties of correlation functions with the order larger than 2 are studied still insufficiently up to now, only the two first terms of expansion were considered in [24, 25]: the first one is being linear dependent on density and the second one is being proportional to the density squared. Thus, the first term describes certain type of independent quasiparticles, characterized by some interaction potential with the test particle, while the second term is responsible for pairwise or reduced triple correlations between field particles.

2.4. Hooper Model. The Hooper model implements Bohm and Pines “collective coordinates method” (CCM) [30, 31]. This method devoted to an attempt to separate formally Hamiltonian of the system of Coulomb particles into two Hamiltonians, characterizing almost independent subsystems one of which represents itself the plasma collective characteristic oscillations, and the other one represents the subsystem of independent quasiparticles “dressed” by the screening due to separated collective degrees of freedom [30, 31]. It was shown [30, 31] that under specific assumptions, this separation is possible to accomplish by applying the specifically defined sequence of canonical transformations of variables. These results had great impact on the further development of ideas of plasma microfield and were used later as a basis in order to determine how to separate the collective microfield component due to the plasma characteristic oscillations from many-body but “individual” microfield component due to particles or quasiparticles [48–51]. Firstly for constructing the static microfield distributions, this method was proposed by Broyles [32, 33]. The Broyles papers [32, 33] contain deep and very interesting original physical analysis of microfield problem, as well as several innovative suggestions for development of appropriate mathematical formalism.

Meanwhile, in the same period of time, the Monte Carlo (MC) procedure was formulated and published providing a powerful tool for consideration of thermodynamically equilibrium conditions and calculations of correlation functions and various static microfield distributions [110] (see [35–39, 111–113]). The overall situation at that time with the Baranger-Mozer results was not clear, and the progress in Monte Carlo and ideas of Broyles inspired Hooper to reconsider the derivation of static microfield distribution functions in some different original way [27–29]. Hooper adopted the ideas of Baranger-Mozer on the separation of high- (electron) and low-frequency (ion) microfield components, but he introduced the separation of the interaction potential into the so-called central (corresponding to the interaction with the test particle) and noncentral (corresponding to the interactions between field particles) parts [27–29]. He also formally included the scalar product of vectorial Fourier variable on the vector of elementary electric field strength of the single particle into the central part of the interaction potential. After this, Hooper constructed the analog of the two term Baranger-Mozer cluster expansion but for complex central potential, which had certain impact on the definition and determination of the correlations functions, for example. It was supposed that the screening of the ion field in the central part of potential is determined by the electronic Debye radius while the screening length for the noncentral part also is described by Debye potential but with a screening length equal to the electronic Debye radius multiplied by fitting parameter “ α ” to be determined later. Using the Bohm and Pines method of collective variables as a mathematical trick according to the Broyles ideas, Hooper was able to derive the formulae for the microfield distribution function that as in the case of Baranger-Mozer is expressed through the finite number of subsidiary integrals and functions [27–29]. Performing calculations along with this derivation and comparing their results with Monte Carlo method for the same values of parameters, Hooper found the rather wide ranges for the “ α ” parameter variation, in which the results of calculations with the prescribed accuracy practically do not alter and coincide with Monte Carlo results for the same set of plasma parameters and assumptions concerning the interaction potential. The examples presented in [27–29] showed that for the low-frequency ionic microfield component, α could change from 1.3 to 1.8 at $a = 0.8$, and from 1.8 to 4.0 at $a = 0.2$. Hence, this strangely means that in some range of fitting parameter variation, the results in question do not depend on its values. When his article was altogether in print [27–29], Hooper became aware of the article of Pfennig and Trefftz [26], and after comparison he found that the results of his calculations do not differ from the improved for digital mistake results of Baranger-Mozer [24, 25]. Thus, it was rather dramatic point because no words the Hooper’s method of derivation was much more complicated and that is why, probably, lesser convincing than the Baranger-Mozer one. However, tables of microfield distributions presented in Hooper’s works became widely used in practical calculations in plasma spectroscopy and thus frequently cited, although their values

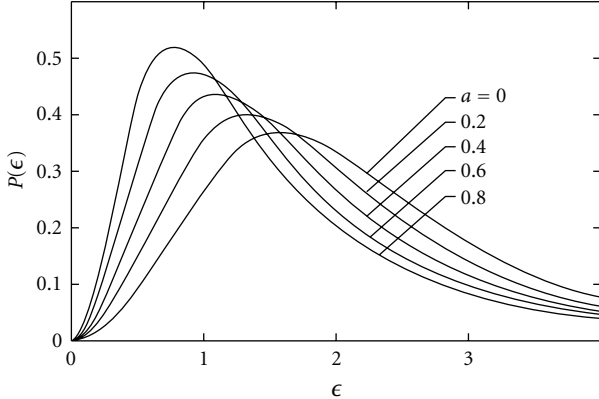


FIGURE 2: Microfield distribution function $P(\epsilon)$ in neutral point for several values of a from [27–29] (designations $\epsilon \equiv \beta$, $W(\beta) \equiv P(\epsilon)$ are the same as in original Hooper paper [27–29]).

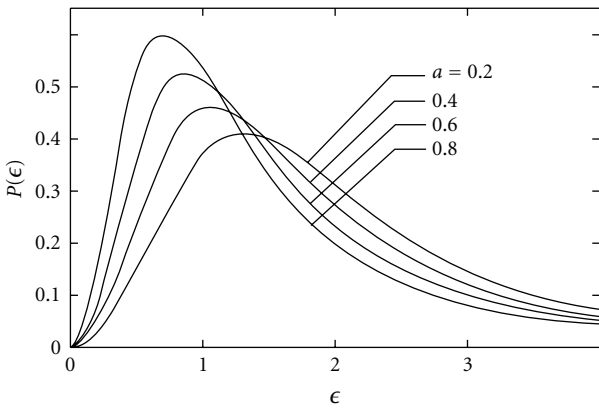


FIGURE 3: Microfield distribution function $P(\epsilon)$ in charged point for several a values according to [27–29] (the designations are the same as in Figure 1).

practically coincide with the values prescribed by Baranger-Mozer approach!

Alas, the derivation of Hooper results is substantially unclear [27–29] mostly due to the very complicated formalism used in [27–29], although initial settings do not differ from Baranger-Moser ones. Hooper also stated that he used nonlinear form of Debye-Hückel correlation function. However, in this case the dependence of the second term of cluster expansion starts to be more complicated and could not be reduced only to the second power of density. Regrettably, the noticeable difference of the effective shielding length from the Debye value did not get any physical treatment in [27–29] and posterior works, exploiting these initial Hooper ideas.

In Hooper works, there are no details on Monte-Carlo method used in the model. The Monte-Carlo method in its essentials corresponds to the infinite interval of time average and thus includes the total ion-ion screening, which is inadmissible in the case of its implementation for the description of quasistatic ion broadening of spectral lines in plasmas. So, now it is well known that the results of Hooper approach do not differ from corrected Baranger-Mozer

results [24, 25]. At the same time Hooper approach is more laborious and could not get unequivocal interpretation. The later Hooper works with coauthors showed that the developed formalism does not have simple extension on the case of arbitrary plasma ionization composition, and even the case of binary composition needs tremendous computing efforts [34]. The Hooper distributions also are limited by values of parameter $a \leq 1$.

In Figure 2, one can see microfield distribution found by Hooper for several values of a in the neutral point, and in Figure 3 in the charged point. Both distributions are calculated for the singly charged field ions and singly charged test ion. The designations in the figures are as in the original Hooper papers. The distribution for $a = 0$ in neutral point coincides with the Holtmark distribution. The other distributions coincide with the Baranger-Mozer ones for the same conditions as mentioned earlier.

The Hooper formalism for construction of distribution functions, based on using in mathematical calculations the collective coordinates method and cluster expansion, could not be generalized directly on quantum case or plasmas with complex ionization composition. In fact, to our knowledge, his results and formalism were never reproduced independently from the author [27–29]. However, the distribution functions presented in [27–29] and other papers are very trusted by professional community and popular in doing practical calculations.

2.5. Monte-Carlo Method. The calculation of microfield distribution functions by Monte-Carlo method (MC) is based on computer statistical sampling of probability of fall-out of various spatial configurations of field particles [35–39].

Firstly, the systematic description of Monte-Carlo method was published in [110] (see also [111–113]) and formally is not limited by only weakly coupled plasmas.

Until recently, the majority of results for microfield distribution functions for strongly coupled plasmas were obtained namely by this method [39]. The notion of strongly coupled plasmas encircles also conditions, when electronic $\Gamma_e = e^2 N_e^{1/3} / T_e$ and ionic plasma parameters $\Gamma_i = Z_p^2 e^2 N_i^{1/3} / T_i$ of coupling exceed unity not at the same time.

In the main part of MC studies up to date, the Debye form is chosen for the initial ionic potential with the effective screening length taking into account the degeneracy of electronic component. The size of the cell L is determined by the density of modeled conditions, namely, by the number of particles in MC simulations N plus the test particle, and connected with the ion density N_i by the relation

$$N_i = \frac{(N+1)}{L^3}. \quad (22)$$

For including the influence of remote particles, the cell is reproduced by its “self-images” with step equal to L , and the total sum of potentials is evaluated by the Evald method [114, 115]. The important advantage of MC is that it easily matches any boundary conditions.

During simulations, the field ion and its location inside the cell are chosen in a random manner. If, during modeling, the ion occurs outside the cell, then it is substituted by its

image. Under the usage of powerful computers like Cray, the first 10^4 configurations were discarded in order to avoid dependence on initial conditions.

For searching equilibrium solution, the Metropolis algorithm is used [105]: the difference of energy ΔW between two consequent configurations is calculated, and if this difference is negative, then the configuration is included with the weight factor equal to 1, and if it is positive then with the weight factor equal to $\exp[-\Delta W/T]$. This allows to avoid the system trapping in local random minima. Evidently, during approaching the equilibrium, $\Delta W \rightarrow 0$. All equilibrium values of microfield are calculated after reaching the equilibrium. For example, in the widely used by experts results of MC modeling [35–39], the number of particles in the cell was 700–800, while the number of configurations after reaching the equilibrium 10^7 . It should be noted that unlike the initial version of method [110], the later results [35–39] are obtained after an average of total potential over the angles of radius vector of test particle, which accelerates the convergence and secure the fulfilment of conditions of isotropy.

In a recent paper [39], the rather simple approximate functions of reduced microfield and coupling parameters for various regions of plasma parameters were proposed during fitting procedure to results of MC calculations of plasma microfield distributions.

In regions of very small and very large reduced microfield values, MC has very large fluctuations and could not provide prescribed accuracy. For description of distribution functions in this regions, the matching with known asymptotic results is applied [21].

2.6. Adjustable Parameter Exponential Approximation. The Hooper's ideas gave rise to another approach in the theory of microfield distribution that is called Adjustable Parameter Exponential Approximation (APEX) developed in series of papers by Iglesias et al. (for current version, see [43, 184–189]). This method was aimed to describe first of all the microfield distribution at highly charged test ions in strongly coupled plasmas, where other theoretical approaches as Baranger-Mozer one fail, while MC at that time was considered as inconvenient and expensive for large-scale calculations together with magneto-hydrodynamic and radiation transfer codes in the laser inertial confinement fusion (LICF) studies [40–42]. Hence, the main motivation for APEX derivation [40–44] was an attempt to give alternative with respect to MC description of microfield distributions at test ions in strongly coupled plasmas. However, APEX from the beginning was formulated as *ad hoc* approach.

APEX also singles out the high frequency-electron and low frequency-ion components of plasma microfield. The constructions of microfield distributions for those components are rather different. The APEX model for high-frequency component could be considered in our classification as a mixed one, because it uses the notion of point separate electrons and the notion of uniform continuous positive background due to ions. In this APEX derivation, the results of the so-called one component plasma model (OCP)

were applied [7–12]. Here, the narration mostly concerns the APEX results for ionic low-frequency part [42–44].

The key point in the APEX construction is the assumption of the Yukawa-type effective interaction potential between ions with the screening length, which is proportional to the adjustable parameter “ α ” to be determined later. Also, APEX utilizes the exact relation that have to be fulfilled at the test particle with charge equal to Z_0 [43]. At the same time if to remember that in the strongly coupled plasma the Debye radius as a rule is less than the mean interparticle distance, the validity and applicability of the Debye potential start to be doubtful for these conditions.

According to the APEX ideology, the introduction of the APEX effective field should account for high-order correlations and thus should make it possible to consider effectively noninteracting quasiparticles [43]. Thus, the initial APEX starting formulation and idea was using transformations of cluster expansion for $\ln A(k)$, like used by Hooper [27–29], to obtain single-term representation of cluster series with the help of more accurate methods for constructing the correlation functions than those provided by Debye approximation [7–12].

For transformation of cluster series to one term it was proposed to substitute in $\ln A(k)$ not a real, but some effective electric field and corresponding distribution of quasiparticles, equating the products of local probability density on the value of local field, namely:

$$\begin{aligned} eC_\sigma Z_\sigma G_\sigma(x) f_\sigma(x) &= eC_\sigma Z_\sigma g_\sigma(x) f(x), \\ G_\sigma(x) &= g_\sigma(x) \frac{f(x)}{f_\sigma(x)}, \\ f_\sigma(x) &= \frac{\exp[-\alpha_\sigma x]}{x^2} (1 + \alpha_\sigma x), \\ f(x) &= \frac{\exp[-a x]}{x^2} (1 + ax), \end{aligned} \quad (23)$$

where $a = R_0/R_{D_e}$; σ designates the field ions species; $C_\sigma = N_\sigma/N$, Z_σ are partial concentration and the charge of field ions species σ correspondingly; $g_\sigma(x)$ is the correlation function of the field and test ions; $f_\sigma(x)$ is the APEX effective field, depending on fitting parameter α_σ ; $G_\sigma(x)$ is the effective distribution function of the field particles density with the charge Z_σ around the test ion with the charge Z_0 ; $f(x)$ is the reduced initial, screened by electrons according to Debye, this “so-called” elementary electric field is the adopted dependence for the electric field of single plasma ion.

Thus, the Hooper ideas of implementation of additional fitting parameter under optimization of distribution functions got in APEX alike, but another realization.

The set of fitting parameter $\{\alpha_\sigma\}$ according to [42] has to be found from the exact relation for mean square of microfield at test ion

$$\begin{aligned} \langle E^2 \rangle &= 4\pi NT \sum_\sigma \frac{C_\sigma Z_\sigma}{Z_0} \psi_\sigma(a), \\ \psi_\sigma(a) &= a^2 \int_0^\infty dx x g_\sigma(x) \exp[-ax], \end{aligned} \quad (24)$$

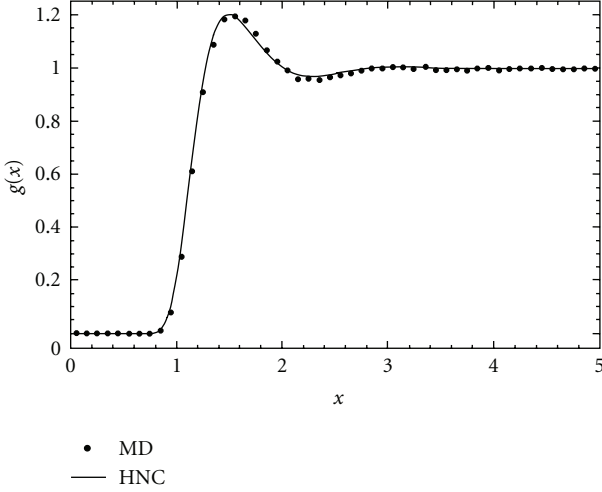


FIGURE 4: Comparison of pairwise radial distribution functions (RDF) for $Z_0 = Z_s = 25$, $T_e = 50$ eV, plasma coupling parameter $\Gamma = 50$ and $N_e = 10^{24}$ cm $^{-3}$ calculated by Molecular Dynamics and in HCN approximation in [43].

where Z_0 is the test ion charge.

The left-hand side of this equation in APEX takes the form [42]

$$\begin{aligned} \sum_{\sigma} Z_{\sigma}^2 C_{\sigma} \int_0^{\infty} dx x^2 g_{\sigma}(x) f_{\sigma}(x) f(x) \\ = \frac{1}{Z_0 \Gamma_i} \sum_{\sigma} Z_{\sigma} C_{\sigma} \psi_{\sigma}(a). \end{aligned} \quad (25)$$

It is assumed in [42] that the solution could be found for each species separately, which gives the set of equations for all σ :

$$Z_{\sigma}^2 \int_0^{\infty} dx x^2 g_{\sigma}(x) f_{\sigma}(x) f(x) = \frac{Z_{\sigma}}{Z_0 \Gamma_i} \psi_{\sigma}(a). \quad (26)$$

The correlation functions could not be determined within APEX. To close APEX scheme, the correlation functions are calculated separately within the hypernetted chain approximation (HCN) [7–12], when the so-called “bridge function” is put to zero [43]. The HCN correlation functions are considered as very precise and remarkably differ from Debye ones for large plasma coupling parameters and reproduce rather well MC and MD correlation functions [7–12, 40–43]. The illustration of correlation function behavior for strongly coupled plasma is shown in Figure 4 from [43]. Utilizing HCN correlation functions is one of the APEX significant advantages that gives possibility to describe microfield distributions in strongly coupled plasmas (SCP) [43]. At the same time as could be judged by laconic APEX papers, the starting potential in HCN is again Debye potential [42], which could be invalid for very large plasma coupling parameters.

The APEX results very well reproduce the MC simulations, considered by the APEX authors as more time consuming than APEX. However, recently MC programs were substantially improved and could compete with APEX speed of computations [37–39]. As shown in APEX publications,

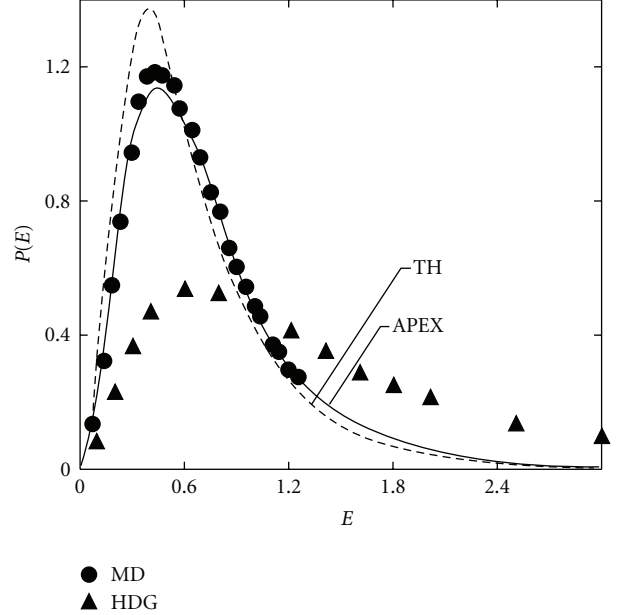


FIGURE 5: Microfield distribution function $P(E)$ in charged point $Z_0 = 9$ in mixture of field ions with charges $Z_1 = 9$ and $Z_2 = 1$, with equal partial concentrations, ($T_e = 0.21$) according to [42]: MC designates Monte-Carlo results, TH are results from [34], HDG are the results of [72, 73] (designations $E \equiv \beta$, $W(\beta) \equiv P(E)$ are the same as in the original paper [42]).

the value of fitting parameter α^{-1} can exceed unity several times [68, 69]. In Figure 5, the example of APEX distribution in the mixture of field ions with equal concentrations and its comparison with the results of other authors is presented [43]. It is seen that the APEX better reproduces MC calculations than it could be done in the frames of TH [34] or HDG [72, 73] approaches, which were not designed to describe strongly coupled plasmas. In Figure 6, the calculated in APEX [68, 69] variation of the reduced fitting parameter α in the reciprocal Debye length units k_{DH} for the hydrogen-like Ar ions at temperature $T_e = 800$ eV is shown versus density. These results demonstrate that the effective APEX potential has all the time the radius of shielding (2 ÷ 4) times less the Debye radius in the interval of density variation of 4 orders of magnitude. So, the effective interaction is more short-ranged in comparison with Debye potential.

The recently improved APEX version [43] can address to nonequilibrium plasma parameter-non-equality of ion T_i and electron T_e temperatures. The example in Figure 7 shows the case when the ion temperature by an order of magnitude less than the electron one could lead to two times difference of the quasistatic Stark line profile halfwidth [43]. The improved APEX scheme allows to consider the degeneracy of electronic component [43]. Although the significance of the degeneracy effects evidently signalize about an uprise of the quantum effects, it has almost no consequences on the derivation of the practically classical microfield distribution function beside changing the screening length of the interaction potential [43]. However, the APEX microfield distribution function itself could be

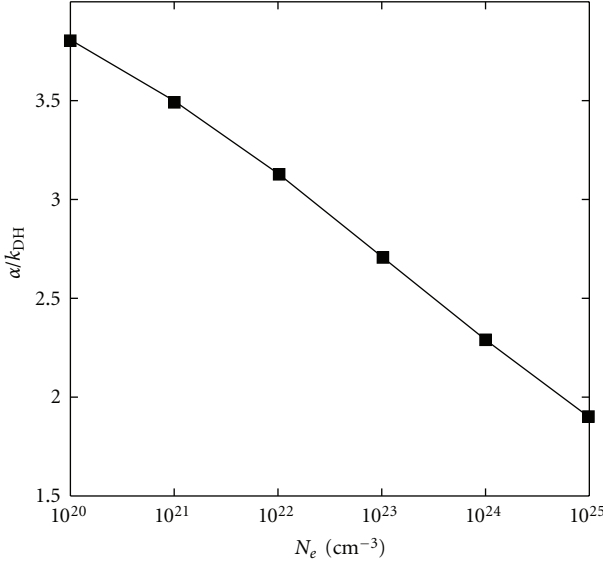


FIGURE 6: APEX α parameter in units of reciprocal Debye length of shielding k_{DH} versus density for hydrogen-like Ar ions at temperature 800 eV according to [68, 69].

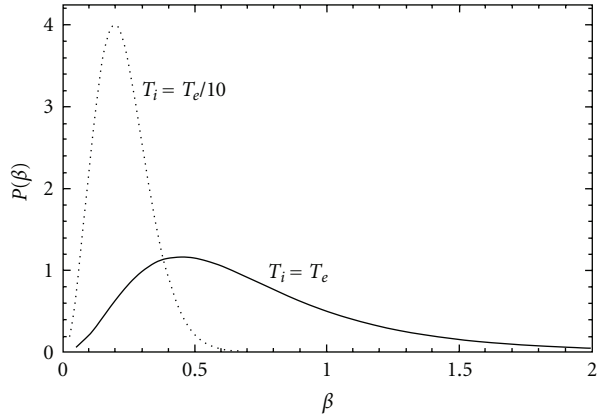


FIGURE 7: The comparison of APEX microfield distributions $P(\beta)$ for $Z_0 = Z_s = 12$, $N_e = 5 \cdot 10^{23}$ cm\$^{-3}\$ at Ar\$^{+17}\$ ion charged point for $T_e = 100$ eV and two values of ion temperature $T_i = T_e$ and $T_i = T_e/10$ from [43] (the reduced field is given in the electron units).

changed quite considerably, which is well illustrated in [43, Figure 8]. It is worthy to discuss the $W(\beta)$ behavior at large Γ_i . In this limit, the pairwise Radial Distribution Function should acquire additional maxima on the scales, corresponding to short-range and long-range ordering. Moreover, it should be escorted by an uprise of pronounced anisotropy. From physical point of view [45] in this case, the distribution function should be alike Gaussian, describing small deviations from equilibrium particles positions in the vicinity of crystallization $\Gamma_i \sim 150$, which was really observed in modeling of strongly coupled plasmas. Hence, the asymptotic of distribution function could not be the nearest neighbor NN distribution [21, 39]. Although it is stated in APEX that at $\Gamma \rightarrow \infty$ the APEX is approaching Gaussian, this transition was not followed in detail, whereas

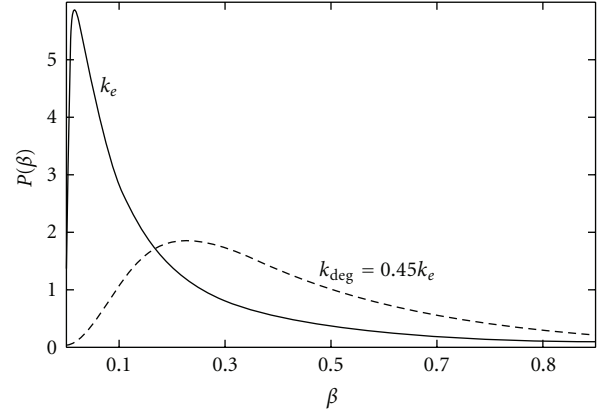


FIGURE 8: Microfield distribution functions $P(\beta)$ in charged point $Z_0 = Z_1 = 1$ with (dashed line) and without (solid line) account of electron degeneracy effects according to APEX [43] ($N_e = 10^{24}$ m\$^{-3}\$, $T_e = 5$ eV, $k_e \equiv r_{de}^{-1}$, k_{deg} is the reciprocal shielding length of electrons with account of degeneracy).

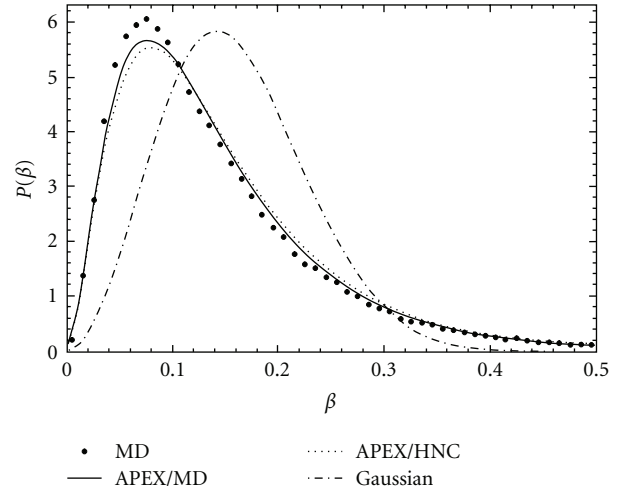


FIGURE 9: Microfield distributions for $Z_0 = Z_s = 25$, $N_e = 10^{24}$ cm\$^{-3}\$, $T_e = 50$ eV, giving $\Gamma = 50$ from [43]; dashed line: APEX with HCN RDF; solid line: APEX with MD RDF; • : MD; dot-dash line: Gaussian approximation.

it is doubtful how so qualitatively different asymptotic laws would replace each other. The available results do not allow to clear this question yet.

In Figure 9 from [43], the microfield distributions for $Z_0 = Z_s = 25$, $N_e = 10^{24}$ cm\$^{-3}\$, $T_e = 50$ eV, giving $\Gamma = 50$ from [43] are presented, where it is seen that at these conditions the APEX is approaching already Gaussian in some regions of β variation. However, APEX asymptotic at $\Gamma = 50$ is still more alike nearest neighbor (NN) [43]. Also, one can see the comparison of APEX distributions constructed with HCN and MD Radial Distribution Functions (RDFs) [43]. The current methods of simulations *ab initio*, the molecular dynamics (MD) [68, 69, 96, 101–109, 135–139] and MC [35–39], provide rather large noise with increasing of reduced microfield values, as was illustrated recently in [43].

For description of microfield distributions in neutral point, the APEX approach was reformulated [44]. In this case, the relations (24)–(26) do not take place. For the case of neutral point, it is suggested to determine α from the condition of equality of the second order derivative over Fourier-variable k to zero at $k = 0$ of any term beside the first one of specially renormalized cluster expansion [44]. If to return to the charged point, then it was stated that the new relation could be reduced to the form introduced for the charged point [44].

The APEX model was recently interestingly combined in works of Nersisyan et al. [184–186] for the classical two component plasmas (TCP) with the “potential-of-mean-force” (PMF) approximation very similar to the earlier work of Yan and Ichimaru [187]. Here the basic APEX ingredients like the expressions for the elementary electric fields are changed and modeled by the Coulomb fields modified in the case of attractive interactions by diffraction corrections [184–186]. The fitting parameter “ α ” is not introduced at all since the second moment relation is satisfied exactly [184–186]. The new model called PMFEX [184–186] preserves the APEX way for generating the correlation functions-HCN approximation and demonstrates rather good coincidence with MD simulations and admirable stability in providing data in the region of large reduced microfield values. Astonishingly, PMFEX has more natural generalization to obtain microfield distribution functions (MDF) in neutral point than APEX itself.

At last, the APEX procedure was generalized to extend it for modeling liquid domain in [189], where additional parameter of scaling is introduced

$$\kappa = \frac{r_{ws}}{\lambda_e}, \quad (27)$$

where r_{ws} is the Wigner-Seitz radius, λ_e is the electron screening length. In this work, the set of analytical formulas are proposed for acceleration of computations depending beside reduced field β on κ and the coupling plasma ion parameter Γ_i , defined as

$$\Gamma_i = \frac{(Z^* \cdot e)^2}{k_B \cdot T \cdot r_{ws}}, \quad (28)$$

alike it was done in [39], where obtained by Dr. Dominique Gilles, data in MC simulations were fitted by multi-parametric approximate expressions. In [189] and the aforementioned expression, the thermodynamic equilibrium is assumed $T = T_i = T_e$, Z^* is the residual ion charge. However, to our opinion, an extension of microfield ideas on liquids with Yukawa type of interaction potential between particles is complicated and disputable subject.

In conclusion of this section, it should be resumed that in spite of evident success of APEX applications, the APEX itself is essentially *ad hoc* semiempirical method, whose reproduction is almost impossible without the help of its authors. At the same time the new APEX modifications evidently expand the range of successful implementation of these ideas.

2.7. Density Functional Theory. The most close to conventional thermodynamic notions method of construction of plasma microfield distribution functions was proposed in the work of Dharma-Wardana and Perrot [46, 47]. This method is based on generalization of local density functional theory of Kohn and Sham (LDFT) [116, 117] to finite temperatures. The outstanding research of these coauthors, who performed a row of fundamental studies, made possible the regular application of LDFT methods in plasmas (see, e.g., [118–123]).

The physical idea of this approach is the implementation of the self-consistent description of dense plasmas, which can reflect the influence of its properties on the quantum characteristics of free electrons with the arbitrary extent of degeneracy and partially ionized core of field ions and actually the states of emitter, determined simultaneously and self-consistently with correlation functions.

The request for self-consistency to some extent corresponds to the solution of kinetic problem, giving the answer on a question what partial concentration, temperature, and effective charge would have that or another plasma component at given temperature and density of free plasma electrons. Namely, relying on this initial information, the distribution functions are constructed in the other nonself-consistent approaches. It is evident that self-consistent approach would be by far more complicated due to necessity to find simultaneously with a distribution function the distribution of electron density, effective charges of ions cores, and various correlation functions.

The range of plasma parameters on which such a description is pretended corresponds to large values of electron plasma-coupling parameter $\Gamma_e \gg 1$ and strong ion-electron correlation due to influence of bounded electron states of emitter and field ions, but at the same time to values of ion plasma coupling parameter mainly less than unity $\Gamma_i < 1$.

The proper *variational* methods of local density functional is finding self-consistent distribution of electron density with simultaneous solution of the Schrödinger equation for determining the wave functions and energy levels in potential, which in its turn is a functional of the electron density distribution [46, 116, 117].

The computational realization of approach is accomplished in the so-called correlation sphere of finite radius. This recalls the principles of mean ion plasma model (MIP), assuming finite size of ion sphere, in which the quasineutrality condition is fulfilled. It is common to refer on this procedure as on solution of DFT-Schrödinger equation [116].

In [46], this distribution of electron density is used further on in solution of Ornstein-Zernike equation in HCN approximation [7–12] for calculations of ion-ion correlation functions $g_{ii}(r)$.

These functions are substituted then in two terms cluster expansion of Baranger-Mozer type [24, 25] for calculations of the logarithm of characteristic function with some amending modifications, connected with possibilities of partial summation of chain terms of higher orders in the so-called “weighted-chain-sum” (WCS) approximation [46].

This amendment functionally is expressed in appearance of majorizing factor for the second-order density term in the Baranger-Mozer expression for the characteristic function logarithm [46].

The principal moments of this approach [46] are (i) the choice of Baranger-Mozer scheme of cluster expansion, that allows generalization on quantum case in distinction from, for example, limited by classical approximation Hooper model; (ii) the criticism of a choice of the Yukawa type potentials for describing pairwise interactions in plasma; (iii) the determination of $g_{ii}(r)$ with the help of special self-consistent procedure within HCN approximation; (iv) the way of calculation of the electric field value at the origin of reference frame due to field ion with the effective charge Z_B according to the exact result of pseudopotential theory of the second order:

$$E(r) = \frac{Z_B}{r^2} + \frac{1}{r^2} \int_0^r \bar{n} [g_{ei}(x) - 1] 4\pi x^2 dx. \quad (29)$$

The expression for $E(r)$ is convenient to represent in the form

$$\begin{aligned} E(r) &= Z_B \frac{\bar{q}(r)}{r^2}, \\ \bar{q}(r) &= 1 - \frac{1}{Z_B} \int_0^r dx 4\pi x^2 \Delta n(x), \\ \Delta n(x) &= \bar{n} [g_{ei}(x) - 1]. \end{aligned} \quad (30)$$

The last equation determines the total nonlinear excess of electron density around ion "B," including exchange and correlations effects, which is found from the solution of DFT-Schrödinger equation in [46, 116, 117]. This pileup of electron density around ion is defined with respect to the level of uniform neutralizing background of free plasma electrons.

It should be noted that ionization equilibrium in DFT [46, 47, 116, 117] does not obey Saha equation because the correct condition of thermodynamic equilibrium is the free energy minimization. To the same resume, Hammer and Michalas arrived at one year later during analysis of the microfields influence on the equation of state [154–156].

At the same time, one drawback of this approach could be hidden here. Indeed, the emitter or field ion of "finite" size is inserted in the uniform electron background, but the plasma effects like lowering of ionization potential and kinetics of establishing of equilibrium with continuous spectra are not included in the description of levels population and realization of the bound electron states of the upper levels, as tried to formulate Hammer and Michalas [154–156].

As could be judged by original formulation [46, 47, 116, 117], it seems that DFT capability to describe nonequilibrium plasma conditions with complex chemical and ionization composition and different temperatures of electron and ion subsystems appears to be doubtful.

In the equation for electric field, the shielding of only one ion (field ion or emitter) is included. Due to the authors statement [46], the accounting for analogous terms for the second ion is beyond the accuracy of the used second-order pseudopotential theory.

It is important to underline that the electric field defined by the aforementioned equations in the quantum case could not be equalled as in the classical limit to the gradient (with opposite sign) of pairwise potential of ion-ion interaction. This is because in these conditions, this gradient will include nonelectrostatic terms connected with exchange and other purely quantum effects. Thereupon in [46] it is demonstrated that the usage of the effective pairwise potential of Yukawa type provides inadequate results.

The discussed approach operates with the following quantities: the effective charge of field ions \bar{Z} and their mean density $\bar{\rho}$, and the mean density of free electrons \bar{n} , associated with quasineutrality condition:

$$\bar{n} = \bar{Z} \bar{\rho}, \quad \frac{4}{3} \pi r_s^3 \bar{n} = 1, \quad (31)$$

where r_s has the sense of the electron sphere radius. The reduced and normal fields are determined by expressions

$$\begin{aligned} \bar{E} &= \frac{E}{E_0}, \\ E_0 &= \frac{Z}{r_0^2}, \\ \frac{4}{15} (2\pi)^{3/2} r_0^3 \bar{n} &= 1, \\ r_0 &= 0.9991178 r_s, \end{aligned} \quad (32)$$

where Z represents itself the charge of field ions. (This choice of the normal field, although admissible in principle, could be misleading. More adequate to our opinion would be $E_{0i} = \bar{Z}/r_{0i}^2$, $(4/15)(2\pi)^{3/2} r_{0i}^3 \bar{\rho} = 1$.) The distribution functions depend on parameter

$$\begin{aligned} a &\equiv r_{mf} = \frac{r_0}{r_{De}} = 0.99912 (3\Gamma_e)^{1/2}, \\ \Gamma_e &= \frac{e^2}{Tr_s} \equiv \frac{r_c}{r_s}, \end{aligned} \quad (33)$$

where the electron Debye radius r_{De} is determined also on the basis of the mean free electrons density \bar{n} , the electron plasma coupling parameter Γ_e is defined in the same way as Hooper did, and r_c is the Coulomb radius.

The classical ion plasma coupling parameter is determined from the expression

$$\Gamma = \frac{Z^2 r_c}{r_{WS}}, \quad r_{WS} = \left(\frac{3}{4\pi\bar{\rho}} \right)^{1/3}, \quad (34)$$

where r_{WS} is the radius of Wigner-Seitz cell. In this model, Z and \bar{Z} are related to each other by

$$\bar{Z} = Z - \bar{n}_b, \quad (35)$$

where \bar{n}_b is the number of bounded electrons per ion, calculated on the basis of DFT approach.

The DFT microfield distribution functions in distinction from the distribution functions in classical plasmas

depending not only on the parameter a but also on the parameter $\tilde{T} = T/T_F$ at least, where T_F is the electron Fermi temperature, defined by the equation

$$kT_F = E_F = \frac{1}{2} (3\pi^2 \bar{n})^{2/3}, \quad \text{a.u.} \quad (36)$$

Moreover, according to authors [46, 47] opinion, the extent of plasma coupling in quantum case is characterized more correctly by parameter $\bar{\Gamma}$, which is determined by the basis of notion about the mean ion radius \bar{R} assigned to each ion, so that the mean number of free electrons per ion \bar{n}_f^i is equal to

$$\bar{n}_f^i = \frac{4}{3}\pi\bar{R}^3\bar{n}_f, \quad (37)$$

where \bar{n}_f ($= \bar{n}$) is the density of plasma free electrons. On the other hand,

$$\begin{aligned} Z &= \bar{n}_b + \bar{n}_f^i, \\ \bar{n}_b &= 2 \int_0^{\bar{R}} 4\pi r^2 n_b(r) f_s(r) dr, \\ \bar{\Gamma} &= \frac{\bar{Z}^2 r_c}{\bar{R}}, \end{aligned} \quad (38)$$

where $\bar{\Gamma}$ could be considered as the effective ionic plasma coupling parameter, corresponding to “equivalent” classical plasma, $f_s(r)$ is the Fermi factor, describing the character of electron states filling and depending on temperature and chemical potential. Thereby, the value \bar{Z} or \bar{n}_b are also the results of self-consistent solution of DFT-Schrödinger equations.

In the first article [46] of the authors of this approach, devoted to constructing microfield distribution functions, the Kirkwood approximation [7–12] was applied for disentanglement of the three particle correlations. This procedure was supplemented by separation of the central and noncentral parts of interactions in [47] on the basis of methods, elaborated in papers for description of quantum Hall effect. In particular, this improvement was connected with the APEX authors criticism of the DFT results for strongly coupled plasmas, where noticeable discrepancy was observed between the predictions of APEX and the first version of DFT-approach [46].

To illustrate this, the results of DFT-approach in comparison with APEX [40, 41] for Al plasma are presented in Figure 10 according to [46]. It is necessary to note that data of [40, 41] correspond to the so-called the high-frequency component of microfield, which describes the distribution of Coulomb electric fields of particles with the charge Z_e [40] or with arbitrary composition of ions of different species [41], inserted in the uniform neutralizing electron background. However, the authors of [46] did not point out for which values of Z or \bar{Z} they took the data from [40, 41]. However, curiously enough, the most open for criticism moment of this approach is its complete self-consistency, which leads to the loss of possibility of the conventional identification of observed spectral transitions. In other words, in this

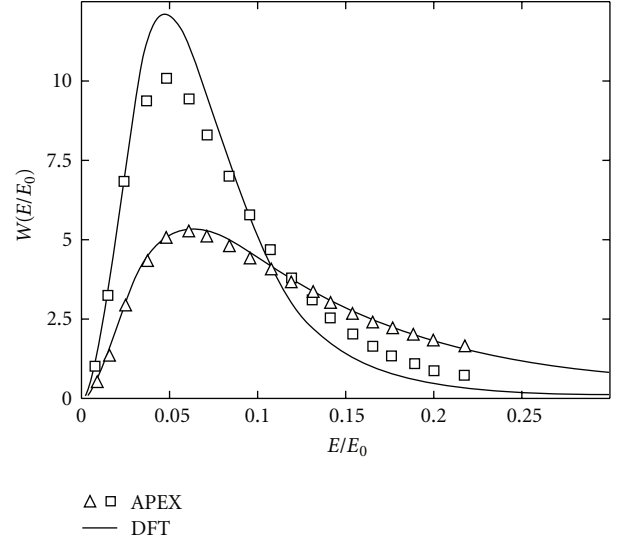


FIGURE 10: DFT-function of microfield distribution $W(E/E_0)$ in neutral (Δ -triangles, lower curves) and charged points (\square squares, upper curves) $Z = 0$ and $Z = 1$ in Al plasma in comparison with APEX results without account of electron degeneracy effects [40, 41] from [46] ($\bar{\Gamma} = 3.47$, $\Gamma = 3.31$, $\tilde{T} \equiv T/T_F = 7.624$, $\bar{Z}_{Al} = 5.178$, $r_s = 3a_0$, $r_{mf} = a = 0.8$, T_F is the electron Fermi temperature see (36)).

DFT version, the self-consistent wave functions and the energy structure of emitters in plasma do not remember the corresponding characteristics of free emitters, which, generally speaking, are tools for decoding of observations.

Probably the cause of that is the insufficient accuracy in the description of the bounded excited states within DFT [46, 47]. The DFT version under discussion, however, could be successfully applied for calculations of the thermodynamic characteristics, when the affixment of results to observed properties of radiation in spectral lines is not important.

Moreover, it is not quite clear how to track the time scales of microfield variations in this approach, and the character of averages, applied in its derivation, more corresponds to purely thermodynamic notions. That is why the doubt arises in possibility to construct with the help of this approach *instantaneous* ion microfield distribution functions. Partially, it is connected with the very orientation of this method on description of quantum effects in the microfield distributions and necessity of possible reexamination of the “instantaneous distribution functions” notion in this case. However, this criticism concerns equally and Monte-Carlo method, and so forth.

In comparison with the other theoretical approaches to the microfield distribution functions construction, touched here, this method is perhaps the most laborious and complicated for realization, as the procedure of finding solution is very complicated and cumbersome, and requires preliminary complex calculations of additional auxiliary functions.

Beside, this method essentially does not give universal results for actually the microfield distribution functions, as the distribution from the very beginning depends on the

specific quantum properties of field ions and the emitter. At the same time, the doubt arises on how adequate and ample the developed notions about the character and the speed of establishing equilibrium between the emitter (test particle) and plasmas. Apparently DFT approach, of course, could not pretend on all completeness of plasma kinetic description, which is necessary for determination of plasma parameters. The latter are necessary as initial (input) data for the calculations of microfield distribution functions. Thus, the self-consistency of DFT approach in certain sense is limited.

Up to now, the DFT calculations of microfield distribution functions are performed only for several concrete cases and did not get wide-spread implementation. It is also unknown if there are any accessible for applied usage DFT codes for calculation of microfield distribution functions that are similar, for example, to APEX, although during the past years after the paper [47], the DFT approach as a method for description of atomic properties was considerably improved [120–123].

At the same time, no essential progress was achieved in the extent of adequateness of description with the help of DFT the excited atomic states, and consequently the radiative processes with their participation [122]. However, the DFT application to calculations of atomic, molecular, and chemical properties are all over considered currently as quite effective from point of view of universality, simplicity, and also due to the high speed of performing corresponding calculations on contemporary computers [123].

However, in spite of pointed out drawbacks the studies, performed within DFT approach, provided very interesting and instructive physical results, which without any doubt are very valuable for the further development in this field.

2.8. Plasma Collective Oscillations.

2.8.1. Microfield Separation on “Individual” and “Collective” Components. As it is evident, the “individual” and “collective” components of microfield are consequences of the same Hamiltonian of plasma charged particles [48]. Thus, many papers, dealing with the problem of microfield distributions of plasma collective oscillations, followed Bohm and Pines [30, 31], attempting to split the system of Coulomb particles with the help of canonical transformations of variables into the two weakly interacting subsystems, which could be considered independently [17, Section 2], [48, 49]. In addition, plasma could usually be considered as uniform and isotropic.

Then, the total distribution function $W(\vec{F})$ of summary microfield \vec{F} under the condition that its components are additive, and the characteristic time scales of their variation are of the same order could be expressed as a convolution [48–50]:

$$W(\vec{F}) = \int d\vec{F}_c d\vec{F}_i W_c(\vec{F} - \vec{F}_i) W_i(\vec{F}_i), \quad (39)$$

where $W_c(\vec{F})$, $W_i(\vec{F})$ are distribution functions of the collective \vec{F}_c and individual \vec{F}_i microfield components correspondingly. The microfield distribution function of individual

component more or less approaches the Baranger-Mozer-type function, whereas the distribution function of collective component is practically Gaussian [48].

However, the final result of such approach happens to depend on the choice of phenomenological parameter, which controls the separation of subsystems, while the satisfactory methods for its exact determination was not ever found [30, 31, 48, 49].

The determination of this parameter invoked certain difficulties already in Bohm and Pines [30, 31] papers. Firstly, it is rather not a parameter but a function in the space of oscillations wave vectors \vec{k} , and secondly the possibility of such separation is valid only in a quite narrow range of plasma parameters [30, 31]. Thereby, this procedure of collective variables extraction is not regular and universal.

In spite of that, it was declared in two publications (see [17, Section 2]), [49] about the realization of such separation after two canonical transformations although no explicit and proving demonstration of this statement was provided. These difficulties, of course, are due to strong interaction between subsystems, when, for example, the usage of the formal technique like the Zwanzig method of projection operators could not be rigorously justified, while the corresponding subsystems of quasiparticles, “dressed by interaction with each other”, could not be managed reasonably in order to separate them by transformations of initial Hamiltonian (see, e.g., [14, 79, 96]).

Basing on sound sense, the separation on “collective” and “individual” subsystems should be possible when the resonance interaction of plasma waves with plasma particles is not essential [6, 50, 82].

So, for these specially stipulated conditions in fact *without proof*, it was conventionally accepted to consider that the two practically independent and noninteracting subsystems of plasma waves and quasiparticles exist, for which it is possible to introduce independent distributions of microfields.

Per se it means the construction of distribution function of collective oscillations on the basis of independent models. Evidently, this question has sense only if the conditions of quasistatics or large modulation depth are fulfilled:

$$\frac{dE_0}{\hbar} \gg \omega_c, \quad (40)$$

where d is the dipole moment of the emitter (test particle), E_0 , ω_c are the amplitude and characteristic frequency of collective plasma electric microfield component.

2.8.2. Rayleigh Distribution. In the assumption of isotropy, multimode property, additivity and randomness of phases of collective oscillations, the distribution of collective microfields is described by Rayleigh function [50]:

$$W_c(\vec{F}) = 3\left(\frac{6}{\pi}\right)^{1/2} \frac{F^2}{\langle F^2 \rangle^{3/2}} \exp\left[-\frac{3F^2}{2\langle F^2 \rangle}\right], \quad (41)$$

$$\langle F^2 \rangle = \int_0^\infty dF F^2 W_c(F).$$

This function is known also under the name of “distribution of random vector,” and by definition, it corresponds to nonpolarized summary field of oscillations.

In one-dimensional case, this distribution has the form

$$W_c(F) = \left(\frac{2}{\pi}\right)^{1/2} \frac{1}{\langle F^2 \rangle^{1/2}} \exp\left[-\frac{F^2}{2\langle F^2 \rangle}\right], \quad (42)$$

and then the electric field of oscillations has definite polarization.

2.8.3. Regular Oscillations. For linearly polarized, one mode, and sinusoidal field, it is possible to introduce instantaneous distribution function [51, 52] in the so-called dynamic case, when the atomic state dipole precession frequency in the electric field is much larger than the frequency of oscillations Ω and the reciprocal life time of atomic state τ_{eff}^{-1} :

$$\frac{dE_0}{\hbar} \gg \Omega \gg \tau_{\text{eff}}^{-1}. \quad (43)$$

This distribution function has the form [48–50]

$$W_c(F) = \frac{1}{\pi} \frac{1}{\sqrt{E_0^2 - F^2}}, \quad (44)$$

where E_0 is the amplitude of sinusoidal oscillations.

2.9. Joint Distributions. In many problems, the information about distribution of the electrical field strength vector only is insufficient, and it is necessary to consider much more complex joint distribution functions of several scalar, vector, or tensor random variables at once [19–21, 53–70, 74–81]. These variables could have some limitations on the intervals of their variation, as, for example, it happens in APEX. Seemingly, the first works, where the joint distributions in ideal gas of Coulomb (gravitating) particles were considered in application to problems of stellar dynamics, belong to Chandrasekhar and von Neuman [19–21].

2.9.1. Distribution of Microfield and Its Space Derivatives. Let us consider the low-frequency ion joint distribution function $W(\vec{F}; \{\partial F_\alpha / \partial x_\beta\})$ of the ion electric microfield vector \vec{F} and its spacial derivatives $\partial F_i / \partial x_k$, forming the symmetric second rank tensor, following [53–62] (compare [63, 64]). The “Spur” of this tensor is not equal to zero for the shielded ions, but is nullified in the case of Coulomb field. The values of arguments are sums of corresponding values of separate field ions, that is, the additivity condition is fulfilled:

$$\vec{F} = \sum_j \vec{F}_j, \quad \frac{\partial F_\alpha}{\partial x_\beta} = \sum_j \frac{\partial (\vec{F}_j)_\alpha}{\partial x_\beta}. \quad (45)$$

In general form, it is rather complex function in 9-dimensional space of variables: the 3 components of electric field vector and the 6 independent components of symmetric tensor of the second rank.

For arbitrary plasma ionization composition, the quasineutrality condition could be expressed as

$$N = N_e = \sum_s Z_s N_s, \quad (46)$$

where Z_s, N_s are the charge and partial concentration of field ions of s species correspondingly.

The general expression for the joint distribution function then could be presented in the form

$$\begin{aligned} W\left(\vec{F}; \left\{ \frac{\partial F_\alpha}{\partial x_\beta} \right\} \right) = & \frac{1}{(2\pi)^9} \int d^3 \vec{\rho} \prod_{m=1}^6 \int_{-\infty}^{+\infty} d\sigma_m \\ & \cdot \exp\left[-i\vec{p}\vec{F} - i \sum_{m=1}^6 \sigma_m \left(\frac{\partial F_\alpha}{\partial x_\beta} \right)_m\right] \\ & \cdot A(\vec{\rho}; \{\sigma_m\}). \end{aligned} \quad (47)$$

For the distribution characteristic function $A(\vec{k})$, the following general exponential representation is valid:

$$A(\vec{\rho}; \{\sigma_m\}) = \exp[-N \cdot C(\vec{\rho}; \{\sigma_m\})]. \quad (48)$$

Using the generalization of Baranger-Mozer cluster expansion [53–58] (compare [63, 64]) on the case of arbitrary plasma composition, the index of exponent of characteristic function could be presented with the accuracy of up to the second-order terms over density in the following recording:

$$\begin{aligned} C(\vec{\rho}; \{\sigma_m\}) = & C^{(o)}(\vec{\rho}; \{\sigma_m\}) - \frac{N}{2!} \cdot C^{(1)}(\vec{\rho}; \{\sigma_m\}), \\ C^{(o)}(\vec{\rho}; \{\sigma_m\}) = & \sum_s C_s \int d^3 \vec{r} \cdot g_{sr}(\vec{r}) \cdot \varphi_s(\vec{\rho}; \vec{r}; \{\sigma_m\}), \\ C^{(1)}(\vec{\rho}; \{\sigma_m\}) = & \sum_{s,s'} C_s C_{s'} \int d^3 \vec{r}_1 \int d^3 \vec{r}_2 \cdot \varphi_s(\vec{\rho}; \vec{r}_1; \{\sigma_m\}) \\ & \cdot \varphi_{s'}(\vec{\rho}; \vec{r}_2; \{\sigma_m\}) \\ & \cdot [g_{ss'}(\vec{r}_1; \vec{r}_2) - g_{sr}(\vec{r}_1) \cdot g_{s'r}(\vec{r}_2)], \\ \varphi_s(\vec{\rho}; \vec{r}; \{\sigma_m\}) = & 1 - \exp[i\Phi_s(\vec{\rho}; \vec{r}; \{\sigma_m\})], \\ \Phi_s(\vec{\rho}; \vec{r}; \{\sigma_m\}) = & \vec{\rho} \vec{E}_s(\vec{r}) + \sum_{m=1}^6 \sigma_m \left(\frac{\partial (\vec{E}_s)_\alpha}{\partial r_\beta} \right)_m. \end{aligned} \quad (49)$$

Here, $C_s \equiv N_s/N$, $g_{sr}(\vec{r})$ is the pair correlation function of field ion from s species with charge Z_s and the test ion with charge Z_0 , immersed in the origin of reference frame, $g_{ss'}(\vec{r}_1; \vec{r}_2)$ is the pair correlation function of field ions between each other with charges Z_s and $Z_{s'}$ in the field of the test ion with charge Z_0 , $\vec{E}_s(\vec{r})$ is the elementary electric field, produced by any field ion (quasiparticle) of “ s ” species in the origin of the reference frame.

This field is determined by the effective interaction potential for such species in plasmas and could be described by the following equations:

$$\begin{aligned}\vec{E}_s(\vec{r}) &= -eZ_s \frac{\vec{r}}{r^3} \cdot [1 - \kappa_s(r)], \\ \operatorname{div} \vec{E}_s(\vec{r}) &= \frac{eZ_s}{r^2} \cdot \frac{\partial \kappa_s(r)}{\partial r} - 4\pi e Z_s \delta(\vec{r}), \\ \oint_{V \rightarrow \infty} d^3 \vec{r} \cdot \operatorname{div} \vec{E}_s(\vec{r}) &= 0.\end{aligned}\quad (50)$$

The latter equations are followed from the properties of screening function $\kappa_s(r)$, connected with its definition: $\kappa_s(0) = 0$, $\kappa_s(\infty) = 1$, so that the excess charge of free electrons around the ion Z_s is determined by the expression

$$\delta n_e^{(s)}(r) = \frac{1}{4\pi} \frac{Z_s}{r^2} \cdot \frac{\partial \kappa_s(r)}{\partial r}. \quad (51)$$

Then the nonuniformity tensor components of elementary electric field are determined from

$$\begin{aligned}G_{ki}^{(s)}(\vec{r}) &\equiv \frac{\partial (\vec{E}_s)_k}{\partial x_i} = \frac{eZ_s}{r^5} \cdot [3x_i x_k - \delta_{ik} r^2] \\ &\cdot \left[1 - \kappa_s(r) + \frac{r}{3} \frac{\partial \kappa_s(r)}{\partial r} \right] \\ &+ \frac{\delta_{ik}}{3} \frac{eZ_s}{r^2} \frac{\partial \kappa_s(r)}{\partial r}.\end{aligned}\quad (52)$$

Hence, it follows that the screening function $\kappa_s(r) \geq 0$ could be found, for example, on the basis of the recent DFT approach receipts [46, 47], and $G_{ki}^{(s)}(\vec{r}) \equiv G_{ik}^{(s)}(\vec{r})$. In assumption that the field ions are bare nuclei here, the equations that determine the bound electrons distributions are not considered. It is assumed that quantum effects [14–17, 46, 47, 71] are not essential in microfield distribution.

The joint distribution obtained earlier provides the instantaneous distribution function of the low-frequency individual ion component of plasma microfield and its spacial derivatives, which per se are defined on time scales τ of the order $\omega_{pe}^{-1} \ll \tau \ll (v_i N_i^{1/3})^{-1}$, where ω_{pe} is the plasma electron frequency, v_i is the relative thermal ion velocity with respect to the test particle, and N_i is the total ion density.

The basic ideas of this derivation were proposed by Baranger and Mozer and did not undergo any essential changes since that time, in spite of certain differences in posterior papers [27–29, 34–81, 96, 97], as they are inherent in microfield formalism.

It is important to underline that plasma polarization effects [46, 47, 53–62] (or in other words appearance of nonuniformity in distribution of plasma electron density) are included in general form in this consideration from the very beginning via screening function and its derivatives. The integration over \vec{F} or over $\partial F_i / \partial x_k$ components leads to separate distributions of microfield or its tensor of nonuniformity, and after implementation of appropriate approximations recovers known earlier results.

One of the most interesting properties of the joint distributions follows from the analysis of its moments $\langle \partial F_i / \partial x_k \rangle_{\vec{F}}$ for a given value of \vec{F} that represent itself the averages of $\partial F_i / \partial x_k$ over the joint distributions for the fixed vector value of \vec{F} :

$$\begin{aligned}W(\vec{F}) \left\langle \frac{\partial F_i}{\partial x_k} \right\rangle_{\vec{F}} &= \frac{N}{(2\pi)^3} \int d^3 \vec{\rho} \cdot \exp[-i\vec{\rho} \cdot \vec{F}] \\ &\cdot A(\vec{\rho}) \cdot \langle G_{ik}(\vec{\rho}) \rangle, \\ \langle G_{ik}(\vec{\rho}) \rangle &= \langle G_{ik}^{(o)}(\vec{\rho}) \rangle + \langle G_{ik}^{(1)}(\vec{\rho}) \rangle, \\ \langle G_{ik}^{(o)}(\vec{\rho}) \rangle &= \sum_s C_s \langle G_{ik}^{(s)}(\vec{\rho}) \rangle, \\ \langle G_{ik}^{(1)}(\vec{\rho}) \rangle &= -\frac{N}{2} \sum_{s,s'} C_s C_{s'} \langle G_{ik}^{(ss')}(\vec{\rho}) \rangle, \\ \langle G_{ik}^{(s)}(\vec{\rho}) \rangle &= \int d^3 \vec{r} \cdot g_{sr}(\vec{r}) \cdot \exp[i\Phi_s(\vec{\rho}; \vec{r})] \\ &\cdot G_{ik}^{(s)}(\vec{r}), \\ \langle G_{ik}^{(ss')}(\vec{\rho}) \rangle &= \int d^3 \vec{r}_1 \int d^3 \vec{r}_2 \\ &\cdot [g_{ss'}(\vec{r}_1; \vec{r}_2) - g_{sr}(\vec{r}_1) \cdot g_{s'r}(\vec{r}_2)] \\ &\cdot \left\{ G_{ik}^{(s)}(\vec{r}_1) \cdot \exp[i\Phi_s(\vec{\rho}; \vec{r}_1)] \right. \\ &\cdot (1 - \exp[i\Phi_{s'}(\vec{\rho}; \vec{r}_2)]) + G_{ik}^{(s')}(\vec{r}_2) \\ &\cdot \exp[i\Phi_{s'}(\vec{\rho}; \vec{r}_2)] \\ &\left. \cdot (1 - \exp[i\Phi_s(\vec{\rho}; \vec{r}_1)]) \right\}.\end{aligned}\quad (53)$$

It was found that the expressions for the first moments of the nonuniformity tensor could be presented via microfield distribution functions in general form [52–55, 59]

$$\begin{aligned}W(\vec{F}) \left\langle \frac{\partial F_i}{\partial x_k} \right\rangle_{\vec{F}} &= N \left[\sum_s C_s \int d^3 \vec{r} \cdot g_{sr}(\vec{r}) \cdot G_{ik}^{(s)}(\vec{r}) \right. \\ &\cdot W(\vec{F} - \vec{E}_s(\vec{r})) - \frac{N}{2} \sum_{ss'} C_s C_{s'} \int d^3 \vec{r}_1 \int d^3 \vec{r}_2 \\ &\cdot [g_{ss'}(\vec{r}_1; \vec{r}_2) - g_{sr}(\vec{r}_1) \cdot g_{s'r}(\vec{r}_2)] \\ &\cdot \left\{ G_{ik}^{(s)}(\vec{r}_1) \cdot \left[W(\vec{F} - \vec{E}_s(\vec{r}_1)) \right. \right. \\ &\left. \left. - W(\vec{F} - \vec{E}_s(\vec{r}_1) - \vec{E}_{s'}(\vec{r}_2)) \right] + G_{ik}^{(s')}(\vec{r}_2) \right. \\ &\cdot \left. \left[W(\vec{F} - \vec{E}_{s'}(\vec{r}_2)) - W(\vec{F} - \vec{E}_s(\vec{r}_1) - \vec{E}_{s'}(\vec{r}_2)) \right] \right\} \Big].\end{aligned}\quad (54)$$

To carry out expressions that could be processed in numerical calculations, it is necessary to apply additional

simplifications and approximations for correlation functions in the aforedescribed general formulas. For this it is presumed that the pair correlation function depends only on the module of particles radii-vectors difference and the Kirkwood approximation is used for disentanglement [7–10] of the three-particle correlations. This yields [55–58, 80, 81]

$$g_{sr}(\vec{r}) \equiv g_{sr}(r),$$

$$g_{ss'}(\vec{r}_1; \vec{r}_2) \simeq g_{ss'}(|\vec{r}_1 - \vec{r}_2|) \cdot g_{sr}(r_1) \cdot g_{s'r}(r_2), \quad (55)$$

$$h_{ss'}(|\vec{r}_1 - \vec{r}_2|) \equiv g_{ss'}(|\vec{r}_1 - \vec{r}_2|) - 1.$$

Then, it is possible to obtain the following general representations of correlation functions in the form of series over harmonics:

$$\begin{aligned} h_{ss'}(|\vec{r}_1 - \vec{r}_2|) &= \sum_{n=0}^{\infty} (2n+1) \cdot P_n \left(\cos \left[\widehat{\vec{r}_1 \vec{r}_2} \right] \right) \cdot h_{ss'}(n; r_1; r_2), \\ h_{ss'}(n; r_1; r_2) &= \int_0^{\infty} dk \cdot k^2 \cdot j_n(kr_1) \cdot j_n(kr_2) \cdot h_{ss'}(k), \\ h_{ss'}(k) &= \frac{1}{(2\pi)^3} \int d^3 \vec{r} \cdot \exp(i\vec{k}\vec{r}) \cdot h_{ss'}(r). \end{aligned} \quad (56)$$

Here, $P_n(z)$ are the Legendre polynomials depending on cosine of the angle between vectors \vec{r}_1 and \vec{r}_2 , where $j_n(y)$ is the spherical Bessel function.

This allows to simplify general results, mentioned earlier, and obtain, for example, the distribution function of reduced microfield values $\beta \equiv F/F_0$ (where F_0 is the value of normal microfield [18]), more general expression than those known before [24, 25] (compare [72, 73, 164]):

$$W(\vec{F}) = 4\pi F^2 \cdot W(F), \quad A(\rho) = A(\rho), \quad (57)$$

$$F_0 = \Lambda e N^{2/3}, \quad \Lambda \equiv 2\pi(4/15)^{2/3},$$

$$W(\beta) = \frac{2\beta}{\pi} \int_0^{\infty} dk \cdot k \cdot \sin k\beta \cdot A(k), \quad (58)$$

$$A(k) = \exp\{-[\Psi_0(k) + \Psi_1(k)]\},$$

$$\begin{aligned} \Psi_0(k) &= \frac{4\pi}{\Lambda^{3/2}} \sum_s C_s I_s(k), \\ \Psi_1(k) &= -\frac{8\pi^2}{\Lambda^3} \sum_{ss'} C_s C_{s'} I_{ss'}(k), \quad r_0 \equiv \left(\frac{e}{F_0} \right)^{1/2}, \end{aligned} \quad (59)$$

$$I_s(k) = \int_0^{\infty} dx \cdot x^2 \cdot g_{sr}(r_0 x) \cdot \left\{ 1 - \frac{\sin k\epsilon_s(x)}{k\epsilon_s(x)} \right\}, \quad (60)$$

$$\begin{aligned} \epsilon_s(x) &= \frac{Z_s}{x^2} [1 - \kappa_s(r_0 x)], \\ I_{ss'}(k) &= \int_0^{\infty} dx_1 \cdot x_1^2 \int_0^{x_1} dx_2 \cdot x_2^2 \cdot g_{sr}(r_0 x_1) \cdot g_{s'r}(r_0 x_2) \\ &\cdot \sum_{n=0}^{\infty} (-1)^n (2n+1) \cdot \{j_n[\epsilon_s(x_1)] - \delta_{on}\} \\ &\cdot \{j_n[\epsilon_{s'}(x_2)] - \delta_{on}\} h_{ss'}(n; r_0 x_1; r_0 x_2). \end{aligned} \quad (61)$$

Here, the function $\Psi_1(k)$ describes ion-ion correlations.

The explicit representation for distribution function allows to obtain analytical expressions for the first moments of nonuniformity tensor, describing its fundamental properties for the fixed value of the ion electric microfield vector:

$$\begin{aligned} \left\langle \frac{\partial F_X}{\partial X} \right\rangle_{\vec{F}} &= -\frac{2\pi Ne}{3} \left\{ B_D(\beta) \left[P_2(\cos \theta) - P_2^{[2]}(\cos \theta) \frac{\cos 2\phi}{2} \right] \right. \\ &\left. - 2B_{DO}(\beta) \right\}, \end{aligned} \quad (62)$$

$$\begin{aligned} \left\langle \frac{\partial F_Y}{\partial Y} \right\rangle_{\vec{F}} &= -\frac{2\pi Ne}{3} \left\{ B_D(\beta) \left[P_2(\cos \theta) + P_2^{[2]}(\cos \theta) \frac{\cos 2\phi}{2} \right] \right. \\ &\left. - 2B_{DO}(\beta) \right\}, \end{aligned} \quad (63)$$

$$\left\langle \frac{\partial F_Z}{\partial Z} \right\rangle_{\vec{F}} = \frac{4\pi Ne}{3} \{B_D(\beta) \cdot P_2(\cos \theta) + B_{DO}(\beta)\}, \quad (64)$$

$$\left\langle \frac{\partial F_Y}{\partial X} \right\rangle_{\vec{F}} = \frac{\pi Ne}{3} \cdot B_D(\beta) \cdot P_2^{[2]}(\cos \theta) \cdot \frac{\sin 2\phi}{2}, \quad (65)$$

$$\left\langle \frac{\partial F_Z}{\partial X} \right\rangle_{\vec{F}} = \frac{2\pi Ne}{3} \cdot B_D(\beta) \cdot P_2^{[1]}(\cos \theta) \cdot \cos \phi, \quad (66)$$

$$\left\langle \frac{\partial F_Z}{\partial Y} \right\rangle_{\vec{F}} = \frac{2\pi Ne}{3} \cdot B_D(\beta) \cdot P_2^{[1]}(\cos \theta) \cdot \sin \phi, \quad (67)$$

where θ and ϕ are the polar and azimuthal angles of vector \vec{F} in the laboratory Cartesian reference frame XYZ, $P_n^{[m]}(x)$ is the generalized Legendre polynomial.

The universal function $B_{DO}(\beta)$ is due to plasma polarization effects [55–59].

The universal functions $B_D(\beta)$ and $B_{DO}(\beta)$ with an account of ion-ion correlations are determined by the expressions, where the terms with upper subindex (1) are connected with ion-ion correlations:

$$\begin{aligned} B_D(\beta) &= B_D^{(o)}(\beta) + B_D^{(1)}(\beta), \\ B_{DO}(\beta) &= B_{DO}^{(o)}(\beta) + B_{DO}^{(1)}(\beta), \\ B_D^{(o)}(\beta) &= \frac{12}{\pi} \frac{\beta^2}{W(\beta)} \sum_s C_s Z_s b_s(\beta), \\ B_D^{(1)}(\beta) &= -\frac{12}{\pi} \frac{\beta^2}{W(\beta)} \sum_{ss'} C_s C_{s'} b_{ss'}(\beta), \\ B_{DO}^{(o)}(\beta) &= \frac{2}{\pi} \frac{\beta^2}{W(\beta)} \sum_s C_s Z_s b_s^{(o)}(\beta), \\ B_{DO}^{(1)}(\beta) &= -\frac{2}{\pi} \frac{\beta^2}{W(\beta)} \sum_{ss'} C_s C_{s'} b_{ss'}^{(o)}(\beta), \end{aligned} \quad (68)$$

The functions, describing the first terms of expansion and connected with quadrupolar tensor $b_s(\beta)$ and scalar $b_s^{(o)}(\beta)$ correspondingly, could be transformed to

the following form:

$$\begin{aligned} b_s(\beta) &= \int_0^\infty dk \cdot k^2 \cdot A(k) \cdot j_2(k\beta) \cdot \Phi_s(k), \\ b_s^{(o)}(\beta) &= \int_0^\infty dk \cdot k^2 \cdot A(k) \cdot j_0(k\beta) \cdot \Phi_s^{(o)}(k), \end{aligned} \quad (69)$$

where the Fourier-components of nonuniformity tensor $\Phi_s(k)$ and its trace $\Phi_s^{(o)}(k)$ of the field ion for “s” species enters the integrands:

$$\begin{aligned} \Phi_s(k) &= \int_0^\infty dx \cdot x^2 \cdot g_{sr}(r_0x) \cdot j_2[k\epsilon_s(x)] \cdot \Phi_s(x), \\ \Phi_s^{(o)}(k) &= 4\pi \int_0^\infty dx \cdot x^2 \cdot g_{sr}(r_0x) \cdot j_0[k\epsilon_s(x)] \cdot \left\{ \frac{r_0^3 \delta n_e^{(s)}(r_0x)}{Z_s} \right\}, \\ \Phi_s(x) &\equiv \frac{1}{x^3} \left[1 - \kappa_s(r_0x) + \frac{x}{3} \frac{\partial \kappa_s(r_0x)}{\partial x} \right]. \end{aligned} \quad (70)$$

It is convenient to represent the next-order functions $b_{ss'}(\beta)$ and $b_{ss'}^{(o)}(\beta)$ due to ion-ion correlations in the following form using the same designations:

$$\begin{aligned} b_{ss'}(\beta) &= \int_0^\infty dk \cdot k^2 \cdot A(k) \cdot j_2(k\beta) \cdot b_{ss'}(k), \\ b_{ss'}^{(o)}(\beta) &= \int_0^\infty dk \cdot k^2 \cdot A(k) \cdot j_0(k\beta) \cdot b_{ss'}^{(o)}(k), \end{aligned} \quad (71)$$

where the corresponding Fourier components of correlation contributions are represented in the series

$$\begin{aligned} b_{ss'}(k) &= \int_0^\infty dx_1 \cdot x_1^2 \int_0^{x_1} dx_2 \cdot x_2^2 \cdot g_{sr}(r_0x_1) \\ &\quad \cdot g_{sr}(r_0x_2) \cdot b_{ss'}(k; x_1; x_2), \\ b_{ss'}(k; x_1; x_2) &= Z_s \cdot \Phi_s(x_1) \\ &\quad \cdot \left\{ j_2[k\epsilon_s(x_1)] \right. \\ &\quad \cdot h_{ss'}(0; r_0x_1; r_0x_2) - \sum_{n=0}^{\infty} (-1)^n (2n+1) \\ &\quad \cdot \left[\left(\frac{3n(n-1)}{2k^2 \epsilon_s^2(x_1)} - 1 \right) j_n[k\epsilon_s(x_1)] \right. \\ &\quad \left. + \frac{3}{k\epsilon_s(x_1)} j_{n+1}[k\epsilon_s(x_1)] \right] \\ &\quad \left. \cdot j_n[k\epsilon_s(x_2)] \cdot h_{ss'}(n; r_0x_1; r_0x_2) \right\}, \\ b_{ss'}^{(o)}(k) &= \int_0^\infty dx_1 \cdot x_1^2 \int_0^{x_1} dx_2 \cdot x_2^2 \cdot g_{sr}(r_0x_1) \\ &\quad \cdot g_{sr}(r_0x_2) \cdot b_{ss'}^{(o)}(k; x_1; x_2), \\ b_{ss'}^{(o)}(k; x_1; x_2) &= 4\pi \cdot r_0^3 \delta n_e(r_0x_1) \\ &\quad \cdot \left\{ j_0[k\epsilon_s(x_1)] \cdot h_{ss'}(0; r_0x_1; r_0x_2) \right. \\ &\quad - \sum_{n=0}^{\infty} (-1)^n (2n+1) \cdot j_n[k\epsilon_s(x_1)] \\ &\quad \left. \cdot j_n[k\epsilon_s(x_2)] h_{ss'}(n; r_0x_1; r_0x_2) \right\}. \end{aligned} \quad (72)$$

Now, it is useful to present substitutions for obtaining previous results [24, 25] in the linearized Debye-Hückel approximation for correlation functions of field particles from expressions, derived earlier:

$$\begin{aligned} \kappa_s(r_0x) &\longrightarrow \kappa_s^D(x) \equiv 1 - \exp[-ax] \cdot (1 + ax), \\ a &\equiv \frac{r_0}{r_D}, \quad r_D \equiv \sqrt{\frac{T_e}{4\pi e^2 N_e}}, \\ g_{sr}(r_0x) &\longrightarrow \exp \left[-Z_0 Z_s \cdot \Theta \cdot a^2 \cdot \frac{\Lambda^{3/2}}{4\pi} \cdot \frac{\exp[-ax]}{x} \right], \\ \Theta &\equiv \frac{T_e}{T_i}, \\ h(n; x_1; x_2) &\longrightarrow -\Theta \cdot a^3 \cdot \frac{\Lambda^{3/2}}{4\pi} \cdot f_n^>(ax_1) \cdot f_n^<(ax_2), \\ f_n^>(z) &\equiv (-1)^n \cdot z^n \cdot \left(\frac{d}{zdz} \right)^n \frac{e^{-z}}{z}, \\ f_n^<(z) &\equiv z^n \cdot \left(\frac{d}{zdz} \right)^n \frac{\sinh(z)}{z}. \end{aligned} \quad (73)$$

In these formulas, the conventional designations from original works [24–26, 72, 73, 164] are used, while T_i, T_e are the electron and ion temperatures correspondingly.

After performing the pointed out simplifications for one sort of field ions, the equations (57)–(61) reproduce the Baranger-Mozer results for low-frequency ion component of plasma microfield distribution function.

In Figure 11 the Baranger-Mozer (BM) functions $W(\beta)$ for several a values, calculated along with this section derivation in the charged point, and the results of corresponding MC calculations are presented. The comparison has shown that within the accuracy of the figure drawing BM and MC data are indistinguishable from each other. It should be noted that the direct calculations of general joint distribution functions is very complicated task even for the current powerful supercomputers. Moreover, sometimes even a definition of such functions is difficult to accomplish. That is why the most accessible approximation is characterizing these functions with the help of its moments of various ranks over different variables.

In practical application, it is important to keep in mind that even in the case of calculations the simplest distribution functions, depending only on the module of reduced field, the known difficulties exist with arising oscillations in results at small and especially at large β due to Fourier transform. That is why the most accepted method of introduction of various distribution functions in calculations is connected with the use of their tables. As a rule under calculations of the sum of terms with ion-ion correlations, the convergence is rather rapid, and it is quite enough to include only 3–4 first terms of the sum [22–26].

In Figure 12, the universal function $B_D(\beta)$ in the charged point $Z_r = Z_1 = 1$ for different values of parameter a is presented [58]. The dashed lines show the results of calculations using only the first two terms of cluster expansion and three terms of expansion over l . The nearest neighbor result is also shown as $2\beta^{3/2}$. Solid lines represent MC results. In

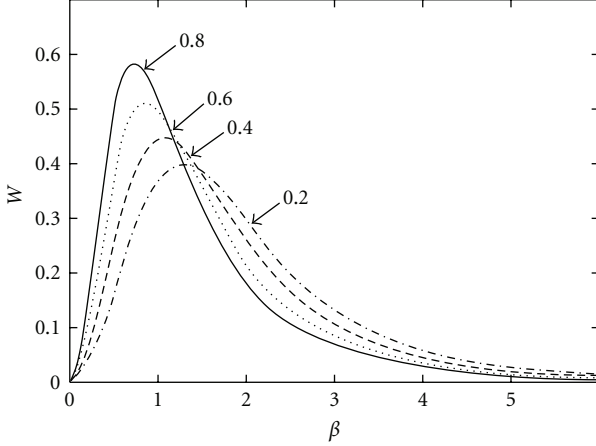


FIGURE 11: Microfield distribution function $W(\beta)$ in charged point $Z_r = 1$ in mixture of field ions with charge $Z = 1$ from [58] calculated within Baranger-Mozer and MC approaches (results of MC and Baranger-Mozer calculations are practically indistinguishable, numbers near arrows label a values).

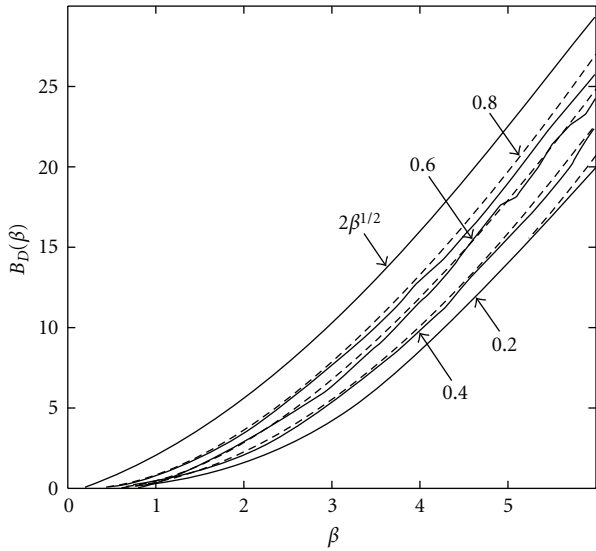


FIGURE 12: Universal functions $B_D(\beta)$ in charged point $Z_r = 1$ for various a values and charge of field ions equal to 1 [58].

Figure 13, the illustration of the universal function $B_{DO}(\beta)$ for different values of parameter a in the charged point $Z_r = Z_1 = 1$, according to [58] similarly to $B_D(\beta)$ is presented. Only the two first terms of cluster expansion and three terms of expansion over l are used. Solid lines show MC results (see [58]). The analysis of $B_{DO}(\beta)$ asymptotic for small β discovers that this function stems to constant at $\beta \rightarrow 0$. Moreover, from graphs, generally speaking, the presence of another constant is evident in asymptotic for large β . These properties have principal significance and signalize on the necessity of simultaneous correct account for electron contribution under consideration of quadrupole interaction, for example, in the spectral lines broadening [59, 60, 62].

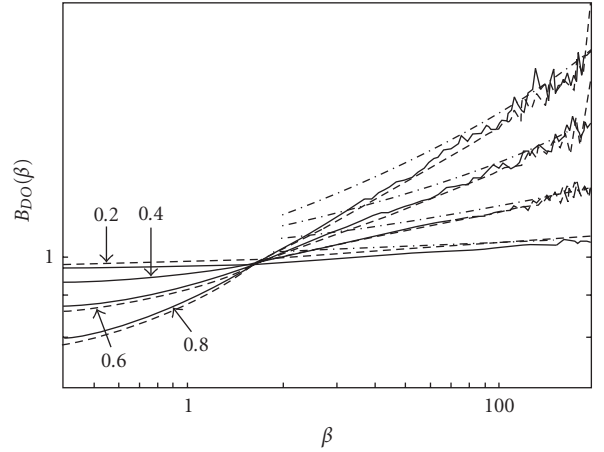


FIGURE 13: Universal functions $B_{DO}(\beta)$ in charged point $Z_r = 1$ for various a values and charge of field ions equal to 1 [58].

The described-here Baranger-Mozer cluster expansion approach for joint distribution function of ion microfield and its nonuniformity tensor with Debye-Hückel correlation functions was firstly proposed by the author of this review in [54] and completely realized in [55, 56], where the functions $B_D(\beta)$ and $B_{DO}(\beta)$ were defined and its asymptotics was described. Two years later and with much less generality, similar results appeared in [64]. Interestingly, the designations in [64] coincide with the corresponding from [55].

In order to obtain results for strongly coupled plasmas, it is necessary to apply MC [57–62], molecular dynamics or APEX approaches. However, the APEX scheme allows only some reformulation of general expression on the basis of (54) relations, and then derivation from it the expressions for the first moments [65, 68, 69]. However, it is not possible to construct with APEX namely the joint distributions and then to derive the first moment from such a function, if it would exist in APEX.

Indeed, within the APEX these operations do not commute (see [58, 65, 68, 69]), and APEX authors avoid the attempts of construction joint distribution functions [165]. Resultantly, they attempt to generalize the relation for the first moment, basing on [165] (where the correlation function in the given electric field $\vec{\epsilon}$ was introduced $g(\vec{r}; \vec{\epsilon})$) and miss the partial derivative from $C(\rho; \sigma_m)$ over one of σ_m components, that during reduction of microfield function to APEX form provides the effective density distribution $g_{\text{eff.APEX}}(r)$ [59, 60], diverging at large values of argument.

For the APEX distribution function itself and the “quadrupole” part of the first moment of nonuniformity tensor, this increase is damped by corresponding decrease of function in (60) (see [57, 58, 80, 81]):

$$\left\{ 1 - \frac{\sin k\epsilon_s(x)}{k\epsilon_s(x)} \right\}, \quad \epsilon_s(x) = \frac{Z_s}{x^2} [1 - \kappa_s(r_0 x)] \quad (74)$$

and function in (70):

$$j_2[k\epsilon_s(x)], \quad (75)$$

but in the scalar part of first moment, this invokes divergence [68, 69, 80, 81].

Thus, pointed out noncommutativity is connected on one hand with the behavior of effective screening α in APEX, which is stronger than the Debye one (see Figure 14), and on the other hand with the outcome to constant for small reduced field values of the polarization (scalar) part of the first moment of nonuniformity tensor (see Figures 12 and 13), which was not taken into account in the first APEX work on the first moment of nonuniformity tensor calculation [65]. These factors both lead to divergence at upper limit in the polarization part of the first moment of nonuniformity tensor if to derive it from expression for the joint distribution function of microfield and its spacial derivatives within APEX (see [57, 58, 65, 68, 69, 76, 80, 81]).

In order to obtain the finite result, APEX authors in fact calculate field derivative, averaged over the APEX distribution function. This way means that such an average could be performed over any microfield distribution, and consequently, the given microfield is associated with the derivative as “if of quite other microfield”. So, the presence of unequivocal connection between the field and its derivative is not requested, which does not correspond to the setting of a problem under consideration, and from the logic point of view is absurd.

Nevertheless, the general derivation in [65] contains several new interesting formal results. Indeed, in [65], the constrained distributions of the nonuniformity tensor components at the fixed value of microfield are introduced instead of joint distribution functions, which formally allows to avoid the approximation of preaveraged Hamiltonian over components of microfield nonuniformity tensor. However, to our opinion, the numerical calculation of such functions is not simpler than the full-joint distribution itself and avoiding the approximation of averaged Hamiltonian has only an illusive character.

The described difficulties are due to the fact that the APEX distribution itself already is derived under certain limitations, imposed by fulfillment of the (24) condition for the second moment of microfield in the charged point. So, trying to preserve the natural asymptotic for large field values on one hand, and on the other hand comprehending well that $g_{\text{eff},\text{APEX}}(r)$ is divergent at large r , the authors of [65, 165] decided not to use the first moment of the joint distribution function, but to use the mean value of derivative over APEX distribution. (The presence of divergence and non-normalization of $g_{\text{eff},\text{APEX}}(r)$ and the information on real values of screening parameter α in comparison with the Debye reciprocal length was not mentioned in previous APEX papers till [68, 69].) Per se introduced in [165], the definitions of averaged values deviate from the conventional approach of Chandrasekhar-von Neuman [19–21] and represent itself some additional approximation that is not connected with formalism of joint distribution functions, and which region of validity is at least unclear.

Besides the fact that APEX in this case does not allow to construct namely *joint* distribution function of the electric field strength vector and its nonuniformity tensor in the

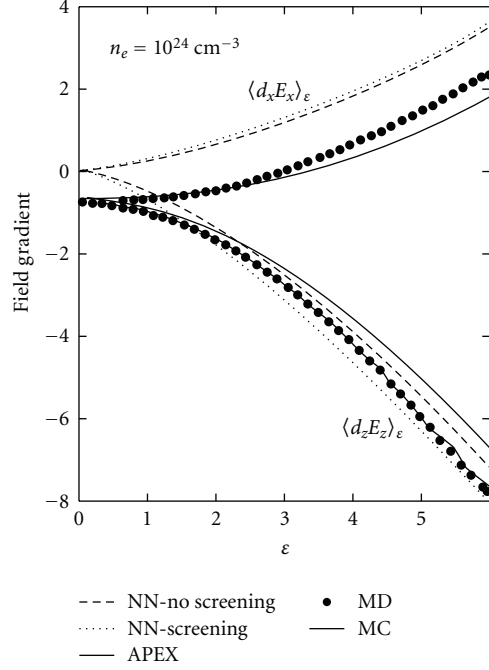


FIGURE 14: First moment components of ion microfield nonuniformity tensor for given value of microfield strength (without separation of quadrupole and scalar parts for MD, MC, and APEX) and nearest neighbor distribution NN (without scalar part) versus microfield-reduced values ϵ according to [68, 69] (MC from [58], MD from [68, 69]).

conventional “Chandrasekhar” sense [19–21], this problem seemingly is connected with inadmissibility of separate consideration of the electron and ion contributions to polarization interaction. Indeed, simultaneous consideration in real physical problems of the ion and electron contributions to polarization interaction lead to conversion to zero, at infinite distances, the constant in summary polarization interaction, and in this way remove the problem of pointed out divergence (see [59, 60]). The physical sense of this is that the distribution of ion charge also becomes nonuniform in response to the nonuniform distribution of electron density (see [59, 60]), and both effects compensate each other at sufficient distances from test charge according to general plasma quasineutrality condition. The alike outlook is presented in the interesting paper of Ortner, Valuev, and Ebeling, where such model is called as OCP on polarizable background (POCP).

On the other hand, it is obvious that up to now, not all variants of joint distribution function construction, using APEX, were analyzed.

The comparison of results for the moments of total nonuniformity tensor (without separation of contributions on tensor and scalar parts) for fixed value of the field ϵ using MD method, APEX (on the basis of relation (54)), and MC (from [58]) for $T = 800 \text{ eV}$ and $N = 10^{24} \text{ cm}^{-3}$ is presented according to [68, 69] in Figure 14 versus the reduced field values. The designations are taken from original work [68,

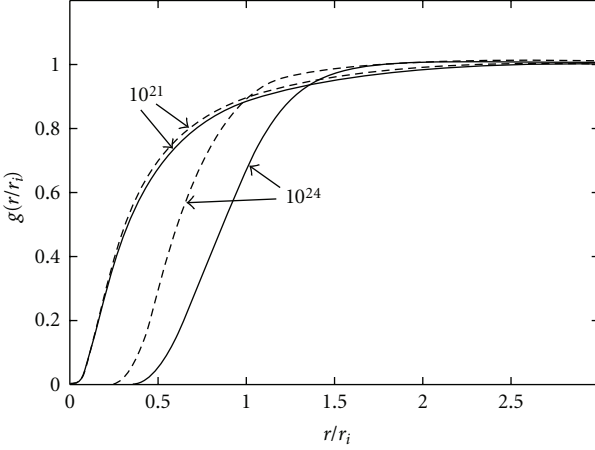


FIGURE 15: Pair radial correlation functions $g(r/r_i)$, calculated within HCN by Rogers code [124] (solid lines) and in Debye approximation (dotted lines) for $N_e = 10^{21} \text{ cm}^{-3}$ and $N_e = 10^{24} \text{ cm}^{-3}$ at $T = 800 \text{ eV}$ according to [58].

69]. The designations in the figure are connected with the conventional ones in the present paper in the following way:

$$\langle d_x E_x \rangle_\epsilon \equiv \left\langle \frac{\partial F_x}{\partial x} \right\rangle_\beta, \quad \langle d_z E_z \rangle_\epsilon \equiv \left\langle \frac{\partial F_z}{\partial z} \right\rangle_\beta, \quad (76)$$

and the results are obtained after average over angles of microfield vector in the expressions (62)–(67).

In Figure 14, the dependencies presented are obtained specially for distribution of nearest neighbor (NN) with screening by plasma electrons and without it, but neglecting the scalar part of nonuniformity tensor. It is seen that the APEX version for *average* values of nonuniformity tensor [68, 69] noticeably deviates at large reduced microfield values from the results of the nearest neighbor distribution. The MD results practically coincide with MC ones, while APEX curves are located inside MC curves in Figure 14. The presence of constant at small values of reduced microfield is confirmed. This comparison shows that the APEX calculation of *averaged* components of nonuniformity tensor in principle gives sound results in the context of coincidence with values of the first moments of nonuniformity tensor, although its derivation within APEX could not be recognized as completely correct and justified.

It seems instructive to demonstrate how with the increase of plasma coupling the differences of radial distribution functions within Debye and HCN approximations become ever more pronounced, which is illustrated in Figure 15. Partially, namely, the implementation of HCN correlation functions provides the APEX success in description of microfield distribution functions for strongly coupled plasmas. As was already mentioned with the increase of plasma coupling, the considerable changes of pair correlation function $g(r)$ occur, which acquires oscillations versus r for large values of Γ , which are due to the formation of the short-range ordering [166, 167]. This is explicitly demonstrated in Figures 16 and 17 within one component plasma model (OCP) for the different values of plasma coupling Γ . The

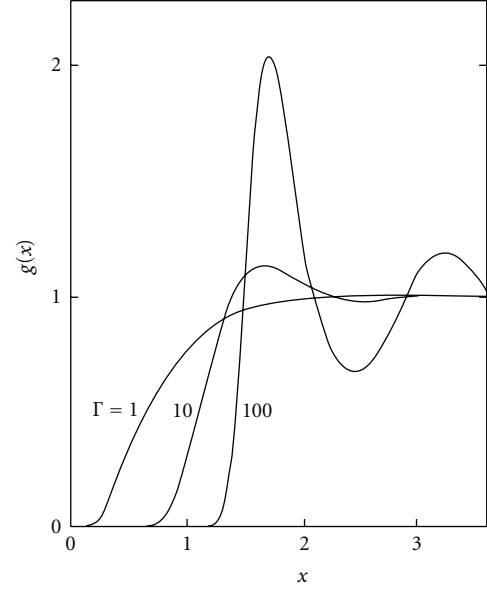


FIGURE 16: Pair radial distribution function $g(r/r_i)$, obtained by MC in OCP model according to [166] (numbers near curves provide corresponding values of plasma coupling parameter Γ).

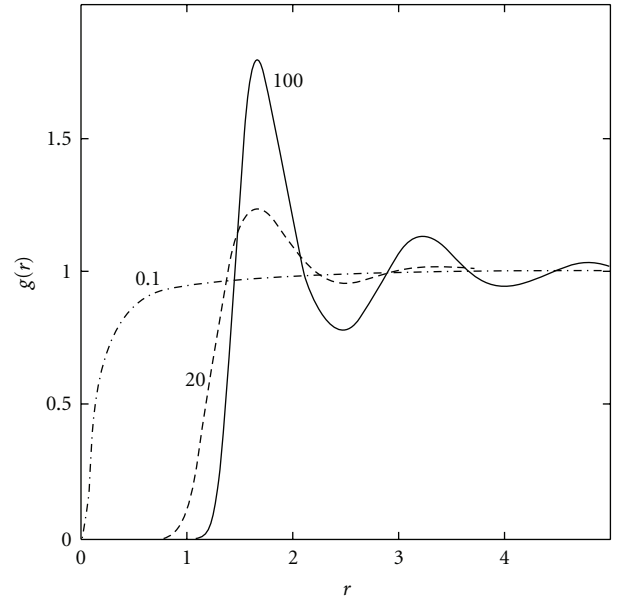


FIGURE 17: Pair radial correlation function $g(r/r_i)$, obtained by MC in OCP model according to [167] (numbers near curves provide corresponding values of plasma coupling parameter Γ).

presented results are obtained by the different authors with ten years interval [166, 167]. These data demonstrate visually qualitative changes of $g(r)$ versus variation of plasma coupling in the range $\Gamma = 0.1 - 1$, $\Gamma = 10 - 20$, $\Gamma \approx 100$. At the same time, the special study, done in [58], showed that using in the Baranger-Mozer scheme HCN correlation functions and MC correlation functions does not eliminate completely the noticeable discrepancies between

APEX and Baranger-Mozer microfield distribution functions for strongly coupled plasmas.

It should be taken into account that the linearization approximation for Debye-Hückel correlation functions is not inalienable part of Baranger-Mozer scheme, which allows the usage of any arbitrary accurate correlation function, including of the nonlinearized Debye-Hückel ones as well.

2.9.2. Distribution of Microfield and Its Time Derivatives. In the most general form, the joint distribution functions of microfield and its time derivatives could be written as Fourier-transform of its characteristic functions analogously to the previous section [19–21, 74–81], if following Chandrasekhar to consider the values of derivatives at initial time $t = 0$. These functions [74–81] describe microfield evolution in time on sufficiently small time intervals.

Without loss of generality, as an example, we present the function $W(\vec{F}; \dot{\vec{F}}; \ddot{\vec{F}})$ [54–56, 80, 81] (compare with [19–21]):

$$\begin{aligned} W\left(\vec{F}; \dot{\vec{F}}; \ddot{\vec{F}}\right) &= \frac{1}{(2\pi)^9} \int d^3\vec{\rho} \int d^3\vec{\sigma} \int d^3\vec{\xi} \\ &\cdot \exp\left[-i\left(\vec{\rho} \cdot \vec{F} + \vec{\sigma} \cdot \dot{\vec{F}} + \vec{\xi} \cdot \ddot{\vec{F}}\right)\right] \cdot A\left(\vec{\rho}; \vec{\sigma}; \vec{\xi}\right), \\ A\left(\vec{\rho}; \vec{\sigma}; \vec{\xi}\right) &= \exp\left[-NC\left(\vec{\rho}; \vec{\sigma}; \vec{\xi}\right)\right]. \end{aligned} \quad (77)$$

It is worthy to underline that in spite of the presence of the first and the second derivatives of microfield over time, this is per se the instantaneous static distribution function. At the same time, of course, it is very complex function in 9-dimensional space of its variables. Using the same designations and plasma composition, we express $\ln A(\vec{\rho}; \vec{\sigma}; \vec{\xi})$ as in the previous section:

$$\begin{aligned} C\left(\vec{\rho}; \vec{\sigma}; \vec{\xi}\right) &= C^{(o)}\left(\vec{\rho}; \vec{\sigma}; \vec{\xi}\right) - \frac{N}{2!} C^{(1)}\left(\vec{\rho}; \vec{\sigma}; \vec{\xi}\right), \\ C^{(o)}\left(\vec{\rho}; \vec{\sigma}; \vec{\xi}\right) &= \sum_s C_s \int d^3\vec{u}_s w_s(\vec{u}_s) \int d^3\vec{r} g_{sr}(\vec{r}) \\ &\cdot \varphi_s\left(\vec{\rho}; \vec{r}; \vec{\sigma}; \vec{\xi}\right), \\ C^{(1)}\left(\vec{\rho}; \vec{\sigma}; \vec{\xi}\right) &= \sum_{s,s'} C_s C_{s'} \int d^3\vec{u}_s w_s(\vec{u}_s) \int d^3\vec{u}_{s'} \\ &\cdot w_{s'}(\vec{u}_{s'}) \int d^3\vec{r}_1 \int d^3\vec{r}_2 \\ &\cdot \varphi_s\left(\vec{\rho}; \vec{r}_1; \vec{\sigma}; \vec{\xi}\right) \varphi_{s'}\left(\vec{\rho}; \vec{r}_2; \vec{\sigma}; \vec{\xi}\right) \\ &\cdot [g_{ss'}(\vec{r}_1; \vec{r}_2) - g_{sr}(\vec{r}_1) g_{s'r}(\vec{r}_2)], \\ \varphi_s\left(\vec{\rho}; \vec{r}; \vec{\sigma}; \vec{\xi}\right) &= 1 - \exp\left[i\Phi_s\left(\vec{\rho}; \vec{r}; \vec{\sigma}; \vec{\xi}\right)\right], \\ \Phi_s\left(\vec{\rho}; \vec{r}; \vec{\sigma}; \vec{\xi}\right) &= \vec{\rho} \cdot \vec{E}_s(\vec{r}) + \vec{\sigma} \cdot \dot{\vec{E}}_s(\vec{r}) + \vec{\xi} \cdot \ddot{\vec{E}}_s(\vec{r}). \end{aligned} \quad (78)$$

In distinction from the previous section, these expressions contain the additional integration over thermal velocities \vec{u}_s of field ions with the velocity distribution function $w_s(\vec{u}_s)$.

Moreover, $\dot{\vec{E}}_s(\vec{r})$ and $\ddot{\vec{E}}_s(\vec{r})$ determine the first and the second time derivatives of elementary electric field, produced by arbitrary field ion of s species in the origin of reference frame and having the same value of relative velocity at $t = 0$:

$$\begin{aligned} \dot{\vec{E}}_s(\vec{r}) &= \frac{eZ_s}{r^3} [3\vec{n}(\vec{n} \cdot \vec{v}_s) - \vec{v}_s] \\ &\cdot \left[1 - \kappa_s(r) + \frac{r}{3} \frac{\partial \kappa_s(r)}{\partial r}\right] + \frac{\vec{v}_s}{3} \frac{eZ_s}{r^2} \frac{\partial \kappa_s(r)}{\partial r}, \\ \ddot{\vec{E}}_s(\vec{r}; \vec{v}_s; \dot{\vec{v}}_s) &= \dot{\vec{E}}_s^{(1)}(\vec{r}; \dot{\vec{v}}_s) + \ddot{\vec{E}}_s(\vec{r}; \vec{v}_s), \\ \dot{\vec{E}}_s^{(1)}(\vec{r}; \dot{\vec{v}}_s) &= \frac{eZ_s}{r^3} [3\vec{n}(\vec{n} \cdot \dot{\vec{v}}_s) - \dot{\vec{v}}_s] \\ &\cdot \left[1 - \kappa_s(r) + \frac{r}{3} \frac{\partial \kappa_s(r)}{\partial r}\right] + \frac{eZ_s}{3} \frac{r}{r^2} \frac{\partial \kappa_s(r)}{\partial r} \dot{\vec{v}}_s, \\ \ddot{\vec{E}}_s(\vec{r}; \vec{v}_s) &= \frac{3eZ_s}{r^4} \left\{ [2\vec{v}_s(\vec{n} \cdot \vec{v}_s) + \vec{n}v_s^2] \right. \\ &\cdot \left[1 - \kappa_s(r) + \frac{r}{3} \frac{\partial \kappa_s(r)}{\partial r}\right] - 5\vec{n}(\vec{n} \cdot \vec{v}_s)^2 \\ &\cdot \left[1 - \kappa_s(r) + \frac{7}{15} r \frac{\partial \kappa_s(r)}{\partial r} \right. \\ &\left. \left. - \frac{r^2}{15} \frac{\partial^2 \kappa_s(r)}{\partial r^2}\right]\right\}, \end{aligned} \quad (79)$$

where $\vec{n} \equiv \vec{r}/r$, and $\vec{v}_s = \vec{u}_s - \vec{u}_r$ is the relative thermal velocity of field ion of “ s ” species with respect to the test particle with velocity \vec{u}_r . It is seen that there are summands, containing $\dot{\vec{u}}_s$, that is,

$$\dot{\vec{v}}_s = \dot{\vec{u}}_s - \dot{\vec{u}}_r = \frac{eZ_s}{m_s} \vec{F}(\vec{r}) - \frac{eZ_r}{m_r} \vec{F}(0), \quad (80)$$

where $\vec{F}(\vec{r})$ is the microfield in the location point of field ion of “ s ” species, and m_s, m_r are masses of the field ion and test particle correspondingly. These terms cause nonlinearity and loss of locality of joint distribution, if to include them into the expression for the second derivative.

Indeed, the microfield distribution at the origin of reference frame becomes dependent on microfield values in the total space. This controversy could be removed, assuming that the thermal velocities of field ions are constant due to stationarity conditions, as it was done in Chandrasekhar papers [19, 20], namely, $\dot{\vec{u}}_s = 0$ for all s . In the opposite case, the back reaction of field ions requests special study, which is beyond the frames of the present work.

On the other hand, there are terms due to polarization effects as well. That is why the results of Chandrasekhar and von Neuman could be reproduced only after discarding the neutralization background of electrons by setting $N_e = 0$. Here, it is supposed as before that all field ions are bare nuclei.

This joint distribution provide instantaneous low-frequency distribution function of individual (but many-body) ion component of plasma microfield and its time derivatives, which are defined on time scales τ of the order of $\omega_{pe}^{-1} \ll \tau \ll (v_i N_i^{1/3})^{-1}$, where ω_{pe} is the electron plasma frequency, v_i is the relative thermal velocity of field ions with respect to the test particle.

We note that this distribution in distinction from Chandrasekhar results includes effects of neutralizing background of plasma electrons and its polarization (or in the other words the appearance of nonuniformity in distribution of free electrons). The convolution over components \vec{F} or $\dot{\vec{F}}$ leads to separate distributions of the field and its derivatives, and after corresponding simplifications reproduces known results.

As it was already pointed out, the computation of joint distributions is very complex problem and it is possible now to present only some unique examples of such calculations [58, 70, 76], which contain as a rule many additional approximations and simplifications (only the projections of such functions are calculated with fixed values of a part of variables).

So, one of few methods to characterize these distributions is the calculations of their moments. This is achieved by the convolution over $d^3 \dot{\vec{F}}$. After that, it is possible to obtain the following expressions for the first moment of $\dot{\vec{F}}$ for a given value of \vec{F} :

$$W(\vec{F}) \langle \dot{\vec{F}} \rangle_{\vec{F}} = \frac{N}{(2\pi)^3} \int d^3 \vec{\rho} \exp[-i\vec{\rho} \cdot \vec{F}] \cdot A(\vec{\rho}) \vec{D}(\vec{\rho}),$$

$$\vec{D}(\vec{\rho}) = \vec{D}^{(o)}(\vec{\rho}) + \vec{D}^{(1)}(\vec{\rho}),$$

$$\vec{D}^{(o)}(\vec{\rho}) = \sum_s C_s \vec{D}_o^{(s)}(\vec{\rho}),$$

$$\vec{D}^{(1)}(\vec{\rho}) = -\frac{N}{2} \sum_{s,s'} C_s C_{s'} \vec{D}^{(ss')}(\vec{\rho}),$$

$$\vec{D}^{(s)}(\vec{\rho}) = \int d^3 \vec{u}_s w_s(\vec{u}_s) \int d^3 \vec{r} g_{sr}(\vec{r}) \cdot \exp[i\Phi_s(\vec{\rho}; \vec{r})] \dot{\vec{E}}_s(\vec{r}),$$

$$\vec{D}^{(ss')}(\vec{\rho}) = \int d^3 \vec{u}_s w_s(\vec{u}_s) \int d^3 \vec{u}_{s'} w_{s'}(\vec{u}_{s'})$$

$$\cdot \int d^3 \vec{r}_1 \int d^3 \vec{r}_2$$

$$\cdot [g_{ss'}(\vec{r}_1; \vec{r}_2) - g_{sr}(\vec{r}_1) \cdot g_{s'r}(\vec{r}_2)]$$

$$\cdot \left\{ \dot{\vec{E}}_s(\vec{r}_1) \exp[i\Phi_s(\vec{\rho}; \vec{r}_1)] \right.$$

$$\cdot (1 - \exp[i\Phi_{s'}(\vec{\rho}; \vec{r}_2)]) + \dot{\vec{E}}_{s'}(\vec{r}_2)$$

$$\cdot \exp[i\Phi_{s'}(\vec{\rho}; \vec{r}_2)] (1 - \exp[i\Phi_s(\vec{\rho}; \vec{r}_1)]) \right\}. \quad (81)$$

These formulas [80, 81] could be rewritten in terms of microfield distribution function similar to previous section:

$$\begin{aligned} W(\vec{F}) \langle \dot{\vec{F}} \rangle_{\vec{F}} &= N \left[\sum_s C_s \int d^3 \vec{u}_s w_s(\vec{u}_s) \int d^3 \vec{r} \right. \\ &\quad \cdot g_{sr}(\vec{r}) \dot{\vec{E}}_s(\vec{r}) W(\vec{F} - \vec{E}_s(\vec{r})) \\ &\quad - \frac{N}{2} \sum_{ss'} C_s C_{s'} \int d^3 \vec{u}_s w_s(\vec{u}_s) \int d^3 \vec{u}_{s'} w_{s'}(\vec{u}_{s'}) \\ &\quad \cdot \int d^3 \vec{r}_1 \int d^3 \vec{r}_2 [g_{ss'}(\vec{r}_1; \vec{r}_2) - g_{sr}(\vec{r}_1) \cdot g_{s'r}(\vec{r}_2)] \\ &\quad \cdot \left\{ \dot{\vec{E}}_s(\vec{r}_1) \left[W(\vec{F} - \vec{E}_s(\vec{r}_1)) \right. \right. \\ &\quad \left. \left. - W(\vec{F} - \vec{E}_s(\vec{r}_1) - \vec{E}_{s'}(\vec{r}_2)) \right] \right. \\ &\quad \left. + \dot{\vec{E}}_{s'}(\vec{r}_2) \left[W(\vec{F} - \vec{E}_{s'}(\vec{r}_2)) \right. \right. \\ &\quad \left. \left. - W(\vec{F} - \vec{E}_s(\vec{r}_1) - \vec{E}_{s'}(\vec{r}_2)) \right] \right\} \right]. \quad (82) \end{aligned}$$

The expressions for $\dot{\vec{F}}$ could be obtained in a similar manner by substitution $\dot{\vec{E}}_s(\vec{r})$ instead of $\dot{\vec{E}}_s(\vec{r})$ in the right part of corresponding equations, if to put $\vec{u}_s = 0$ for all $\{s\}$ as was pointed out earlier.

To obtain results in more detail, the approach, presented in the previous section, and the connection of spatial and time derivatives of the field, produced at test particle with the velocity \vec{v} in the origin of reference frame, are used (compare with [19–21]):

$$\langle \dot{\vec{F}}_i \rangle_{\vec{F}} = \left\langle \frac{\partial F_i}{\partial x_k} \right\rangle_{\vec{F}} \langle \dot{x}_k \rangle_{\vec{v}} \vec{e}_i, \quad (83)$$

where \vec{e}_i are unit vectors of Cartesian reference frame, and the symbol $\langle \dots \rangle_{\vec{v}}$ designates the average over thermal velocities of field ions. Substituting then in these expressions, the first moments of nonuniformity tensor, obtained in the previous section, we come to the next compact formulae (compare with [19–21]):

$$\left\langle \frac{\partial F_i}{\partial x_k} \right\rangle_{\vec{F}} = \frac{2\pi e N}{3} \left\{ B_D(\beta) \left(\frac{3F_i F_k}{F^2} - \delta_{ik} \right) + 2 \delta_{ik} B_{DO}(\beta) \right\}, \quad (84)$$

where the universal functions $B_D(\beta)$ and $B_{DO}(\beta)$ are determined in the previous section.

After substitution and convolution over indexes of components of \vec{F} and \vec{u}_r the sought result is

$$\begin{aligned} \langle \dot{\vec{F}} \rangle_{\vec{F}} &= -\frac{2\pi e N}{3} \{ B_D(\beta) (3 (\vec{n}_F \cdot \vec{u}_r) \vec{n}_F - \vec{u}_r) \\ &\quad + 2 B_{DO}(\beta) \vec{u}_r \}, \quad n_F \equiv \frac{\vec{F}}{F}. \quad (85) \end{aligned}$$

The contribution from microfield variation disappears due to assumed isotropy of velocity distribution function of field ions.

It is seen that contributions of polarization effects, included in $B_D(\beta)$ and $B_{DO}(\beta)$, have different signs in the expression for vector oriented along \vec{u}_r , but, as it is possible to assure, they do not compensate each other due to the different symmetry of interactions (quadrupolar and scalar). This does happen in the coefficient in front of \vec{F} . Using the relation

$$\dot{\vec{u}}_r = \frac{eZ_r}{m_r} \vec{F}(0), \quad (86)$$

where m_r is the mass of test particle, it is possible to write down the part of the moment over the second field derivative, assuming $\dot{\vec{u}}_s = 0$ for all $\{s\}$ due to the independence of ensemble of field particles on time:

$$\left\langle \frac{\ddot{F}^{(1)}}{\vec{F}} \right\rangle = -\frac{4\pi e^2 Z_r N}{3} [B_D(\beta) + B_{DO}(\beta)] \frac{\vec{F}(0)}{m_r}. \quad (87)$$

This expression with the opposite sign is proportional to “zz” component of microfield nonuniformity tensor in the reference frame, in which \vec{F} is directed along \vec{OZ} :

$$\left\langle \frac{\ddot{F}^{(1)}}{\vec{F}} \right\rangle = -eZ_r \left\langle \frac{\partial F_z}{\partial Z} \right\rangle_{\vec{F} \parallel \vec{OZ}} \frac{\vec{F}(0)}{m_r}. \quad (88)$$

This result describes the influence of neutralizing background on dynamical friction [80, 81], that is, the consequence of plasma polarization effects. These terms do not disappear in the (OCP) limit for ions, when the neutralizing background has the constant density. So, the complete recover of the Chandrasekhar and von Neuman results [19–21] is possible only if to equal artificially this density to zero. The other results on this issue could be found in [76–79], where for advancing in the region of strongly coupled plasmas, the MD methods and models, used in theory of liquids, are applied.

It should be noted that in a row of problems on ion dynamics, the joint distribution functions of microfield and its time derivatives were also introduced in the case, when the total field is simultaneously defined by its individual and collective components. This question was considered in detail in [80, 81, 168]. In particular, the derivation of the expression for the second moment of the first derivative of total microfield was analyzed:

$$\left\langle \frac{\dot{F}_{\perp}^2}{F^2} \right\rangle_{\vec{F}}, \quad (89)$$

which plays dominating role in the consideration of fluctuating microfield time evolution (ion dynamics) on small in comparison with $\omega_{pi}^{-1} \gg (N_i^{1/3} v_{Ti})^{-1}$ (or $R_{Di} N_i^{1/3} \gg 1$) time scales [80, 81]. The principal result of [80, 81] is that the asymptotic of this moment for small values of reduced summary field does not change in comparison with the results of Chandrasekhar and von Neuman (see

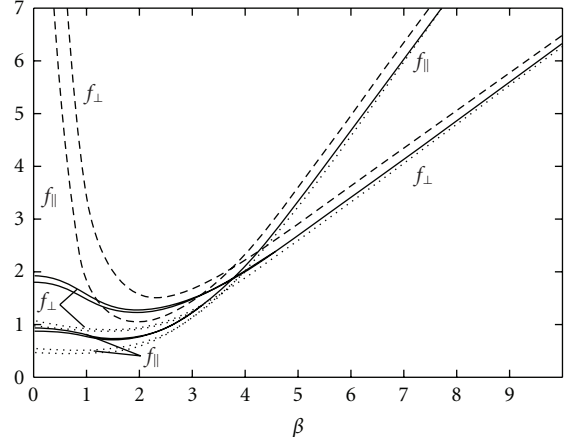


FIGURE 18: Reduced values of longitudinal and perpendicular second moments according to [170, 171]: dashed curves correspond to Chandrasekhar and von Neuman results [19–21] for fixed velocity values of test particle; solid curves are erroneous results [170, 171] with account of Doppler broadening (see [170]); the upper curves according to [170, 171] correspond to $N = 10^{17} \text{ cm}^{-3}$, $T = 12\ 700 \text{ K}$, and lower curves to $N = 3\ 10^{17} \text{ cm}^{-3}$, $T = 14\ 800 \text{ K}$; dotted curves the results that account for Debye screening due to authors [170] statements; the axis of abscissas shows the reduced microfield values.

[17, 19–21, 80, 81, 168]) in the case of three-dimensional isotropic distribution of collective fields and with account of the electron Debye screening and ion-ion correlations in individual component. Thereby, it was shown that Griem result [169–171] about the finiteness of the second moment values in the limit of small values of summary field is incorrect, but is the consequence of inconsistent performing of averaging and violation of the additivity condition in [169–171]. As these incorrect results [169–171] look like graphically the finiteness of the second moment (89) in the limit of small values of summary microfield is shown in Figure 18 from [170].

Alas it is worthy to note that the results presented in this figure, as if corresponding to the account of Debye screening, are obtained with the help of rather unfounded and unreliable procedure (see [80, 81, 172, 173]). It must be noted that in Griem papers [169–171], the derivation of results from [168] was repeated word to word, except absent in [168] incorrect resume on finiteness of the second moment (89) in the limit of small values of summary microfield. It follows from this analysis that the collective component becomes more rapid than individual one with increase of plasma coupling, and at $\Gamma \sim 1$, the characteristic scales of their time variation are of the same order of magnitude.

In conclusion of this section, it is necessary to mention that the first attempt to generalize Chandrasekhar and von Neuman results [19–21] for the first and the second moments of the first time derivative of microfield accounting for Debye screening but without ion-ion correlations in the middle of seventieth was made by Hey and Griem [172, 173]. They used expansion over parameter a . In this

respect, it is similar to Margenau approach, who attempted by expansion over parameter R_c/R_0 (R_c is the Coulomb radius, R_0 is the mean interparticle distance) to account for the influence of ion-ion repulsion on distribution functions [174]. Regrettably, such types of expansions are poor even for establishing asymptotic limits and in fact integrally are inapplicable for these functions due the absence of a real small expansion parameter. Related to these approaches is the method of the characteristic functions (or thermodynamic potentials) expansion over Fourier variable in the absence of any parameter of infinitesimality, which very often resort to in theory of liquids, where it appears under term of “ λ ” expansion [8]. The similar mathematical problems arise in the method of collective variables of Bohm and Pines [30, 31] also. The development of microfield theory has shown that there is no proof of convergence of such a type of expansions, and thereby their application is unjustified [80, 81].

2.10. Asymptotic Expansions. As was already noted, in fact, all distribution functions and connected with them universal functions have universal form of asymptotic at large and small values of reduced field, but at the same time, the procedure of those asymptotic derivation from general expressions as a rule is rather complicated and laborious. In the case of not so large plasma coupling, at large values of reduced microfield asymptotic should approach the distribution of nearest neighbor NN. For ions of the same species with the charge Z , the following relations are valid [53–62, 72, 73, 80, 81]:

$$\begin{aligned} W_{NN}(\beta) &= \frac{15}{4(2\pi)^{1/2}Z^2} \frac{y^5 g(y)}{1 + ay + a^2 y^2/2} \\ &\quad \cdot \exp\left[ay - \frac{1}{Z} \frac{15}{2\sqrt{2\pi}} \int_0^y dx x^2 g(x)\right], \\ B_{NN,D}(\beta) &= \frac{3}{Z W_{NN}(\beta)} \frac{y^2 (1 + ay + a^2 y^2/3) g(y)}{1 + ay + a^2 y^2/2} \\ &\quad \cdot \exp\left[-\frac{1}{Z} \frac{15}{2\sqrt{2\pi}} \int_0^y dx x^2 g(x)\right] \\ &\approx \frac{4\sqrt{2\pi} Z}{5 y^3} \left(1 + ay + \frac{a^2 y^2}{3}\right) \exp(-ay), \\ B_{NN,DO}(\beta) &= C_\infty + \frac{1}{2 Z W_{NN}(\beta)} \frac{a^2 y^4 g(y)}{1 + ay + a^2 y^2/2} \\ &\quad \cdot \exp\left[-\frac{1}{Z} \frac{15}{2\sqrt{2\pi}} \int_0^y dx x^2 g(x)\right] \\ &\approx C_\infty + \frac{2(2\pi)^{1/2} a^2 Z \exp(-ay)}{15 y}, \end{aligned} \quad (90)$$

where the quantity y is expressed in units of r_0 and is determined by

$$\beta = Z \frac{\exp(-ay)}{y^2} (1 + ay), \quad (91)$$

and C_∞ is determined from the other relation (see [57–62]). When ay is small enough, $\beta \approx Z/y^2$, then

$$\begin{aligned} B_{NN,D}(\beta) &\approx \frac{4\sqrt{2\pi}}{5} \frac{\beta^{3/2}}{Z^{1/2}}, \\ B_{NN,DO}(\beta) - C_\infty &\approx \frac{2(2\pi)^{1/2} a^2}{15} (Z\beta)^{1/2} \exp\left(-a\left(\frac{Z}{\beta}\right)^{1/2}\right). \end{aligned} \quad (92)$$

3. Fluctuating Microfields in Plasmas

As was already mentioned several times, the thermodynamic formalism not always happens to be adequate for problems, where the dynamics of time evolution of dipole interactions and actually plasma microfields is essential. Especially, this became critical for the sufficiently large effective time scales of evolution. However, in these cases, the statistical methods of modeling were developed, including as a rule two stages: (i) statistical modeling of system time dynamics, (ii) statistical average over random sampling from results of previous stage. The systems that require such an approach conventionally are called the systems “with partial memory loss” [7], when in spite of stochastic character of the process, the result often depends on prehistory of system evolutional dynamics.

3.1. Correlation Function Expansion over Time. In a row of problems and approaches, it is sufficient to follow only the very initial stage of microfield time evolution. Then it is possible to use the expansion over time of the state evolution operator, and reduce the problem solution to finding various moments of joint distribution functions of microfield over the microfield time derivatives at the starting moment of evolution ($t = 0$) [17, 19–21, 54–56, 74–81]. Chandrasekhar and von Neuman [19–21] and V. I. Kogan were the first who used this. This method could be applied to characterize the evolution of microfield distributions [19–21, 74–81, 104, 105] itself. In particular, this method allows to separate the ion dynamics contributions due to the different physical effects like the amplitude (rotation of microfield vector) and phase modulations (variation of microfield module) and the finite life time of Stark substates due to electronic collisions [168].

3.2. Method of Model Microfield. The method of model microfield (MMM) is known for providing the closed analytical expression for the spectrum of evolution operator $U(t)$ [86–94, 146], reducing the time dependent problem to the statistical average of static evolution operators $U_{St}(t)$ over quasistatic distributions of microfield:

$$\begin{aligned} \langle U(\omega) \rangle_{\text{MMM}} &= \langle U_{St}(\omega + i\nu) \rangle + \langle \nu U_{St}(\omega + i\nu) \rangle \\ &\quad \cdot \langle \nu I - \nu^2 U_{St}(\omega + i\nu) \rangle^{-1} \langle \nu U_{St}(\omega + i\nu) \rangle, \end{aligned} \quad (93)$$

where ν designates $\nu(\vec{F})$ (the frequency of jumps in the MMM Kangaroo-process), $U_{\text{St}}(\omega + i\nu)$ is the Laplace transform at $z = -i\omega + \nu$ of the static evolution operator, the symbol $\langle \dots \rangle$ designates the average over the static microfield distribution function $W(F)$, I is the unit operator. This expression is valid if the evolution operator is the function of only the difference between final and initial moments of time. Hence, MMM is applicable only in the absence of the $U(t)$ explicit time dependence. There is essential assumption in the derivation of this general result that microfield changes in time by jumps and only by their amplitude. The frequency of jumps $\nu(F)$ depends on the microfield value F at the given time moment. This character of changes was called Kangaroo-process [86–94, 146]. To close the procedure, it is necessary to know $\nu(F)$. The most wide-spread way to close the MMM system of equations and definition of $\nu(F)$ is based on equating the microfield correlator $C(t)$ to the mean square of microfield with the weight function equal to the product of the static microfield distribution function $W(F)$ and the factor $\exp[-|\nu(F)| \cdot t]$ with the exponential decay in time with the rate $|\nu(F)|$ [86–94]:

$$C(t) = \langle \vec{F}(t) \cdot \vec{F}(0) \rangle = \int_0^\infty dF W(F) F^2 \exp[-\nu(F)t]. \quad (94)$$

This significant correlation function $\langle \vec{F}(t) \cdot \vec{F}(0) \rangle$ was considered in many works: in the absence of Debye screening implicitly by Cohen, Spitzer and Routly [128]; for the gas of Coulomb particles by Kogan [129]; in the general form on the basis of kinetic plasma theory by Rosenbluth and Rostocker [130, 131]; by Taylor [132]; with account to Debye screening by Lewis [133]. This correlation function could be expressed via integral from the plasma structure factor $S(k, \omega)$ [4, 5, 7–10] and has direct connections with the problems of collisional transport and determination of plasma conductivity. (In recent work of Gordienko [134] an attempt was made to reconsider the canonical results that the microfield correlator effectively acquires binary form in the process of average [129]. In [134], on the basis of quite unclear and entangled computations, the statement is made about the existence of nonbinary, many-body and essential contribution to the microfield correlator. However, augmentations and derivations in [134] are based on a row of rather strong, unreliable, and difficult to test assumptions of statistical and mathematical character, which does not allow to consider the results of [134] as correct.) Thus, in MMM, the known analytical expression is substituted in the left-hand side of (94), derived in [89, 90] for classical plasmas in assumption of rectilinear trajectories and static Debye screening in the neutral point:

$$C(t) = \frac{4\pi N e^2}{D} \left\langle \left(\frac{D}{vt} - \frac{1}{2} \right) \exp\left(-\frac{vt}{D}\right) \right\rangle_v, \quad (95)$$

where $\langle \dots \rangle_v$ designates the average over velocities of

field particles and

$$\begin{aligned} C(t) &= \frac{4\pi N e^2}{t} \left\langle \frac{1}{\nu} \right\rangle_v \left[1 + x^2 - \pi^{1/2} x \left(x^2 + \frac{3}{2} \right) \right. \\ &\quad \left. \cdot \exp(x^2) \operatorname{erfc}(x) \right], \\ \operatorname{erfc}(y) &= \frac{2}{\sqrt{\pi}} \int_y^\infty \exp(-s^2) ds, \quad x \equiv \frac{\omega_p t}{\sqrt{2}}, \\ \left\langle \frac{1}{\nu} \right\rangle_v &= \left(\frac{2 m}{\pi k_B T} \right)^{1/2}. \end{aligned} \quad (96)$$

Often the paper of Rosenbluth and Rostocker [130, 131] is unreasonably connected with this result.

In MMM additionally the μ -ion model (or the ion of reduced mass, corresponding to the masses of perturbing and test particles) is used. The result for $C(t)$ is applied to the same extent as for electrons and as for ions, because the values of Debye radius, density, velocity, and reduced mass of the pair of test and perturbing particles D, N, v, m correspondingly are not specified.

The account of trajectory curvature in the case of calculations of $\langle \vec{F}(t) \cdot \vec{F}(0) \rangle$ in the charged point was performed numerically in [94]. However, it is not sufficient especially for strongly coupled plasmas.

The application of these methods [86–94, 128–134] to ions suffers from essential defect in determining $\nu(F)$. The thing is that the correlator of the fields at test-charged particle could be expressed as the correlator of accelerations, the integral of which over time should be equal to zero [8, 9]. At the same time, the analytical result for such a correlator is unknown, and that is why often the correlator in neutral point is used, which does not satisfy this condition.

It is worthy to note that MMM practical realization requests usage of rather tedious and complex procedure for the reduction of multiple products of irreducible spherical operators, that is not published yet.

For the case of charged test particle, Boercker et al. proposed the kinetic model [95], analogous to used in theory of liquids [8–12]. In this model, the frequency of microfield changes is constant $\nu(F) = \text{const}$, and does not depend on microfield value. By special selection of parameters, based on the introduction of the dependence on frequency detunings $\Delta\omega$, and using the relation with diffusion coefficient, the authors were able to satisfy the condition of conversion to zero of the integral of $\langle \vec{F}(t) \cdot \vec{F}(0) \rangle$ over time in the charged point [95]. At the same moment, this model contains a good few of other assumptions, which could not allow to give unequivocally the preference to that or another method in the case of the electric field description at test ion.

For calculations of this correlator, the MD methods are applied also, but each concrete case corresponds to the fixed plasma parameters, and it is difficult to detect scaling. The study of this correlator in strongly coupled plasmas using methods from the theory of liquids and Molecular Dynamics (MD) simulations was performed in the series of papers by Dufty et al. [79, 96, 104–107]. In [79, 96], certain criticism

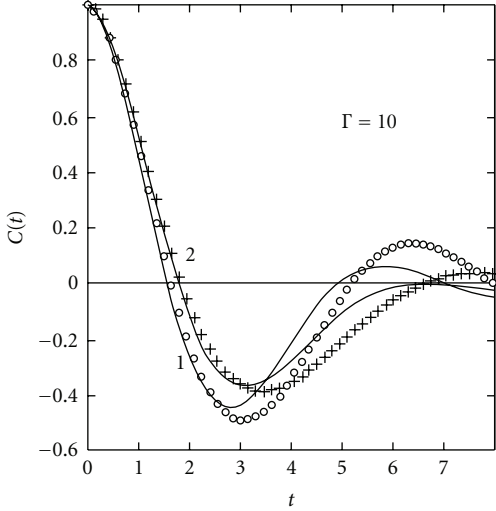


FIGURE 19: Model microfield correlation function $C(t)$ according to [96] in charged point for $\Gamma = 10$: 1 Coulomb interaction; 2 with account to Debye screening for $k = r_{De}/R_i = 1$; points—results of MD simulations.

on MMM is expressed in the case of its application for description of microfield fluctuations at charged test particle. This nevertheless seems rather strange, since MMM could allow any closing in the sense of $\nu(F)$ calculations. For example, the corresponding results for $C(t) \equiv \langle \vec{F}(t) \cdot \vec{F}(0) \rangle$ for small values of electron plasma-coupling parameter (when $R_{De} = R_i$, R_i is the ion sphere radius in OCP) from [96] are presented in Figure 19. It should be pointed out that the parameter of screening k in this model is uniquely related to plasma coupling parameter Γ , which in this example is about 10. As could be seen in Figure 19, $C(t)$ is alternating-sign function that assures the conversion to zero of $\int_0^\infty dt C(t) = 0$. There were also attempts to derive the expression for correlator in the neutral point on the basis of cluster expansion formalism [97] (see also [79]), however, the application of these results in MMM itself led to appearance of strange, nonphysical consequences [98].

In this respect, it is necessary to take caution to progress in the construction of $\nu(F)$ and $C(t)$ because insignificant peculiarities in the behavior of this quantities could lead to unforeseen nonphysical spectrum singularities. This is the reflection of the fact that per se here there is situation of the so-called “ill-posed inverse problem.”

Currently, there is also another significantly developed method of Frequency Fluctuation Model (FFM) [99, 100], ideologically adjoining to MMM. However, its principal difference is that this model to the more extent than MMM is a way to describe the spectra in the fluctuating microfield than the method to describe microfield characteristics itself. It is based on the assumption of the microfield fluctuation frequency independence from the value of the electric microfield strength, and in total, the statistical problem settings correspond more to Kubo resolvent (see [88, 146]). On the other hand, there is a possibility to model this frequency using the methods from theory of liquids. Due to

application of the latter effectively the fluctuation frequency starts to depend on frequency detunings from the line center [95, 99, 100]. Then, the limits of small and large frequency detunings could be expressed via “fundamental” parameters (see [79, 95, 99, 100]). It was already mentioned that for some time, the used $\nu(F)$ was obtained also in the process of special MD simulations for corresponding parameters, which up to now is rather laborious procedure. Regretfully, the details of published FFM formulation do not allow to use it freely for practical calculations.

3.3. Method of Molecular Dynamics. The method of molecular dynamics is the simultaneous self-consistent solution of equations of motion for the finite number of particles N in the finite cell and allows to determine the time evolution of summary electric microfield, acting on the test particle [101–109].

The cell size is defined from the similar considerations as in the Monte-Carlo method [34–39]. However, the simultaneous modeling of electrons and ions was not managed to succeed even on the current supercomputers not only due to the large difference of characteristic time scales but also due to the complexity of sound accounting for the effects of attraction between particles with the opposite signs of charge.

As a rule, the quasiparticles are used with Debye screening by plasma electrons. The numerical calculations could be performed, for example, in cubic cell with periodic boundary conditions, or elastic, or isotropic scattering on its borders [108, 109]. If to use in calculations ensembles from 50 and 120 particles, the accuracy of results makes up about $\sim 10\%$. The trajectories in the system are evaluated on time scales much larger than the correlation time $\tau_c \sim r_0/v_i$, where $r_0 \sim (N_e/Z)^{-1/3}$ is the mean distance between ions, v_i the mean ion velocity with respect to the emitter at rest. During integration, the conservation of the total energy of the system is controlled. Also, the test calculations on reproduction of results for the static distribution functions are performed [104–106], and on their basis, the additional subsidiary algorithms for convergence acceleration are introduced [104–107]. The other methods for acceleration of convergence and reduction of fluctuations in the results of computations with regard to the concrete mathematical setting of that or another physical problem are used as well.

In the majority of performed MD calculations, the μ -ion model was used. Nevertheless, the separate modeling of the test particle motion is possible as well. The final result is obtained by an average over the large number of “histories” of time evolution. Following large effective time intervals, MD had rather large fluctuations that, for example, made difficult to recover impact limit in broadening by ions [101–109].

The MD was used to study the dependencies of microfield time evolution [105, 106, 135–137], the characteristic time and spacial scales of screening setting during simulations of microfield distribution functions [135–137] (compare [84, 85, 125–127]). However, in [135–137] the particles with negative sign had the same mass as positive

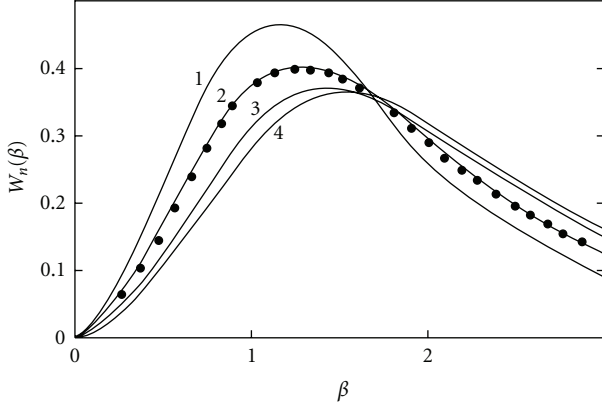


FIGURE 20: Distribution of static ion microfield [135], produced by finite number \mathcal{N} of noninteracting particles, placed in cube: 1 $\mathcal{N} = 4$; 2 $\mathcal{N} = 27$; 3 $\mathcal{N} = 1000$; 4 Holtsmark distribution; points—microfield distribution for 27 particles, placed in sphere.

ions, which did not allow to model the real plasma screening of ions by electrons. In series of papers of these authors, the attention was payed to the effect of finiteness of particles number in the effective sphere of interaction, which formally did not permit to switch to thermodynamic limit:

$$N = \lim_{\mathcal{N} \rightarrow \infty, V \rightarrow \infty} \frac{\mathcal{N}}{V}, \quad (97)$$

being the key condition during conducting of thermodynamic averages. Here, \mathcal{N} is the total number of particles, V is the total volume, N is the particles density. The display of the finiteness of particles number effects could be followed by results of modeling [135], presented in Figure 20. On the other hand, it is seemed that, particularly, the damping of this influence is achieved by operation with the large number of tracked microfield time evolutions (configurations) during the statistical average and the reduction of results dispersion [101–109]. It follows from results of modeling [135–137], presented in Figure 21, that Coulomb interaction shifts somehow the maximum of distribution in the direction of small fields with respect to the case of ideal plasma with noninteracting quasiparticles. However, this shift is much smaller than the shift, arisen due to hypothetic Debye screening [135–137]. In other words, according to [135–137], the distribution of instantaneous microfields does not coincide with Debye field, which is evidently the result of average over sufficiently large time interval. At the same time the distribution of summary field experience more essential shift [135–137] than the distribution of ion field, as far as the correlation of like sign charges is less essential than the correlation of charges with opposite signs.

At the same moment in cited works [135–137], the question of applicability of static Debye shielding to the modeling of the electric fields of plasma ions was considered. However, as was assumed from intuitive notions, the Debye shielding is settled for rather large time intervals in comparison with characteristic time scales of the plasma electrons electric fields variation. That is why the MD instantaneous microfield distribution for this case becomes more similar to the

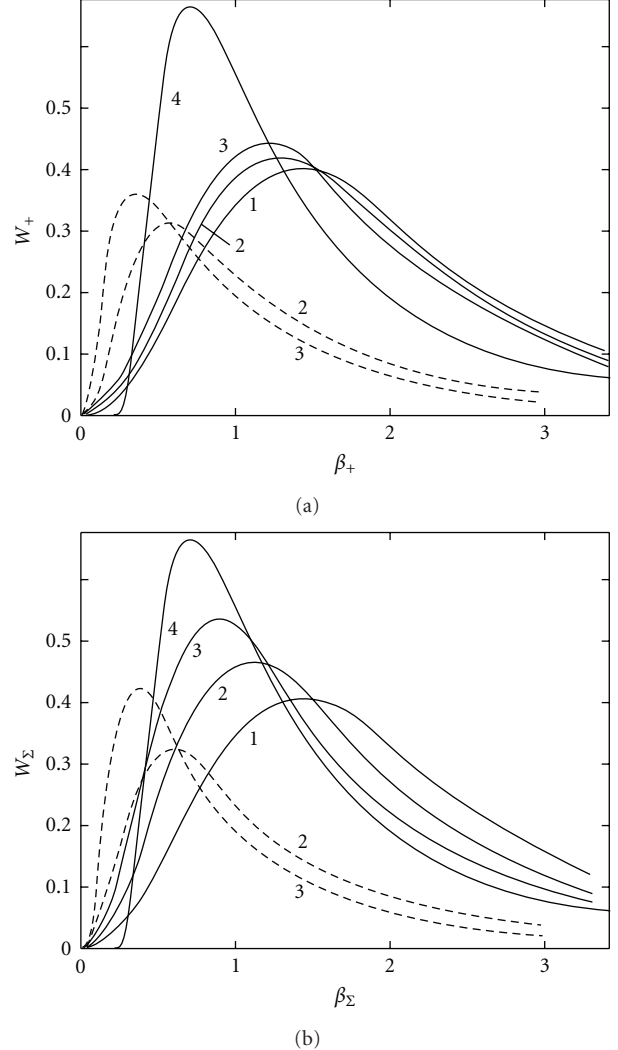


FIGURE 21: Distribution of static ion microfield [135], produced by positive charges (a) and by charges of both signs (b) (solid lines correspond to Coulomb interaction, dashed lines to hypothetic microfield distribution with Debye screening): 1: $T \rightarrow \infty$ modified Holtsmark distribution accounting to finite number of particles in modeling; 2: $T = 1$ eV, plasma coupling parameter $d \equiv (r_c/R_0)^3 = 0.006$; 3: $T = 0.5$ eV, $d = 0.05$; 4 is nearest neighbor distribution $W(\beta) = (3/2) \beta^{-5/2} \exp[-\beta^{-3/2}]$ (solid lines are normalized by condition $\int d\beta W(\beta) = 1$, dashed ones by $\int d\beta W(\beta) = 1/2$; density of like-sign charges $N = \mathcal{N}/R^3 = 10^{18} \text{ cm}^{-3}$, $\mathcal{N} = 27$, $R = 0.03\mu$; total density of particles $2N$, $2\mathcal{N} = 54$; $\beta_+ = F_+/F_{+,0}$, $\beta_\Sigma = F_\Sigma/F_{\Sigma,0}$, $F_{+,0} = (4\pi \mathcal{N}/3)^{2/3} e$, $F_{\Sigma,0} = 2^{2/3} F_{+,0}$).

Holtsmark distribution [135–137] than to the Ecker-Müller one. At the time when the works of Yakovlenko et al. were performed, it was not yet possible to judge on the validity of conventional results for the microfield distribution functions (MDFs) of the low-frequency ion component of plasma microfield with static Debye screening, since they could manage joint simulations with only heavy negative particles, not electrons. However, after several decades, the power of computers allowed to consider and realize such task. Professor Sergey Yakovlenko spoke against implementation

of the term “molecular dynamics” in the case of plasma proposing instead the term “method of dynamics of many particles.”

Indeed, recently within the certain assumptions on interaction potentials, MD modeling of plasma electrons and ions electric fields action on the emitter was realized simultaneously on the same footing with account of correlations between them [138, 139, 182, 183]. The principal moment, which allows to perform such modeling, is the replacing of attracting ion-electron Coulomb potential at the small distances either by finite potential or by potential of “impermeable sphere.” Moreover, of course, this becomes possible also due to the evident significant progress in recent MD programming, that allowed to consider now the very tiny time steps and huge numbers of evolution histories [182].

In [138, 139], the results of these rather detailed and interesting studies were related only to consideration of evolution of plasma electrons microfield simultaneously with the evolution of ion field with switched off and switched on interaction between electrons and ions. Firstly, this program was realized in [182]. These results were further developed in [182, 183] that we follow in what follows. In [182, 183], the interaction potential of particles with the same sign is taken in the form

$$V_{ee,ii}(r) = \frac{e^2}{r} \exp\left(-\frac{r}{\lambda}\right), \quad (98)$$

where λ is taken to be about a half of the size of simulation cubic cell $\sim s/2$. The electron-ion potential is approximated with the function

$$V_{ei}(r) = -\frac{e^2}{r} \left[1 - \exp\left(-\frac{r}{\delta}\right) \right] \exp\left(-\frac{r}{\lambda}\right), \quad (99)$$

where the short-range regularization parameter δ is chosen to satisfy in the limit of small r the value of ionization potential of hydrogen atom. The total electric microfield is evidently represented as the sum of summary plasma ions and electrons fields, which is subdivided into slow \mathcal{S} and fast \mathcal{F} microfield components:

$$\vec{E}(t) = \vec{E}_i(t) + \vec{E}_e(t) = \vec{E}_{\mathcal{S}}(t) + \vec{E}_{\mathcal{F}}(t). \quad (100)$$

Introducing in [182] the average of the electron summary field $\overline{\vec{E}_e(t)}_{\Delta t}$ over variable time interval Δt provides the tool for analysis of stochastic fluctuations:

$$\overline{\vec{E}_e(t)}_{\Delta t} = -\frac{1}{\Delta t} \int_{-\Delta t/2}^{\Delta t/2} dt' \vec{E}_e(t-t'). \quad (101)$$

After that, the slow \mathcal{S} and fast \mathcal{F} components are defined as

$$\begin{aligned} \vec{E}_{\mathcal{S}}(t) &= \vec{E}_i(t) + \overline{\vec{E}_e(t)}_{\Delta t}, \\ \vec{E}_{\mathcal{F}}(t) &= \vec{E}(t) - \vec{E}_{\mathcal{S}}(t) = \vec{E}_e(t) - \overline{\vec{E}_e(t)}_{\Delta t}. \end{aligned} \quad (102)$$

At the same time, due to ergodicity [182],

$$\lim_{\Delta t \rightarrow \infty} \overline{\vec{E}_e(t)}_{\Delta t} = \langle \vec{E}_e(t) \rangle = 0. \quad (103)$$

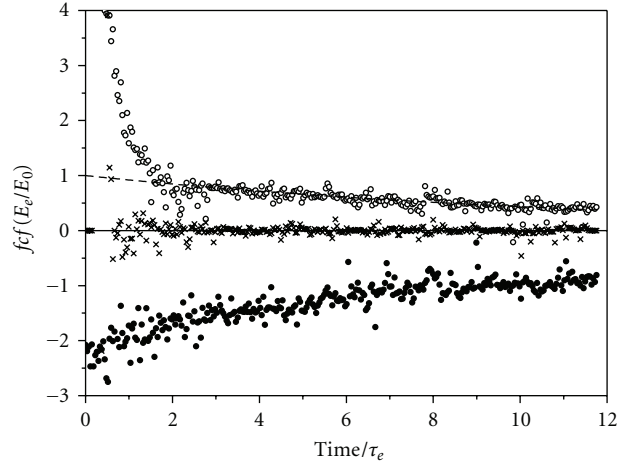


FIGURE 22: MD correlation functions of electric fields for $a = 0.8$ from [182] at neutral point: black circles is correlation of summary ion and summary electron fields $\langle \vec{E}_{\text{ion}}(0) \cdot \vec{E}_e(t) \rangle$; open circles $\langle \vec{E}_e(0) \cdot \vec{E}_e(t) \rangle$; crosses is a correlation function of fast component of total microfield $\langle \vec{E}_{F,\Delta t}(0) \cdot \vec{E}_{F,\Delta t}(t) \rangle$ for $\Delta t = 0.4 \cdot \tau_e$; dashes-exponential fit.

The conventional parameters of simulations are the electron-electron and ion-ion mean distance $r_0 = (3/4\pi N_e)^{1/3}$, the mean electric field modulus $E_0 = e^2/r_0^2$, the electron thermal velocity $v_e = (k_B T_e/m_e)^{1/2}$, the electron and proton coupling constants $\Gamma = e^2/(r_0 k_B T_e)$, and Debye length $r_D = (k_B T_e/4\pi N_e e^2)^{1/2}$, $\tau_e \sim r_0/v_e$. The conditions were considered with $a = 0.4$ and $a = 0.8$, $N_e = 10^{18} \text{ cm}^{-3}$, $T_e \sim 1 \text{ eV}$. During simulations, the cell is taken about $s \sim 3r_D$, and the number of particles in the cell is $N \sim 1000$. The introduction of λ screening ensures the more rapid convergence of results but has no deal with much more stronger Debye screening [182]. As usual, the periodic boundary conditions allow to address the infinite homogeneous system. During simulations, the total energy is preserved with accuracy about 1%. The authors of [182] correctly noticed that the fast component could not represent the electron fields due to correlations between ion and electrons, while all definitions are the functions of the average time interval Δt that have to be determined from physical peculiarities of the problem, which are beyond the model. To our opinion in the case of line broadening, the detuning from the line center could be such a parameter to require $\Delta\omega\Delta t \sim 1$.

The results for correlation functions presented in Figure 22 along with [182] are very instructive and physically reasonable. The symbol $\langle \dots \rangle$ means as usual the average over ensemble of microfield evolution histories. The correlation functions itself are common and valuable additional tool for study of fluctuations. In Figure 22, the fast component loses correlation very soon, and the strong anticorrelation of ionic and electron fields is pronounced. The statistical independence of introduction slow and fast microfield components is clearly demonstrated in Figure 22 too.

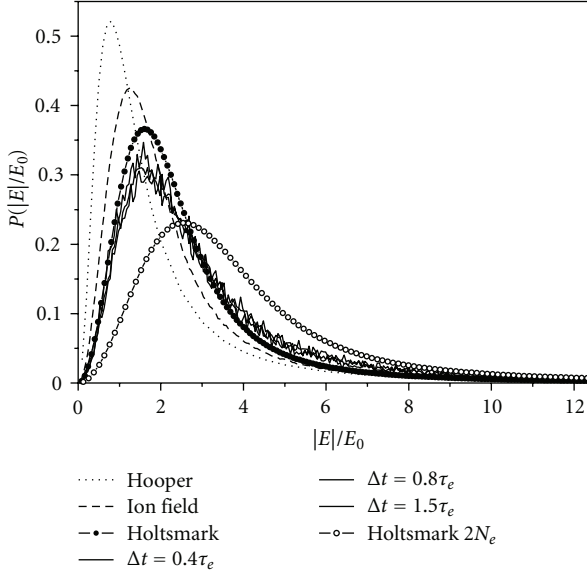


FIGURE 23: MD distributions at neutral emitters for slow component of total plasma microfield \mathcal{S} from [182] for $a = 0.8$ monotonously shifted to smaller reduced microfield values versus increasing intervals of time average Δt .

Astonishingly, the results of simulations in Figures 23 and 25 for slow component qualitatively coincide with previously obtained results [135–137] for heavy negatively charged particles in Figures 20 and 21. So, the main resume is that for instantaneous microfields, the Debye shielding is not realized, while the correlation between electrons and ions shifts the realistic distribution for slow component somewhere in between two Holtsmarkians corresponding to densities N_e and $2N_e$ in opposite direction from Hooper or Baranger results, corresponding to the static Debye screening model. However, additionally, it is seen that the ion field distribution function obtained from the slow component in the limit $\Delta t \rightarrow \infty$ interestingly differs from the Hooper result, thus showing that in this case the screening effect is not static either.

This shift also detects the electron contribution into the ionic distribution function. In Figure 24, the fast component distribution functions are shifted more far from the ordinate axis as the Δt increases. This is opposite to the behavior of the slow microfield component in Figure 23, which is shifted toward smaller fields while the Δt increases. The authors of [182] thus reasonably state that due to symmetry relations for $\Delta t \rightarrow \infty$, both the slow and fast MDF should converge to the same limit—common MDF. It should be noted that the authors of [182] soundly outline the characteristic time scales τ of processes for which the definitions of the fast and slow components are introduced. Of course, like in the works of BM, τ is related to inequality $\tau_e < \tau < \tau_i$ [182]. Resuming discussion of MD simulations in [182], it is worthy to remind earlier attempts of separation of slow and fast microfield components on the basis of rather vague consideration in [180], where no constructive instruments that could allow to

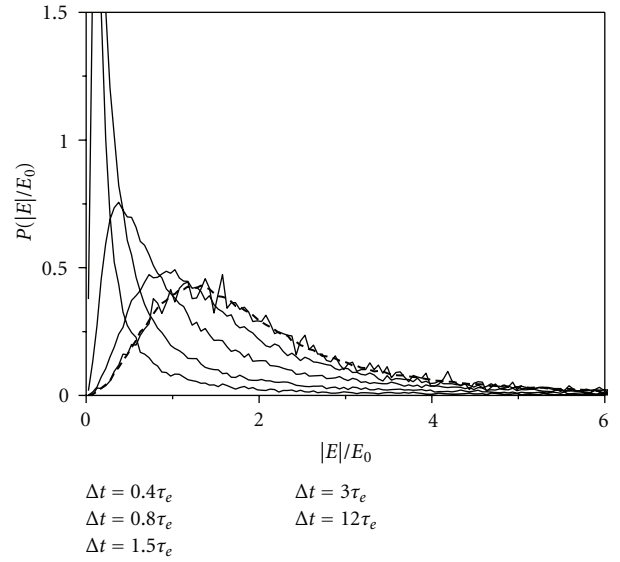


FIGURE 24: MD distribution functions at neutral emitters for fast component of total plasma microfield \mathcal{F} and for electron distribution function (dashes) from [182] for $a = 0.8$, monotonously shifted to larger reduced microfield values versus increasing intervals of time average Δt .

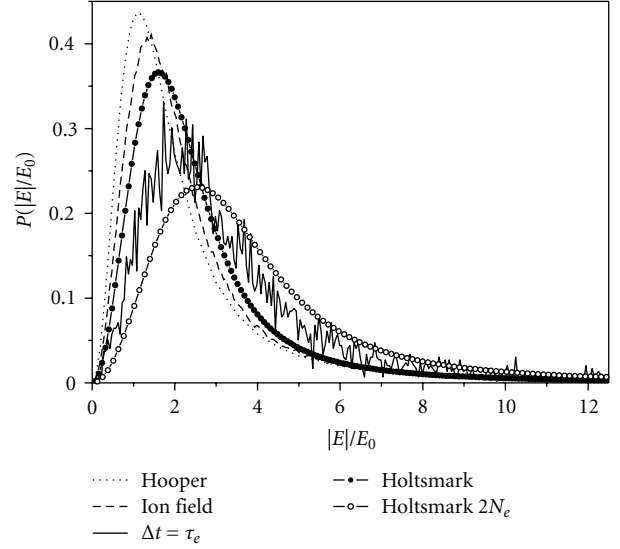


FIGURE 25: MD distribution function at neutral emitters for slow component of total plasma microfield from [182] for $a = 0.4$.

realize this general idea were proposed. In contrast, in [182], the logically clear *ab initio* MD simulation method enabling to perform this separation and study physical characteristics of slow and fast components of microfield is created.

The obtained in [182, 183] results put under doubt practically all ones, which were previously obtained on the subject, and bid their reconsideration and confirmation.

Due to its complexity the MD method is computationally time-consuming, and that is why more simple approach of modeling using the motion of particles along the prescribed

type of trajectories becomes sometimes more appropriate. This latter approach could assure the achievement of the same accuracy of calculations as MD using at least the quasi-particle models with the lesser expenditure of computational resources.

3.4. Modeling along Trajectories. The methods of computer simulations using prescribed type of trajectories for particles motion for modeling the microfield time evolution were developed in works of Voslamber and Stamm [101–103], Seidel and Stamm [101–103], Stamm-Smith-Talin and Cooper [104, 105], Gigosos and Cardenoso [140, 141], Hegerfeldt and Kesting [142], Gigosos et al. [143, 144], Kesting [145], and Stambulchik [190].

The method of modeling along the straight or hyperbolic trajectories also uses the finite number of particles N in the spherical cell of the finite radius “ R ” [140, 141], which is determined by given plasma density. The trajectory characteristics and localization of the particles inlet are sampled randomly [140, 141], and the particle velocity is sampled with the Maxwell distribution [140, 141]. The interval of velocities is split into N equal regions, having equal probability of sampling. To preserve isotropy, the orientation of collision plane is spread over angles evenly, and the range of impact parameters b is divided into N identical regions, having the equal sampling probability, in which the impact parameter value is generated using the following distribution:

$$P(b)db = \frac{3}{R^3} b\sqrt{R^2 - b^2} db. \quad (104)$$

The trajectory of collision is described in terms of the μ -ion model. After the particle leaves the cell, another particle instead of it is injected randomly for conserving the total number of particles in the cell [140, 141]. During this, the module of particle impulse is attributed to the new particle for the fulfillment of the conservation law of system energy. Moreover, the impact parameter of the new particle had to correspond to the same range of impact parameters, to which belonged the impact parameter of a particle that left the cell.

Simultaneously, the evolution of summary electric field of all particles produced at the place of test particle localization is followed. The final result was determined by the average over set of generated time histories, the number of which could approach up to 20000 for the achievement of appropriate accuracy not lower than $\sim 10\%$. In order to decrease the number of those histories, the average over the initial configurations is performed with special discretization, which is the request to reproduce with the help of this average the statistical microfield distribution functions. This method allowed to perform simultaneously the joint modeling of electric fields of ions and electrons [143, 144], which provides valuable tool for implementation in plasma spectroscopy, for example. The electric elementary ion field is approximated using Debye potential for the approximate account of electron-ion correlations.

Kesting managed to go beyond the frames of μ -ion model, and elaborated more complex procedure for modeling the motion of test particle [145] as well.

4. Kinetic Plasma Theory

4.1. Microfield Distribution Functions Accounting to Dynamical Electron Screening. As was mentioned, the construction of the distribution function and its properties depend on those time scales, during which the average over ensemble is performed [24, 25].

The application of microfield distribution, for example, in theory of spectral line broadening brings forward rather tough requests. For small values of detunings from the line center, the effective time of average are large, and the screening of ions by electrons could be considered static. However, with the extent of advancing into the line wings, the effective average times become shorter, and static screening does not have enough time to be settled [24, 25]. That is why the approaches are necessary in which the screening changes would be adequately accounted for in construction of microfield distribution functions. To some extent, this could be said about insufficiency of thermodynamic approach for this row of problems, as far as in thermodynamics two procedures of average could not exist at the same time.

One of the ways to this could be the representation of elementary electric field of separate field ion via the dielectric plasma permeability [3–6]:

$$\begin{aligned} \vec{E}_{\text{eff}}(\vec{r}; t) &= \frac{Ze}{2\pi^3 i} \int d^3 k \left\{ \frac{\vec{k}}{k^2 \epsilon_l(k, \omega)} + \frac{\vec{v} - (\vec{k}(\vec{k}\vec{v})/k^2)}{\omega[\epsilon_t(k, \omega) - (k^2 c^2 \omega^2)]} \right\} \\ &\cdot \exp[i(\vec{k}\vec{r} - \omega t)]. \end{aligned} \quad (105)$$

The study of this expression had showed that the extent of screening of the potential of field particle in collisionless plasma is the complex function of its velocity value and the distance to the point, where its electric field is detected, as well as the angle between the velocity direction and the radius-vector of observation point [125–127]. Meanwhile, the extent of potential screening decreases with the increase of velocity value and the radius-vector module. So, the Debye screening could be possible only for particles at rest [3–6, 125–127].

However, the straightforward implementation of this expression for derivation of the instantaneous microfield distribution function of low-frequency plasma microfield component is difficult, as this field depends on time and contains nonelectrostatic summand—the second term in the curly brackets, describing the transversal electric field. Moreover, the question arises what effects of interaction are included in dielectric permeability? Presently, the methods of account of plasma coupling effects (electron-electron or ion-ion correlations) to dielectric permeability still are not elaborated, and it is calculated in assumption of straight trajectories of free particles. One more general objection stems from the fact that per se the notion of dielectric permeability is related to macroscopic method of description, that is, it

is valid at scales $L \gg r_{D_{e,i}}$ and thereby unable in principle to describe processes on lesser scales, on which actually the microfield notion is introduced.

Nevertheless, the formal substitution of this expression in characteristic function is possible. As the notions and, moreover, the methods of calculations of correlations functions, depending on time, were not elaborated, in this case, one could speak about the calculations of microfield distribution functions only for noninteracting quasiparticles. However, it is known that this procedure reproduces the Debye screening of electric field [3–6].

For the separation of low-frequency component, the dielectric permeability should be represented as the sum of ion and electron contributions, and then the contribution of the poles residuals of ion summand should be taken. As the dynamical screening depends on the direction of particle velocity with respect to its radius vector to the test particle, as well as on the value of particle velocity [3–6, 125–127], this considerably complicates not only the calculations but also the interpretation of results.

The attempts of realization of this approach firstly are based on discarding the nonelectrostatic terms in the expression for the electric field of moving field particle in terms of dielectric permeability [82, 83]. In the paper of Ecker and Schumacher [82], it is shown that the contribution of nonelectrostatic terms converges to zero on time scale $t_{\min} \gg 1/\omega_{pi}$ that in truth exceeds the characteristic time scale of forming the distribution function of instantaneous low-frequency microfield component $1/\omega_{pi} \gg 1/(v_T N_i^{1/3}) \gg t_{\text{eff}} \gg 1/\omega_{pe}$ at least for ideal or weakly coupled plasmas. According to the authors' statement, it is equivalent to condition $N_i r_{D_e}^3 \gg 1$ that by now does not allow to consider the region of parameters $a \sim 1$ reasonably. Moreover, from the previous sections, it is evident that the distribution function corresponding to time scales $t_{\text{eff}} \gg 1/(v_T N_i^{1/3})$ no longer could describe the instantaneous distribution of individual component of ion microfield.

As one of their main results, the authors presume the demonstration of factorization of the total distribution function into two independent distributions of high-frequency and low-frequency microfield components. In assumption of straight path trajectories firstly the substitution $\omega = \vec{k} \cdot \vec{v}_{oi}$, corresponding to the major contribution, which is provided by the function $\epsilon_l^{-1}(\vec{k}; \omega)$, and then the change of variables $\vec{r}_{0i} + \vec{v}_{0i}t = \vec{r}$, which removes the explicit dependence on time [62] and means the transition to the intrinsic reference frame of the given particle, are performed. Then similar to Hooper [27–29] and later to APEX [40–44], the fitting parameter ξ is inserted inside the value of the Debye screening radius of separate statically screened ion. After that, it is assumed that the main term in the expansion of natural logarithm of characteristic function describes the microfield distribution with the elementary ion field in the form of statically screened according to Debye $\vec{E}^0(\vec{r}; \xi)$. The second term of expansion is chosen in the form $i\vec{q}[\vec{E}_{\text{eff}}(\vec{r}; \vec{v}) - \vec{E}^0(\vec{r}; \xi)]\exp[-i\vec{q} \cdot \vec{E}^0(\vec{r}; \xi)]$, defining some corrective function similar to the Baranger-Mozer papers. However, the corrective function does not contain

in the integrand any correlation functions in distinction from the Baranger-Mozer approach. The fitting parameter value ξ was determined from the condition of the optimal convergence of computations and turned out to be equal $\sqrt{3/2}$. The resulting distribution shifted with respect to the Baranger-Mozer distribution sideways small field values, but did not reach the Ecker-Müller distribution, which is localized still more nearer to the ordinate axis.

The other result, using this representation, was derived within implementation of some version of Green function formalism [83]. The distribution function in [83] depends not only on the reduced field value but also on the value of detuning from the line center with regard to problems of spectral lines broadening [1, 2]. In this work, the second nonelectrostatic summand in the expression for the field of single charge in terms of plasma dielectric permeability was discarded without any discussion or comments [83]. Regrettably, although the idea of the paper is physically sound, the derivation itself is not quite clear, and alas did not get confirmation in other papers.

In total, the results of this approach were not further developed and were not carried to the form that is necessary for practical calculations, and, moreover, there are certain doubts about the range of its validity.

The questions about time and spacial scales for fixing Debye screening in plasmas [125–127] again became the subject of detailed analytical and computational studies in the recent instructive works of Trofimovich and Krainov [84, 85]. However, alas up to now it is not clear how it would be possible to use these results in the theory of distribution functions. Nevertheless, it is evident that they are related to the functional choice of interaction potential and its dependence on space and time variables.

4.2. Microfields due to Plasma Fluctuations. The theory of plasma fluctuations has the whole row of interesting and useful general relations for the correlation functions of the current density, the charge density, the strengths of electrical and magnetic fields [3–6, 147]. Nevertheless, the physical settings that would allow within the fluctuations theory notions and formalism to construct the microfield distribution functions are unknown yet.

For the case of electrical fields in most general assumptions from the theory of fluctuations in plasma, it is possible to obtain the following expressions for the Fourier components of correlation functions of fluctuating electrical fields in isotropic plasmas $\langle E_j E_i \rangle_{\vec{k}, \omega}$ [4, 5]:

$$\begin{aligned} \langle E_j E_i \rangle_{\vec{k}, \omega} = & 8\pi \frac{\hbar}{\exp[(\hbar \omega)/T] - 1} \\ & \cdot \left\{ \frac{k_i k_j}{k^2} \frac{\text{Im } \epsilon_l}{|\epsilon_l|^2} + \left(\delta_{ij} - \frac{k_i k_j}{k^2} \right) \frac{\text{Im } \epsilon_t}{|\epsilon_t - \eta^2|^2} \right\}, \end{aligned} \quad (106)$$

where l, t are the indecies of longitudinal and transverse electrical fields correspondingly; $\epsilon(\omega, \vec{k})$ is the dielectric

permeability; $\eta = k c/\omega$ is the index of refraction of the plasma wave with the cyclic frequency ω and the wave vector \vec{k} in the isotropic case.

Up to the moment the dielectric function is known practically only for weakly coupled plasmas. Although for strongly coupled plasmas recently a row of model representations was developed for the dielectric function, this problem in total is not studied quite enough first of all due to the variety of physical conditions realizable in strongly coupled plasma [3–12, 148–159].

In the case of isothermal ideal isotropic classical plasmas $T \gg \hbar\omega$, this expression for $\langle E_j E_i \rangle_{\vec{k}, \omega}$ might be reduced for the Maxwell distributions over electrons and ions velocities to the form [4, 5]

$$\begin{aligned} & \langle E_j E_i \rangle_{\vec{k}, \omega} \\ &= \frac{32\pi^2}{\omega} \left\{ \frac{k_i k_j}{k^2} \frac{1}{|\epsilon_i|^2} \left(T_e \operatorname{Im} \kappa_l^e + T_i \operatorname{Im} \kappa_t^i \right) \right. \\ & \quad + \left(\delta_{ij} - \frac{k_i k_j}{k^2} \right) \frac{1}{|\epsilon_t - \eta^2|^2} \\ & \quad \cdot \left. \left(T_e \operatorname{Im} \kappa_t^e + T_i \operatorname{Im} \kappa_t^i \right) \right\}, \end{aligned} \quad (107)$$

where $T_{i,e}$ are ion and electron temperatures correspondingly; $\kappa^{e,i}(\omega, \vec{k})$ are the electron and ion electrical susceptibilities correspondingly.

The dielectric permeability of ideal collisionless plasma is determined by the expressions (compare with [4, 5])

$$\begin{aligned} \epsilon_l(k, \omega) &= 1 + \frac{1}{r_{\text{De}}^2 k^2} \left\{ 1 - \phi(z) + t [1 - \pi(\mu z)] + i\sqrt{\pi} z \right. \\ & \quad \cdot (\exp[-z^2] + t\mu \exp[-\mu^2 z^2]) \left. \right\}, \\ \epsilon_t(k, \omega) &= 1 - \frac{\omega_{pe}^2}{\omega^2} \left\{ \phi(z) + \frac{t}{\mu} \phi(\mu z) - i\sqrt{\pi} z \right. \\ & \quad \cdot \left. \left(\exp[-z^2] + \frac{t}{\mu} \exp[-\mu^2 z^2] \right) \right\}, \\ \phi(z) &= 2z \exp[-z^2] \int_0^z dz \exp[z^2], \\ \omega_{pe} &= \sqrt{\frac{4\pi e^2 n_e}{m}}, \\ z &= \sqrt{\frac{3}{2}} \frac{\omega}{kv_e}, \quad t = \frac{T_e}{T_i}, \quad \mu^2 = \frac{M}{m} \frac{T_e}{T_i}, \\ v_e^2 &= \frac{3T_e}{m}, \quad r_{\text{De}}^2 = \frac{T_e}{4\pi e^2 n_e}. \end{aligned} \quad (108)$$

The expressions for $\kappa^{e,i}(\omega, \vec{k})$ in the case of ideal collisionless plasma have the forms (compare with [4, 5])

$$\begin{aligned} \kappa_l^e(\omega, \vec{k}) &= \frac{1}{4\pi r_{\text{De}}^2 k^2} \{1 - \phi(z) + i\sqrt{\pi} z \exp(-z^2)\}, \\ \kappa_l^i(\omega, \vec{k}) &= \frac{t}{4\pi r_{\text{De}}^2 k^2} \{1 - \phi(\mu z) + i\sqrt{\pi} \mu z \exp(-\mu^2 z^2)\}, \\ \kappa_t^e(\omega, \vec{k}) &= -\frac{1}{4\pi} \frac{\omega_{pe}^2}{\omega^2} \{\phi(z) - i\sqrt{\pi} z \exp(-z^2)\}, \\ \kappa_t^i(\omega, \vec{k}) &= -\frac{t}{4\pi \mu} \frac{\omega_{pe}^2}{\omega^2} \{\phi(\mu z) - i\sqrt{\pi} z \exp(-\mu^2 z^2)\}. \end{aligned} \quad (109)$$

As it is known, all these expressions could be reproduced starting from the notions of elementary currents, produced by non-interacting between each other charged plasma particles moving randomly along straight line trajectories [3]. The generalization of these formulas and their asymptotic under account of collisions could be found in the kinetic approach for description of fluctuations in [6]. In spite of absence of interactions, these particles, nevertheless, create the Debye screening of the electric field in plasmas. Indeed, integrating over cyclic frequencies the expression for the correlation functions of microfields in the simplest case $T_i = T_e$ and converging it over indexes $i = j$, after the inverse Fourier transform, we obtain the expression [4, 5]

$$\langle E^2 \rangle_{\vec{r}} = 8\pi T \left\{ \delta(\vec{r}) + \frac{1}{8\pi r_{\text{De}}^2} \frac{\exp(-r/r_{\text{De}})}{r} \right\}. \quad (110)$$

The first summand in $\langle E^2 \rangle_{\vec{r}}$ contains the divergence at zero which is interpreted as being due to the absence of spacial correlations [6], whereas the integral from $\langle E^2 \rangle_{\vec{r}}$ over volume is finite and equal, being divided on 8π , to the energy content W per one structureless particle:

$$W = \oint_V d^3 r \frac{1}{8\pi} \langle E^2 \rangle_{\vec{r}} = \frac{3}{2} T. \quad (111)$$

This result again raises the question about proportions of contributions into the obtained density of plasma energy content $\langle E^2 \rangle_{\vec{r}}$ by plasma collective oscillations, which are forming the plasma dielectric permeability, and by the electrical fields from the individual particles that rapidly decrease on the scales larger than Debye radius.

As the plasma dielectric permeability is a macroscopic characteristic, the collective oscillations have macroscopic origin either. This means that the characteristic spacial scale of their variations at least for weakly coupled plasmas is much larger than the Debye radius. At less scales, these fields decay rapidly and thereby do not provide the essential contribution into the individual microfield component, whose scale of variation is less than the Debye radius in ideal plasmas.

As all derivations of these results were based on collective plasma oscillations, it would seem that it would be possible to state that there is no contribution from the individual component of the electric field, which in principle has

nonthermodynamic origin. However, on the other hand, these results could be derived just from simple notions about the straight line trajectories of particles, having the Maxwell distribution over velocities, and thus should correspond to the individual plasma microfield component. However, both statements are not quite correct as the energy is drawn from the same fixed source $(3/2)\mathcal{N}T$.

In truth, in order to make conclusion about the ratio of energy density between the collective and individual microfield components to $\langle E^2 \rangle_r$, it is necessary to study the contributions from resonance regions under integration of $\langle E_j E_i \rangle_{\vec{k},\omega}$ in the space (ω, \vec{k}) , which actually are responsible for collective plasma oscillations. Few examples of such studies could be found in textbooks on plasma physics [191, 192].

Nevertheless, still the certain difficulties with the notions about separation of individual and collective variables for Hamiltonian of Coulomb particles do exist even for the switched off interaction between them.

4.3. Dissolution Effect and Statistical Sums. One of the known problems in thermodynamics of plasma and gas is the divergence of statistical sums for bound states of partially ionized atoms and ions at arbitrary finite temperatures [7, 10].

However, in the external electric field, the upper excited atomic states are ionized due to the distortion of potential and nonequal to zero probability of penetration under the barrier so-called tunnel effect [146]. In plasma, the microfield plays the role of such external electric field, devastating the upper levels. This effect leads to the finite number of really existing excited states and ensures the convergence of statistical sums. The other physical consequence is the lowering of ionization potential, which influences on relation of equilibrium concentrations of atoms and ions, and thereby on the degree of plasma ionization [146, 148–159]. These tendencies both are visualized in observations by decreasing of spectral line intensities, originating from the upper levels to the extent of advancing to the continuum. This phenomenon conventionally is called as the dissolution effect of spectral lines.

The pointed out effects turn out to be very important for plasma equation of state. Ones of the first Hammer, Michalas [154–159] and Dappen [154–157] payed attention on the microfield influence on plasma equation of state. In recent works, the sensitivity of seismological Sun data treatment to the choice of microfield distribution functions was demonstrated [157], and the comparison of implementation of microfield distributions due to Hooper, APEX, and Holtsmark was performed.

Not all the questions in this complex problem are completely clear and actively disputed up to now (see, e.g., [158, 159, 161, 162]).

4.4. Microfield Influence on Rate Coefficients. The influence of microfield on probabilities of elementary processes in plasma leads to variation of the rate coefficients [146, 162], entering in the balance equations for populations of atomic levels.

This influence is known for processes of excitation and ionization (due to the lowering of ionization potential), charge exchange, photoionization, autoionization and dielectronic recombination (due to the levels structure change) [146], and so forth. The electrical field influences also on the absorption processes, the localization of continuum edge, bremsstrahlung, and other processes, which could in its turn determine the plasma thermodynamic characteristics, and, in particular, the equation of state. However, this subject, due to its extensiveness, complexity, and diversity, needs the special analysis that is beyond the frames of the present work (see, e.g., [146–159, 161, 162]).

5. Discussion

(i) It should be noted that convergence of cluster expansion series of Baranger-Mozer and Hooper, and so forth, for plasma microfield could not be recognized as rigorously proved. In fact, these methods are based on practical convergence of the terms of the first and second order of density for the logarithm of characteristic function. The next terms of expansion after the second cluster expansion term, corresponding to more higher orders over density is difficult to estimate strictly due to the lack of reliable data about correlation functions of the third order and more higher ones. Nevertheless, the results of these papers are physically obvious and do not contradict to existing experimental data.

(ii) Numerous works, in which the cluster expansion is built up with the help of diagrammatic technique, were not considered. In series of papers, there were attempts to renormalize electron-ion interaction, especially in the range of noticeable plasma nonideality.

However, due to the long-range character of Coulomb interaction in plasma, the convergence of renown Bogolubov-Born-Green-Kirkwood-Yvon (BBGKY) chain of equations [6–12] in this case is not rigorously proved [11, 12, 160] at least within the classic theory domain for point particles. The convergence of BBGKY chain in plasmas is possible only for modified Coulomb potential at small distances with the help of the introduction of strong repulsion or various forms of pseudopotentials [7–12, 160] or, in particular, for particles with finite sizes.

On the other hand, it is well known that the sum of only ring diagrams is quite sufficient to reproduce static Debye potential [7–12, 160]. However, in literature, devoted to derivations of cluster expansions of characteristic functions of plasma microfield distributions functions within diagrammatic technique, the results depend on what type of diagrams could be summed and calculated at least partially. The substantial analysis of these questions is a very complex problem and is beyond the scope of present consideration.

(iii) Remind, that the necessity to consider, namely, the conception of instantaneous distribution functions, which we adhere to in the present review, generally speaking, is also under debate. In this discussion, it is stated that test particle is a merely microprobe, detecting the state of a medium, which had enough time to be set long ago before the measurement process. Hence, from this point of view, the implementation

of methods of conventional thermodynamics is sufficient to perform averages. At the same time, the process of the test particle equilibration with the medium and its dynamics represent the separate problem, which has as thermodynamic as statistical aspects.

(iv) We have to recognize that rather complicated theory of joint distribution functions has a number of unresolved questions up to now, connected, for example, with treatment of the shifts of the microfield tensor of nonuniformity distributions [19–21, 35, 66, 67], which appear also during numerical modeling by Monte-Carlo method [37, 38]. These results hold even for the gas of Coulomb particles, and seemingly contradict to initial conditions of plasma isotropy [66, 67]. Meanwhile, these results also depend on the sequence of integration in the corresponding multidimensional integrals. All this did not get clear understanding so far.

(v) The recent results [182, 183] of *ab initio* MD joint simulations of plasma ion and electron fields, and the proposed procedure of their separation into slow and fast microfield components together with the study of its behavior versus the value of average time interval (see [182, 183] and Section 3.3) opens the new era in the investigations of plasma microfield properties and their applications. This will cause obviously serious reanalysis and reconsideration of many questions and notions. For example, it could have drastic impact on the possible magnitude of the aforementioned inhomogeneity effects due cancellation of contributions from ions and electrons, the extent of which could not be predicted from general consideration.

(vi) Thus we see that the whole row of calculations performed in quasistatic approximation and in MD simulations [135–137, 182, 184–189] demonstrate the significance of correlations between subsystems with opposite signs of charges and the necessity to develop and apply TCP models. The more realistic distributions are localized between Holtsmark for N_e and Holtsmark $2N_e$ distributions [182, 187, 188]. In TCP again, we face the divergence of the second microfield moment, which was made convergent in the Debye screened OCP model after divergence for the Holtsmark distribution of noninteracting field particles.

(vii) In consideration of thermodynamic properties as already was discussed earlier, the implementation of static screening notions within conventional thermodynamic ideas is quite sufficient. However, the model of Debye screening was criticized for many inconsistencies [46, 47, 154–156]. The discussion and search of more consistent models of screening and more realistic potentials in plasmas is still continuing (see, e.g., [193, 194] and references therein) as for static and for dynamic conditions [182].

(viii) In some cases, as the attentive reader could see, we preserved the title of articles in the reference list in attempt to underline its significance for the development of the subject and draw attention to their original results.

It should be noted that beside the covered in this review problems, there are also many other interesting ones (see recent reviews [195–198]) or other connected with microfield notion, regrettably not touched here. For example, these are an idea of “mean ion” [158], the so-called NNN distribution [161], the distribution of microfields due

to third particle, peculiarities of microfield distributions in dusty plasmas [163], and so on. At the same time, the choice of works in the reference list was based on some balanced merits: firstly, physical significance of ideas; secondly, adequately chosen formalism that does not reduce the work mainly to its study; thirdly, the final results available for applications. However, of course, the reader must know that this review is focused mainly on conceptual aspects of the problem and only a highly condensed sketch of original scientific papers, which contain much more detailed and ample information on particular studies.

Acknowledgments

The author thanks G. V. Sholin, V. S. Lisitsa, V. I. Kogan, A. N. Starostin, Yu. K. Zemtsov, E. A. Oks, M. D. Ginzburg, D. A. Shapiro, A. E. Bulyshev and A. E. Suvorov, D. Voslamber, D. Kelleher, H. R. Griem, J. Hey, J. Seidel, Nguyen Hoe, C. Stehlé, D. Gilles, Ch. Hooper, R. Stamm, V. Kesting, B. Jancovici, F. Perrot, G. Massacrier, B. Talin, A. Calisti, S. Ferri, G. Kalman, J. Dufty, D. Boercker, C. A. Iglesias, F. J. Rogers, R. W. Lee, R. Mancini, M. Zoppi, M.-M. Gombert, J. L. Lebowitz, D. P. Kilcrease, M. W. C. Dhama-wardana, M. A. Gigosos, M. A. Gonzalez, S. I. Yakovlenko, A. A. Knizhnik, I. L. Iosilevski, and F. Rosmej for cooperation, correspondence, explanations, and discussions on the subject during the last four decades. At the same time, the author’s point of view could differ from expertise of thanked above renown scientists. The author is grateful to Dr. Bernard Talin for permission to use the data from [182] before publication. It is a pleasure to thank V. Khudjakov, D. Nikolić, S. Djurović for generous valuable help in collecting literature, resolving LaTeX problems, and improving figures, and referees of IJS for valuable comments.

References

- [1] H. R. Griem, *Spectral Line Broadening by Plasmas*, Academic Press, New York, NY, USA, 1974.
- [2] I. I. Sobelman, *Introduction to Atomic Spectra*, Pergamon Press, Oxford, UK, 1972.
- [3] V. D. Shafranov, “Electromagnetic waves in plasmas,” in *Reviews on Plasma Physics*, M. Gosatomizdat, Ed., vol. 3, pp. 3–140, 1963.
- [4] N. Rostoker, “Fluctuations of a plasma,” *Nuclear Fusion*, vol. 1, pp. 101–120, 1961.
- [5] A. G. Sitenko, *Electromagnetic Fluctuations in Plasmas*, KhGU, Khar’kov, Ukraine, 1965.
- [6] A. I. Akhiezer, *Plasma Electrodynamics*, Nauka, Moscow, Russia, 1974.
- [7] A. Isihara, Ed., *Statistical Physics*, Academic Press, New York, NY, USA, 1971.
- [8] J.-P. Hansen and I. R. McDonald, *Theory of Simple Liquids*, Academic Press, New York, NY, USA, 1976.
- [9] M. Baus and J.-P. Hansen, “Statistical mechanics of simple coulomb systems,” *Physics Reports*, vol. 59, no. 1, pp. 1–94, 1980.
- [10] Ph. A. Martin, “Sum rules in charged fluids,” *Reviews of Modern Physics*, vol. 60, no. 4, pp. 1075–1127, 1988.

- [11] A. B. Schmidt, *Statistical Thermodynamics of Classical Plasmas*, Energoizdat, Moscow, Russia, 1991.
- [12] G. A. Martynov, *Fundamental Theory of Liquids*, Adam Hilger, New York, NY, USA, 1992.
- [13] E. Oks, "Advance in diagnostics for high-temperature plasmas based on the analytical result for the ion dynamical broadening of hydrogen spectral lines," *Physical Review E*, vol. 60, no. 3, pp. R2480–R2483, 1999.
- [14] J. W. Dufty, "The microfield formulation of spectral line broadening," in *Spectral Line Shapes*, B. Wende, Ed., vol. 1, pp. 41–61, W. de Gruyter, Berlin, Germany, 1981.
- [15] C. F. Hooper, "Electric microfield distribution functions: past and present," in *Spectral Line Shapes*, R. J. Exton, Ed., vol. 4, p. 161, Deepak, Hampton, UK, 1987.
- [16] J. W. Dufty, "Electric microfield distributions," in *Strongly Coupled Plasma Physics*, F. J. Rogers, Ed., p. 493, Plenum Press, New York, NY, USA, 1987.
- [17] V. S. Lisitsa, V. I. Kogan, and G. V. Sholin, "Broadening of spectral lines in plasmas," in *Reviews on Plasma Physics*, B. B. Kadomtsev and M. Energoatomizdat, Eds., vol. 13, pp. 205–261, 1984.
- [18] J. Holtsmark, "Über die verbreiterung von spektrallinien," *Annalen der Physik*, vol. 58, no. 4, pp. 577–630, 1919.
- [19] S. Chandrasekhar and J. von Neuman, "The statistics of the gravitational field arising from a random distribution of stars. I. The speed of fluctuations," *The Astrophysical Journal*, vol. 95, pp. 489–531, 1942.
- [20] S. Chandrasekhar and J. von Neuman, "The statistics of the gravitational field arising from a random distribution of stars II," *The Astrophysical Journal*, vol. 97, pp. 1–27, 1943.
- [21] S. Chandrasekhar, "Stochastic problems in physics and astronomy," *Reviews of Modern Physics*, vol. 15, no. 1, pp. 1–89, 1943.
- [22] G. Ecker, "Das Mikrofeld in Gesamtheiten mit Coulombscher Wechselwirkung," *Zeitschrift für Physik*, vol. 148, no. 5, pp. 593–606, 1957.
- [23] G. Ecker and K. G. Müller, "Plasmapolarisation und Trägerwechselwirkung," *Zeitschrift für Physik*, vol. 153, no. 3, pp. 317–330, 1958.
- [24] M. Baranger and B. Mozer, "Electric field distributions in an ionized gas," *Physical Review*, vol. 115, no. 3, pp. 521–525, 1959.
- [25] B. Mozer and M. Baranger, "Electric field distributions in an ionized gas. II," *Physical Review*, vol. 118, no. 3, pp. 626–631, 1960.
- [26] H. Pfennig and E. Trefftz, "Die Druckverbreiterung der diffusen Heliumlinien, Vergleich zwischen messung und Theorie im quasistatischen Bereich," *Zeitschrift für Naturforschung A*, vol. 21, p. 697, 1966.
- [27] C. F. Hooper Jr., "Electric microfield distributions in plasmas," *Physical Review*, vol. 149, no. 1, pp. 77–91, 1966.
- [28] C. F. Hooper Jr., "Low-frequency component electric microfield distributions in plasmas," *Physical Review*, vol. 165, no. 1, pp. 215–222, 1968.
- [29] C. F. Hooper Jr., "Asymptotic electric microfield distributions in low-frequency component plasmas," *Physical Review*, vol. 169, no. 1, pp. 193–195, 1968.
- [30] D. Bohm and D. Pines, "A collective description of electron interactions: II. Collective vs individual particle aspects of the interactions," *Physical Review*, vol. 85, pp. 338–353, 1952.
- [31] D. Bohm and D. Pines, "A collective description of electron interactions: III. Coulomb interactions in a degenerate electron gas," *Physical Review*, vol. 92, no. 3, pp. 609–625, 1953.
- [32] A. A. Broyles, "Stark fields from ions in a plasma," *Physical Review*, vol. 100, no. 4, pp. 1181–1187, 1955.
- [33] A. A. Broyles, "Calculation of fields on plasma ions by collective coordinates," *Zeitschrift für Physik*, vol. 151, pp. 187–201, 1958.
- [34] R. J. Tighe and C. F. Hooper, "Low-frequency electric microfield distributions in a plasma containing multiply-charged ions: extended calculations," *Physical Review A*, vol. 15, no. 4, pp. 1773–1779, 1977.
- [35] D. Gilles and A. Angelie, "Monte-Carlo distributions of electric microfield," *Annales de Physique*, vol. 11, no. 3, supplement 3, p. 157, 1986.
- [36] J. M. Caillol and D. Gilles, "Monte Carlo simulations of the Yukawa one-component plasmas," *Journal of Statistical Physics*, vol. 100, no. 5–6, pp. 933–947, 2000.
- [37] D. Gilles, "Calcul de la repartition statistique du microchamp électrique dans les plasmas," Internal CEA-Report, 1997.
- [38] D. Gilles, *Méthode de Monte-Carlo en Mécanique Statistique Appliquée à la Physique des Plasmas*, Laboratoire de Physique des Gaz et des Plasmas, Université Paris XI, Lecture Notes, Orsay, France, 1997.
- [39] A. Y. Potekhin, G. Chabrier, and D. Gilles, "Electric microfield distributions in electron-ion plasmas," *Physical Review E*, vol. 65, no. 3, Article ID 036412, 12 pages, 2002.
- [40] C. A. Iglesias, J. L. Lebowitz, and D. MacGowan, "Electric microfield distributions in strongly coupled plasmas," *Physical Review A*, vol. 28, no. 3, pp. 1667–1672, 1983.
- [41] C. A. Iglesias and J. L. Lebowitz, "Electric microfield distributions in multicomponent plasmas," *Physical Review A*, vol. 30, no. 4, pp. 2001–2004, 1984.
- [42] C. A. Iglesias, H. E. DeWitt, J. L. Lebowitz, D. MacGowan, and W. B. Hubbard, "Low-frequency electric microfield distributions in plasmas," *Physical Review A*, vol. 31, no. 3, pp. 1698–1702, 1985.
- [43] C. A. Iglesias, F. J. Rogers, R. Shepherd, et al., "Fast electric microfield distribution calculations in extreme matter conditions," *Journal of Quantitative Spectroscopy and Radiative Transfer*, vol. 65, no. 1–3, pp. 303–315, 2000.
- [44] J. W. Dufty, D. B. Boercker, and C. A. Iglesias, "Electric field distributions in strongly coupled plasmas," *Physical Review A*, vol. 31, no. 3, pp. 1681–1686, 1985.
- [45] H. Mayer, "Method of opacity calculations," Tech. Rep. LA-647, Los Alamos Scientific Laboratory, 1947.
- [46] M. W. C. Dharma-Wardana and F. Perrot, "Electric microfield distributions in plasmas of arbitrary degeneracy and density," *Physical Review A*, vol. 33, no. 5, pp. 3303–3313, 1986.
- [47] F. Perrot and M. W. C. Dharma-Wardana, "Ion correlations and ion microfields at impurities in dense plasmas," *Physical Review A*, vol. 41, no. 6, pp. 3281–3293, 1990.
- [48] G. H. Ecker and K. G. Fisher, "Individual and collective aspects of microfield distribution," *Zeitschrift für Naturforschung*, vol. 26a, pp. 1360–1365, 1971.
- [49] K.-H. Spatschek, "Collective contributions to the electric microfield distribution in a turbulent plasma," *Physics of Fluids*, vol. 17, no. 5, pp. 969–972, 1974.
- [50] E. A. Oks and G. V. Sholin, "Stark profiles of hydrogen lines in a plasma with low-frequency turbulence," *Zhurnal Tekhnicheskoi Fiziki*, vol. 46, pp. 254–264, 1976 (Russian).
- [51] H. H. Klein and N. A. Krall, "Probability distribution of electric fields in thermal and nonthermal plasmas," *Physical Review A*, vol. 8, no. 2, pp. 881–886, 1973.
- [52] E. A. Oks, *Plasma Spectroscopy with Quasi-Monochromatic Electric Fields*, M. Energoatomizdat, 1990.

- [53] A. V. Demura and G. B. Sholin, "Theory of asymmetry of hydrogen-line Stark profiles in dense plasma," *Journal of Quantitative Spectroscopy and Radiative Transfer*, vol. 15, no. 10, pp. 881–899, 1975.
- [54] A. V. Demura, *Certain questions in theory of hydrogen spectral lines broadening in plasmas*, Ph.D. thesis, I.V. Kurchatov Institute of Atomic Energy, Moscow, Russia, 1976.
- [55] A. V. Demura, "Theory of ion microfield distributions and its space and time derivatives in plasmas with complex ionization composition," preprint IAE-4632/6, TsNIIatominform, Moscow, Russia, pp. 1–17, 1988.
- [56] A. V. Demura, "First moments of joint distribution function of electric Ion microfield and it's spatial and time derivatives in a plasma with weak nonideality," in *Proceedings of the 9th International Conference on Spectral Line Shapes (ICSLS '88)*, Nicolas Copernicus University Press, Torun, Poland, 1988, abstract no. A39.
- [57] A. V. Demura and C. Stehlé, "Effects of microfield nonuniformity in dense plasmas," in *Spectral Line Shapes*, Vol. 8, D. May, J. Drummond, and E. Oks, Eds., vol. 328 of *AIP Conference Proceedings*, pp. 177–208, American Institute of Physics, New York, NY, USA, 1995.
- [58] A. V. Demura, D. Gilles, and C. Stehlé, "Comparative study of microfield nonuniformity in plasmas," *Journal of Quantitative Spectroscopy and Radiative Transfer*, vol. 54, no. 1-2, pp. 123–136, 1995.
- [59] C. Stehlé, D. Gilles, and A. V. Demura, "Asymmetry of Stark profiles. The microfield point of view," *The European Physical Journal D*, vol. 12, no. 2, pp. 355–367, 2000.
- [60] A. V. Demura, D. Gilles, and C. Stehlé, "Asymmetry of stark profiles in nonuniform fluctuating microfield," in *Spectral Line Shapes*, Vol. 11, J. Seidel, Ed., vol. 559 of *AIP Conference Proceedings*, pp. 99–107, American Institute of Physics, New York, NY, USA, 2001.
- [61] A. V. Demura and C. Stehlé, "Asymmetry in wings of stark profiles in dense plasmas," in *Spectral Line Shapes*, Vol. 11, J. Seidel, Ed., vol. 559 of *AIP Conference Proceedings*, pp. 111–113, American Institute of Physics, New York, NY, USA, 2001.
- [62] A. V. Demura, D. Gilles, and C. Stehlé, "On plasma statistics of microfield gradients and line asymmetries," in *Strongly Coupled Coulomb Systems*, G. J. Kalman, J. M. Rommel, and K. Blagoev, Eds., pp. 377–380, Plenum Press, New York, NY, USA, 1998.
- [63] R. F. Joyce, L. A. Woltz, and C. F. Hooper Jr., "Asymmetry of Stark-broadened Lyman lines from laser-produced plasmas," *Physical Review A*, vol. 35, no. 5, pp. 2228–2233, 1987.
- [64] J. Halenka, "Asymmetry of hydrogen lines in plasmas utilizing a statistical description of ion-quadrupole interaction in Mozer-Baranger limit," *Zeitschrift für Physik D*, vol. 16, no. 1, pp. 1–8, 1990.
- [65] D. P. Kilcrease, R. C. Mancini, and C. F. Hooper Jr., "Ion broadening of dense-plasma spectral lines including field-dependent atomic physics and the ion quadrupole interaction," *Physical Review E*, vol. 48, no. 5, pp. 3901–3913, 1993.
- [66] K. G. Müller, "Influence of field inhomogeneity on ionic line broadening," *Journal of Quantitative Spectroscopy and Radiative Transfer*, vol. 5, no. 2, pp. 403–423, 1965.
- [67] V. S. Millianchuk, thesis doctor of science, L'vov State University, L'vov, Ukraine, 1956.
- [68] M. S. Murillo, D. P. Kilcrease, and L. A. Collins, "Dense plasma microfield nonuniformity," *Physical Review E*, vol. 55, no. 5, pp. 6289–6292, 1997.
- [69] D. P. Kilcrease, M. S. Murillo, and L. A. Collins, "Theoretical and molecular dynamics studies of dense plasma microfield nonuniformity," *Journal of Quantitative Spectroscopy and Radiative Transfer*, vol. 58, no. 4–6, pp. 677–686, 1997.
- [70] D. P. Kilcrease and M. S. Murillo, "The ion electric microfield gradient joint probability distribution function for dense plasmas," *Journal of Quantitative Spectroscopy and Radiative Transfer*, vol. 65, no. 1–3, pp. 343–352, 2000.
- [71] C. A. Iglesias and C. F. Hooper, "Quantum corrections to the low-frequency-component microfield distributions," *Physical Review A*, vol. 25, no. 3, pp. 1632–1635, 1982.
- [72] B. Held, C. Deutsch, and M. M. Gombert, "Low-frequency electric microfield in dense and hot multicomponent plasmas," *Physical Review A*, vol. 29, no. 2, pp. 880–895, 1984.
- [73] B. Held and P. Pignolet, "Low-frequency electric microfield calculations by iterative methods," *Journal de Physique*, vol. 48, no. 11, pp. 1951–1961, 1987.
- [74] V. I. Kogan, "Broadening of spectral lines in high temperature plasmas," in *Plasma Physics and Problem of Controlled Thermonuclear Reactions*, M. A. Leontovich, Ed., vol. 4, pp. 258–304, AS USSR, 1958.
- [75] L. J. Roszman and C. F. Hooper, "Distribution of the time-dependent microfield in a plasma," *Physical Review A*, vol. 7, no. 6, pp. 2121–2130, 1973.
- [76] A. Alastuey, J. L. Lebowitz, and D. Levesque, "Time-dependent statistical properties of the electric microfield seen by a neutral radiator," *Physical Review A*, vol. 43, no. 6, pp. 2673–2693, 1991.
- [77] J. W. Duffy and L. Zogaib, "Electric-field dynamics in plasmas: theory," *Physical Review A*, vol. 44, no. 4, pp. 2612–2624, 1991.
- [78] J. W. Duffy and L. Zogaib, "Short-time electric-field dynamics at a neutral point in strongly coupled plasmas," *Physical Review E*, vol. 47, no. 4, pp. 2958–2961, 1993.
- [79] M. Berkovsky, J. W. Duffy, A. Calisti, R. Stamm, and B. Talin, "Nonlinear response of electric fields at a neutral point," *Physical Review E*, vol. 51, no. 5, pp. 4917–4929, 1995.
- [80] A. V. Demura, "Instantaneous joint distributions of ion microfield and its time derivatives and effects of dynamical friction in plasmas," *Journal of Experimental and Theoretical Physics*, vol. 83, pp. 60–72, 1996.
- [81] A. V. Demura, "Microfield fluctuations in plasmas with low frequency oscillations," in *Proceedings of the 19th International Conference on Phenomena in Ionized Gases (ICPIG '90)*, vol. 2, pp. 352–353, Beograd, Serbia, 1990.
- [82] G. H. Ecker and A. Schumacher, "Dynamic screening model of the electric microfield distribution," *Zeitschrift für Naturforschung A*, vol. 30, p. 413, 1975.
- [83] L. E. Pargamanik and M. D. Ginzburg, "Distribution function of ionic microfields in plasma," *Ukraine Physical Journal*, vol. 22, pp. 938–943, 1977.
- [84] E. E. Trofimovich and V. P. Krainov, "Setting in of Debye screening in a Maxwellian plasma," *Zhurnal Eksperimentalnoi i Teoreticheskoi Fiziki*, vol. 102, pp. 71–77, 1992.
- [85] E. E. Trofimovich and V. P. Krainov, "Shielding of a moving charge in a Maxwellian plasma," *Zhurnal Eksperimentalnoi i Teoreticheskoi Fiziki*, vol. 104, pp. 3971–2329, 1993.
- [86] U. Frisch and A. Brissaud, "Theory of Stark broadening—I soluble scalar model as a test," *Journal of Quantitative Spectroscopy and Radiative Transfer*, vol. 11, no. 12, pp. 1753–1766, 1971.

- [87] A. Brissaud and U. Frisch, "Theory of Stark broadening-II exact line profile with model microfield," *Journal of Quantitative Spectroscopy and Radiative Transfer*, vol. 11, no. 12, pp. 1767–1783, 1971.
- [88] A. Brissaud and U. Frisch, "Solving linear stochastic differential equations," *Journal of Mathematical Physics*, vol. 15, no. 5, pp. 524–534, 1973.
- [89] A. Brissaud, C. Goldbach, J. Leorat, A. Mazure, and G. Nollez, "On the validity of the model microfield method as applied to Stark broadening of neutral lines," *Journal of Physics B*, vol. 9, no. 7, pp. 1129–1146, 1976.
- [90] A. Brissaud, C. Goldbach, J. Leorat, A. Mazure, and G. Nollez, "Application of the model microfield method to Stark profiles of overlapping and isolated neutral lines," *Journal of Physics B*, vol. 9, no. 7, pp. 1147–1162, 1976.
- [91] J. Seidel, "Effects of ion motion on hydrogen stark profiles," *Zeitschrift für Naturforschung A*, vol. 32a, pp. 1207–1214, 1977.
- [92] J. Seidel, "Hydrogen stark broadening by ion impacts on moving emitters," *Zeitschrift für Naturforschung A*, vol. 34a, pp. 1385–1397, 1979.
- [93] J. Seidel, "Theory of hydrogen stark broadening," in *Spectral Line Shapes*, B. Wende, Ed., vol. 1, pp. 3–39, Walter de Gruyter, Berlin, Germany, 1981.
- [94] C. Stehlé, "Stark Profiles of He^+ ," *Astronomy and Astrophysics*, vol. 292, p. 699, 1994.
- [95] D. B. Boercker, C. A. Iglesias, and J. W. Dufty, "Radiative and transport properties of ions in strongly coupled plasmas," *Physical Review A*, vol. 36, no. 5, pp. 2254–2264, 1987.
- [96] M. A. Berkovsky, J. W. Dufty, A. Calisti, R. Stamm, and B. Talin, "Electric field dynamics at a charged point," *Physical Review E*, vol. 54, no. 4, pp. 4087–4097, 1996.
- [97] S. Sorge, S. Günter, and G. Röpke, "On the consequences of a realistic conditional covariance in MMM-calculations," *Journal of Physics B*, vol. 32, no. 3, pp. 675–681, 1999.
- [98] A. Könes, S. Günter, and G. Röpke, "On the time evolution of the ionic microfield in plasmas," *Journal of Physics B*, vol. 29, p. 6091, 1999.
- [99] B. Talin, A. Calisti, S. Ferri, et al., "Ground work supporting the codes based upon the frequency fluctuation model," *Journal of Quantitative Spectroscopy and Radiative Transfer*, vol. 58, no. 4–6, pp. 953–964, 1997.
- [100] B. Talin, A. Calisti, S. Ferri, C. Mossé, and B. Talin, "Frequency fluctuation model survey," in *Spectral Line Shapes, Vol. 12*, C. Back, Ed., vol. 645 of *AIP Conference Proceedings*, pp. 247–251, American Institute of Physics, New York, NY, USA, 2002.
- [101] R. Stamm and D. Voslamber, "On the role of ion dynamics in the stark broadening of hydrogen lines," *Journal of Quantitative Spectroscopy and Radiative Transfer*, vol. 22, no. 6, pp. 599–609, 1979.
- [102] J. Seidel and R. Stamm, "Effects of radiator motion on plasma-broadened hydrogen Lyman- β ," *Journal of Quantitative Spectroscopy and Radiative Transfer*, vol. 27, no. 5, pp. 499–503, 1982.
- [103] R. Stamm, "Simulation studies of the dynamics of plasma microfields," in *Spectral Line Shapes*, K. Burnett, Ed., vol. 2, pp. 3–29, Walter de Gruyter, Berlin, Germany, 1983.
- [104] E. W. Smith, R. Stamm, and J. Cooper, "Discussion of the conditional-probability function for electric fields in a plasma," *Physical Review A*, vol. 30, no. 1, pp. 454–467, 1984.
- [105] R. Stamm, E. W. Smith, and B. Talin, "Study of hydrogen Stark profiles by means of computer simulation," *Physical Review A*, vol. 30, no. 4, pp. 2039–2046, 1984.
- [106] E. L. Pollock and W. C. Weisheit, "Local fields in strongly coupled plasmas," in *Spectral Line Shapes*, F. Rostas, Ed., vol. 3, p. 181, W. de Gruyter, New York, NY, USA, 1985.
- [107] R. Stamm, B. Talin, E. L. Pollock, and C. A. Iglesias, "Ion-dynamic effects on the line shapes of hydrogenic emitters in plasmas," *Physical Review A*, vol. 34, no. 5, pp. 4144–4152, 1986.
- [108] A. V. Anufrienko, A. E. Bulyshev, A. L. Godunov, et al., "Nonlinear interference effects and ion dynamics in the kinetic theory of stark broadening of the spectral lines of multicharged ions in a dense plasma," *Journal of Experimental and Theoretical Physics*, vol. 78, pp. 219–227, 1993.
- [109] A. E. Bulyshev, A. V. Demura, V. S. Lisitsa, A. N. Starostin, A. E. Suvorov, and I. I. Yakunin, "Redistribution function for resonance radiation in a hot dense plasma," *Journal of Experimental and Theoretical Physics*, vol. 81, pp. 113–121, 1995.
- [110] S. G. Brush, H. L. Sahlin, and E. Teller, "Monte Carlo study of a one-component plasma. I," *The Journal of Chemical Physics*, vol. 45, no. 6, pp. 2102–2118, 1966.
- [111] V. M. Zamalin, G. E. Norman, and V. S. Filinov, *Monte-Carlo Method in Statistical Thermodynamics*, Nauka, Moscow, Russia, 1977.
- [112] P. H. Acioli, "Review of quantum Monte Carlo methods and their applications," *Journal of Molecular Structure*, vol. 394, no. 2–3, pp. 75–85, 1997.
- [113] I. K. Kamilov, A. K. Murtazaev, and Kh. K. Aliev, "Monte Carlo studies of phase transitions and critical phenomena," *Uspekhi Fizicheskikh Nauk*, vol. 169, no. 7, p. 795, 1999 (Russian).
- [114] P. P. Ewald, "Die berechnung optischer und eletrostatischer gitterpotentiale," *Annals of Physics*, vol. 64, pp. 253–287, 1921.
- [115] C. Kittel, *Introduction to Solid State Physics*, John Wiley & Sons, New York, NY, USA, 1986.
- [116] P. Hohenberg and W. Kohn, "Inhomogeneous electron gas," *Physical Review B*, vol. 136, no. 3, pp. B864–B871, 1964.
- [117] W. Kohn and L. J. Sham, "Self-consistent equations including exchange and correlation effects," *Physical Review A*, vol. 140, no. 4, pp. A1133–A1138, 1965.
- [118] F. Perrot and M. W. C. Dharma-Wardana, "Exchange and correlation potentials for electron-ion systems at finite temperatures," *Physical Review A*, vol. 30, no. 5, pp. 2619–2626, 1984.
- [119] F. Perrot and M. W. C. Dharma-Wardana, "Embedding an iron atom in a plasma: influence of the host plasma on the photoeffect," *Physical Review A*, vol. 31, no. 2, pp. 970–979, 1985.
- [120] J. Chihara, "Dharma-wardana Perrot theory and the quantal hypernetted-chain equation for strongly coupled plasmas," *Physical Review A*, vol. 44, no. 2, pp. 1247–1256, 1991.
- [121] G. Massacrier, "Self-consistent schemes for the calculation of ionic structures and populations in dense plasmas," *Journal of Quantitative Spectroscopy and Radiative Transfer*, vol. 51, no. 1–2, pp. 221–228, 1994.
- [122] R. Singh and B. M. Deb, "Developments in excited-state density functional theory," *Physics Report*, vol. 311, no. 2, pp. 47–94, 1999.

- [123] W. Kohn, “Nobel lecture: electronic structure of matter—wave functions and density functional,” *Reviews of Modern Physics*, vol. 71, no. 5, pp. 1253–1266, 1999.
- [124] F. J. Rojers, “Integral-equation method for partially ionized plasmas,” *Physical Review A*, vol. 29, no. 2, pp. 868–879, 1984.
- [125] A. A. Vlasov, *Theory of Many Particles*, Gostekhizdat, Moscow, Russia, 1950.
- [126] A. A. Vlasov, *Statistical Distribution Functions*, Nauka, Moscow, Russia, 1966.
- [127] A. A. Vlasov, *Nonlocal Statistical Mechanics*, Nauka, Moscow, Russia, 1978.
- [128] R. S. Cohen, L. Spitzer Jr., and P. McR. Routly, “The electrical conductivity of an ionized gas,” *Physical Review A*, vol. 80, no. 2, pp. 230–238, 1950.
- [129] V. I. Kogan, “Fluctuating microfield and multiple collisions in gas of charged (or gravitating) particles,” *Doklady USSR*, vol. 135, p. 1374, 1960.
- [130] M. Rosenbluth and N. Rostoker, “Test particles in a completely ionized plasma,” *Physics of Fluids*, vol. 3, no. 1, pp. 1–14, 1960.
- [131] M. N. Rosenbluth and N. Rostoker, “Scattering of electromagnetic waves by a nonequilibrium plasma,” *Physics of Fluids*, vol. 5, no. 7, pp. 776–788, 1962.
- [132] J. B. Taylor, “Electric field correlation and plasma dynamics,” *Physics of Fluids*, vol. 3, no. 5, pp. 792–796, 1960.
- [133] M. Lewis, “Stark broadening of spectral lines by high-velocity charged particles,” *Physical Review A*, vol. 121, no. 2, pp. 501–505, 1961.
- [134] S. N. Gordienko, “Multiparticle nature of collisions in plasma and a unique feature of Coulomb interaction,” *Fizika Plazmy*, vol. 26, no. 6, pp. 519–528, 2000 (Russian).
- [135] S. A. Majorov, A. N. Tkachev, and S. I. Yakovlenko, “Thermodynamic parameters and distributions of instantaneous microfield values in nonideal plasmas,” *Doklady USSR*, vol. 290, no. 1, pp. 106–109, 1988.
- [136] S. A. Majorov, A. N. Tkachev, and S. I. Yakovlenko, “Thermodynamic parameters and debye screening in coulomb gas with small numbers of particles in debye sphere,” *Pisma v ZhTF*, vol. 14, no. 4, pp. 354–359, 1988.
- [137] S. A. Majorov, A. N. Tkachev, and S. I. Yakovlenko, “Modeling of fundamental Coulomb plasmas properties by method of dynamics of many particles,” in *Nonequilibrium Plasma of Multiply Charged Ions*, vol. 40 of *Proceedings of General Physics Institute of Russian Academy of Science*, pp. 4–43, Nauka, Moscow, Russia, 1992.
- [138] B. Talin, A. Calisti, and J. Dufty, “Classical description of electron structure near a positive ion,” *Physical Review E*, vol. 65, no. 5, Article ID 056406, 11 pages, 2002.
- [139] B. Talin, E. Dufour, A. Calisti, et al., “Molecular dynamics simulation for modelling plasma spectroscopy,” *Journal of Physics A*, vol. 36, no. 22, pp. 6049–6056, 2003.
- [140] M. A. Gigosos and V. Cardenoso, “Study of the effects of ion dynamics on Stark profiles of Balmer- α and - β lines using simulation techniques,” *Journal of Physics B*, vol. 20, no. 22, pp. 6005–6019, 1987.
- [141] M. A. Gigosos and V. Cardenoso, “New plasma diagnosis tables of hydrogen Stark broadening including ion dynamics,” *Journal of Physics B*, vol. 29, no. 20, pp. 4795–4838, 1996.
- [142] G. C. Hegerfeldt and V. Kesting, “Collision-time simulation technique for pressure-broadened spectral lines with applications to Ly- α ,” *Physical Review A*, vol. 37, no. 5, pp. 1488–1496, 1988.
- [143] A. Barbés, M. A. Gigosos, and M. Á. González, “Analysis of the coupling between impact and quasistatic field mechanisms in Stark broadening,” *Journal of Quantitative Spectroscopy and Radiative Transfer*, vol. 68, no. 6, pp. 679–688, 2001.
- [144] M. A. Gigosos, M. Á. González, and V. Cardeñoso, “Computer simulated Balmer- α , - β and - γ Stark line profiles for non-equilibrium plasmas diagnostics,” *Spectrochimica Acta*, vol. 58, no. 8, pp. 1489–1504, 2003.
- [145] V. Kesting, “Joint stark-doppler broadening of hydrogen lines in plasma,” in *Spectral Line Shapes*, R. Stamm and B. Talin, Eds., vol. 7, pp. 103–117, Science Nova, New York, NY, USA, 1993.
- [146] L. A. Bureeva and V. S. Lisitsa, *Perturbed Atom*, Izdat, Moscow, Russia, 1997.
- [147] M. L. Levin and S. M. Rytov, *Theory of Equilibrium Thermal Fluctuations in Electrodynamics*, Nauka, Moscow, Russia, 1967.
- [148] L. M. Biberman, V. S. Vorob’ev, and I. T. Yakubov, *Kinetics of Non-Equilibrium Low Temperature Plasmas*, Nauka, Moscow, Russia, 1982.
- [149] G. E. Norman and A. N. Starostin, “Thermodynamics of a strongly nonideal plasma,” *Teplofizika Visokikh Temperatur*, vol. 8, no. 2, pp. 381–408, 1970.
- [150] V. S. Vorob’ev and A. A. Likal’ter, “Physical properties of strongly coupled plasmas,” in *Plasma Chemistry*, B. M. Smirnov, Ed., vol. 15, pp. 163–208, Energoatomizdat, Moscow, Russia, 1989.
- [151] V. E. Fortov, I. T. Yakubov, and A. G. Krapak, *Physics of Strongly Coupled Plasma*, Clarendon Press, Oxford, UK, 2006.
- [152] L. P. Kudrin, *Statistical Plasma Physics*, Atomizdat, Moscow, Russia, 1974.
- [153] W. Ebeling, W. D. Kraeft, and D. Kremp, *Theory of Bound States and Ionization Equilibrium in Plasmas and Solids*, Academie, Berlin, Germany, 1976.
- [154] D. G. Hummer and D. Mihalas, “The equation of state for stellar envelopes. I. An occupation probability formalism for the truncation of internal partition functions,” *Astrophysical Journal*, vol. 331, pp. 794–814, 1988.
- [155] D. Mihalas, W. Däppen, and D. G. Hummer, “The equation of state for stellar envelopes. II. Algorithm and selected results,” *Astrophysical Journal*, vol. 331, pp. 815–825, 1988.
- [156] W. Däppen, D. Mihalas, D. G. Hummer, and B. W. Mihalas, “The equation of state for stellar envelopes. III. Thermodynamic quantities,” *Astrophysical Journal*, vol. 332, pp. 261–270, 1988.
- [157] A. Nayfonov, W. Däppen, D. G. Hummer, and D. Mihalas, “The MHD equation of state with post-Holtsmark microfield distributions,” *Astrophysical Journal*, vol. 526, no. 1, pp. 451–464, 1999.
- [158] D. V. Fisher and Y. Maron, “Effective statistical weights of bound states in plasmas,” *European Physical Journal D*, vol. 18, no. 1, pp. 93–111, 2002.
- [159] W. Ebeling and S. Hilbert, “On Saha’s equation for partially ionised plasmas and Onsager’s bookkeeping rule,” *European Physical Journal D*, vol. 20, no. 1, pp. 93–101, 2002.
- [160] K. P. Gurov, *Basics of Kinetic Theory*, Mir, Moscow, Russia, 1966.
- [161] D. V. Fisher and Y. Maron, “Statistics of inter-particle distances and angles in plasmas,” *European Physical Journal D*, vol. 14, no. 3, pp. 349–359, 2001.
- [162] M.-Y. Song and Y.-D. Jung, “Screening and collective effects on electron-impact excitation of hydrogen-like ions in nonideal plasmas,” *Journal of Physics B*, vol. 36, no. 10, pp. 2119–2128, 2003.

- [163] A. Bouchoule, Ed., *Dusty Plasmas Physics, Chemistry and Technological Impacts in Plasma Processing*, John Wiley & Sons, New York, NY, USA, 1999.
- [164] G. Peach, "Theory of the pressure broadening and shift of spectral lines," *Advances in Physics*, vol. 30, no. 3, pp. 367–474, 1981.
- [165] F. Lado and J. W. Dufty, "Charge distribution in plasmas with field constraint," *Physical Review A*, vol. 36, no. 5, pp. 2333–2337, 1987.
- [166] J. P. Hansen, "Statistical mechanics of dense ionized matter. I. Equilibrium properties of the classical one-component plasma," *Physical Review A*, vol. 8, no. 6, pp. 3096–3109, 1973.
- [167] F. J. Rogers, D. A. Young, H. E. Dewitt, and M. Ross, "One-component plasma structure factor in tabular form," *Physical Review A*, vol. 28, no. 5, pp. 2990–2992, 1983.
- [168] A. V. Demura, V. S. Lisitsa, and G. V. Sholin, "Effect of reduced mass in stark broadening of hydrogen lines," *Journal of Experimental and Theoretical Physics*, vol. 46, pp. 209–215, 1977.
- [169] H. R. Griem, "Broadening of the Lyman- α line of hydrogen by low-frequency electric fields in dense plasma," *Physical Review A*, vol. 20, no. 2, pp. 606–615, 1979.
- [170] H. R. Griem and G. D. Tsakiris, "Broadening of the Lyman- β line of hydrogen by low-frequency electric fields in dense plasma," *Physical Review A*, vol. 25, no. 2, pp. 1199–1202, 1982.
- [171] R. Cauble and H. R. Griem, "Broadening of Lyman lines of hydrogen and hydrogenic ions by low-frequency fields in dense plasmas," *Physical Review A*, vol. 27, no. 6, pp. 3187–3199, 1983.
- [172] J. D. Hey and H. R. Griem, "Central structure of low-n Balmer lines in dense plasmas," *Physical Review A*, vol. 12, no. 1, pp. 169–185, 1975.
- [173] J. D. Hey, "Ion dynamical corrections to the Holtsmark theory of spectral line broadening," *Transactions of the Royal Society of South Africa*, vol. 42, part 1, pp. 81–101, 1976.
- [174] H. Margenau and M. Lewis, "Structure of spectral lines from plasmas," *Reviews of Modern Physics*, vol. 31, p. 56, 1983.
- [175] G. J. Dalenoort, "The Holtsmark-continuum model for the statistical description of a plasma," *Zeitschrift für Physik*, vol. 248, no. 1, pp. 22–40, 1971.
- [176] R. Gans, "Das elektrische molekularfeld," *Annalen der Physik*, vol. 66, p. 396, 1921.
- [177] K. Weise, "The probability distributions of the electric and magnetic microfield in a relativistic plasma," *Zeitschrift für Physik*, vol. 212, no. 5, pp. 458–466, 1968.
- [178] K. Hunger and R. W. Larenz, "Das mikrofeld im plasma," *Zeitschrift für Physik*, vol. 163, no. 3, pp. 245–261, 1961.
- [179] V. I. Kogan and A. D. Selidovkin, "About fluctuating microfield in system of charged particles," *Beiträge aus der Plasma Physik*, vol. 9, no. 3, pp. 199–216, 1969.
- [180] S. Alexiou, "Collective coordinates for ion dynamics," *Journal of Quantitative Spectroscopy and Radiative Transfer*, vol. 54, no. 1-2, pp. 1–26, 1995.
- [181] S. Alexiou, A. Calisti, P. Gauthier, et al., "Aspects of plasma spectroscopy: recent advances," *Journal of Quantitative Spectroscopy and Radiative Transfer*, vol. 58, no. 4–6, pp. 399–412, 1997.
- [182] A. Calisti, S. Ferri, C. Mossé, et al., "Slow and fast microfield components in warm and dense hydrogen plasmas," <http://arxiv1.library.cornell.edu/abs/0710.2091v1>.
- [183] A. Calisti, S. Ferri, C. Mossé, et al., "Electric microfield in simulated two component plasmas," in *Spectral Line Shapes*, Vol. 15, M. A. Gigosos and M. Á. González, Eds., vol. 1058 of *AIP Conference Proceedings*, pp. 27–33, Science Nova, New York, NY, USA, 2008.
- [184] H. B. Nersisyan, C. Toepffer, and G. Zwicknagel, "Microfield distributions in strongly coupled two-component plasmas," *Physical Review E*, vol. 72, no. 3, Article ID 036403, 14 pages, 2005.
- [185] H. B. Nersisyan and G. Zwicknagel, "Microfield distributions in a classical two-component plasma," *Journal of Physics A*, vol. 39, no. 17, pp. 4677–4681, 2006.
- [186] H. B. Nersisyan, D. A. Osipyan, and G. Zwicknagel, "Renormalized cluster expansion of the microfield distribution in strongly coupled two-component plasmas," *Physical Review E*, vol. 77, no. 5, Article ID 056409, 2008.
- [187] X.-Z. Yan and S. Ichimaru, "Theory of interparticle correlations in dense, high-temperature plasmas. VI. Probability densities of the electric microfields," *Physical Review A*, vol. 34, no. 3, pp. 2167–2172, 1986.
- [188] J. Ortner, I. Valuev, and W. Ebeling, "Electric microfield distribution in two-component plasmas. Theory and simulations," *Contributions to Plasma Physics*, vol. 40, no. 5-6, pp. 555–568, 2000.
- [189] S. Laulan, C. Blancard, and G. Faussurier, "Fast electric microfield distribution calculations in strongly coupled Yukawa plasmas," *High Energy Density Physics*, vol. 4, no. 3-4, pp. 131–141, 2008.
- [190] E. Stambulchik and Y. Maron, "A study of ion-dynamics and correlation effects for spectral line broadening in plasma: K-shell lines," *Journal of Quantitative Spectroscopy and Radiative Transfer*, vol. 99, pp. 730–749, 2006.
- [191] N. A. Krall and A. W. Trivelpiece, *Principles of Plasma Physics*, McGraw-Hill, New York, NY, USA, 1973.
- [192] S. Ichimaru, *Basic Principles of Plasma Physics*, Benjamin, Reading, Mass, USA, 1973.
- [193] A. A. Mihajlov, Y. Vitel, and Lj. M. Ignjatović, "The new screening characteristics of strongly non-ideal and dusty plasmas—part 1: single-component systems," *High Temperature*, vol. 46, no. 6, pp. 737–745, 2008.
- [194] A. A. Mihajlov, Y. Vitel, and Lj. M. Ignjatović, "The new screening characteristics of strongly non-ideal and dusty plasmas—part 2: two-component systems," *High Temperature*, vol. 47, no. 1, pp. 1–12, 2009.
- [195] A. V. Demura, "Statistical and thermodynamical aspects of microfield conception in plasmas," in *Encyclopedia of Low Temperature Plasmas: Volume II, Thermodynamics of Plasma*, I. Iosilevski and A. Starostin, Eds., pp. 163–202, Fizmatlit, Moscow, Russia, 2004.
- [196] A. V. Demura and D. Gilles, "Overview of plasma microfield in Stark broadening of spectral lines," in *Proceedings of the 17th International Conference on Spectral Line Shapes*, E. Dalimier, Ed., pp. 121–128, Frontier Group, Paris, France, 2004.
- [197] A. V. Demura, "Evolution of plasma microfield notion," in *Proceedings of the 22nd Summer School and International Symposium on Physics of Ionized Gases (SPIG '04)*, L. Hadzievski, T. Grozdanov, and N. Bibic, Eds., vol. 740 of *AIP Conference Proceedings*, pp. 297–308, AIP, Bajina Basta, Serbia and Montenegro, August 2004.
- [198] C. Stehle, D. Gilles, M. Busquet, and A. Demura, "On Stark broadening as a tool for diagnostics of high density plasmas," *Laser and Particle Beams*, vol. 23, no. 3, pp. 357–363, 2005.

